國立交通大學

電信工程學系

博士論文

交錯耦合微帶線濾波器的調整與診斷

Tuning and Diagnosis of Cross-Coupled Microstrip Filters

研究生：廖竟谷　　　　　(Ching-Ku Liao)

指導教授：張志揚 博士（Chi-Yang Chang)

中華民國　九十六　年　六　月

交錯耦合微帶線濾波器的調整與診斷

Tuning and Diagnosis of Cross-Coupled Microstrip Filters

研 究 生：廖竟谷　　　　Student：Ching-Ku Liao

指導教授：張志揚　　　　Advisor：Chi-Yang Chang

國 立 交 通 大 學

電 信 工 程 學 系

博 士 論 文

A Dissertation Submitted to

Department of Communication Engineering

College of Engineering

National Chiao Tung University

in Partial Fulfillment of the Requirements

in

Communication Engineering

June 2007

Hsinchu, Taiwan, Republic of China

中華民國九十六年六月

推 薦 函

一、事由：本校電信研究所博士班研究生 廖竟谷 提出論文以參加國立交通大學

博士班論文口試。

二、說明：本校電信研究所博士班研究生 廖竟谷 已完成本校電信研究所規定之

學科課程及論文研究之訓練。

有關學科部分，廖君已修滿十八學分之規定（請查閱學籍資料）並通過資格

考試。

有關論文部分，廖君已完成其論文初稿，相關之論文亦分別發表於國際期刊

（請查閱附件）並滿足論文計點之要求。

總而言之，廖君已具備國立交通大學電信研究所應有之教育及訓練水準，因

此特推薦

廖君參加國立交通大學電信工程學系博士班論文口試。

交通大學電信工程學系教授　　張　志　揚

國 立 交 通 大 學

論 文 口 試 委 員 審 定 書

本校＿＿＿＿電 信 工 程＿＿＿＿學系博士班＿＿＿廖 竟 谷＿＿＿君

所提論文　交錯耦合微帶線濾波器的調整與診斷
　　　　　Tuning and Diagnosis of Cross-Coupled Microstrip filters

合於博士資格水準、業經本委員會評審認可。

口試委員：　＿＿＿＿＿＿＿＿＿＿　　＿＿＿＿＿＿＿＿＿＿

指導教授：　＿＿＿＿＿＿＿＿＿＿　　＿＿＿＿＿＿＿＿＿＿

系 主 任：　　　　　　　　　教授

中 華 民 九 十 六 年 四 月 二 十 七 日

Department of Communication Engineering
National Chiao Tung University
Hsinchu, Taiwan, R.O.C.

Date: <u>April 27, 2007</u>

We have carefully read the dissertation entitled

Tuning and Diagnosis of Cross-Coupled Microstrip Filters

submitted by <u>Ching-Ku Liao</u> in partial fulfillment of the requirements of the degree of DOCTOR OF PHILOSOPHY and recommend its acceptance.

Thesis Advisor: _____

Chairman
Department of Communication Engineering:_____

國 立 交 通 大 學

博碩士論文全文電子檔著作權授權書

（提供授權人裝訂於紙本論文書名頁之次頁用）

本授權書所授權之學位論文，為本人於國立交通大學＿＿電信工程＿＿＿系所＿＿電波＿＿組，＿＿95＿＿學年度第＿2＿學期取得博士學位之論文。

論文題目：交錯耦合微帶線濾波器的調整與診斷

指導教授：張志揚

■ 同意　□不同意

本人茲將本著作，以非專屬、無償授權國立交通大學與台灣聯合大學系統圖書館：基於推動讀者間「資源共享、互惠合作」之理念，與回饋社會與學術研究之目的，國立交通大學及台灣聯合大學系統圖書館得不限地域、時間與次數，以紙本、光碟或數位化等各種方法收錄、重製與利用；於著作權法合理使用範圍內，讀者得進行線上檢索、閱覽、下載或列印。

論文全文上載網路公開之範圍及時間：	
本校及台灣聯合大學系統區域網路	■ 中華民國 96 年 9 月 1 日公開
校外網際網路	■ 中華民國 96 年 9 月 1 日公開

授 權 人：廖竟谷

親筆簽名：＿＿廖竟谷＿＿

中華民國　96　年　6　月　20　日

國 立 交 通 大 學

博碩士紙本論文著作權授權書

（提供授權人裝訂於全文電子檔授權書之次頁用）

本授權書所授權之學位論文，為本人於國立交通大學____電信工程____系所__電波____組，__95__學年度第__2_學期取得碩士學位之論文。

論文題目：交錯耦合微帶線濾波器的調整與診斷

指導教授：張志揚

■ 同意

本人茲將本著作，以非專屬、無償授權國立交通大學，基於推動讀者間「資源共享、互惠合作」之理念，與回饋社會與學術研究之目的，國立交通大學圖書館得以紙本收錄、重製與利用；於著作權法合理使用範圍內，讀者得進行閱覽或列印。

本論文為本人向經濟部智慧局申請專利(未申請者本條款請不予理會)的附件之一，申請文號為：_____，請將論文延至____年____月____日再公開。

授 權 人：廖竟谷

親筆簽名：____廖竟谷____

中華民國　　96　年　　6　月　20　日

國家圖書館博碩士論文電子檔案上網授權書

ID:GT009213815

本授權書所授權之論文為授權人在國立交通大學_電機資訊_學院_電信工程_系所 ___電波__ 組 _95_學年度第__2_學期取得博士學位之論文。

論文題目：交錯耦合微帶線濾波器的調整與診斷

指導教授：張志揚

茲同意將授權人擁有著作權之上列論文全文（含摘要），非專屬、無償授權國家圖書館，不限地域、時間與次數，以微縮、光碟或其他各種數位化方式將上列論文重製，並得將數位化之上列論文及論文電子檔以上載網路方式，提供讀者基於個人非營利性質之線上檢索、閱覽、下載或列印。

※ 讀者基於非營利性質之線上檢索、閱覽、下載或列印上列論文，應依著作權法相關規定辦理。

授權人：廖竟谷

親筆簽名：＿＿＿廖竟谷＿＿＿

民國　96　年　6　月　20　日

交錯耦合微帶線濾波器的調整與診斷

研究生:廖竟谷 　　　　　　　　　　　　　　指導教授:張志揚博士

國立交通大學電信工程學系（研究所）博士班

摘要

　　本論文主要在研究如何萃取交錯耦合濾波器之等效電路參數，進而調整濾波器使其達到預先設定之響應。一般而言，交錯耦合濾波器之等效電路參數可由一個耦合矩陣來表示，文中將對耦合矩陣的萃取與合成方法有詳盡的討論。同時文中也提出了系統化的設計與調整濾波器的步驟。而這樣的方法與步驟可有效地用來分析微帶線濾波器中的交錯耦合效應、共振腔頻率校正等問題。其中，對於具有源級與負載相耦合(source-load coupling)的四角互耦(quadruplet)結構有詳盡的討論。此外，文中也提出了如何快速設計具高止帶頻率選擇性的串接三角互耦(cascade trisection)濾波器。除了在單模濾波器的應用外，文中也深入探討了如何混用單模與雙模共振腔來實踐具廣義查比雪夫響應之似盒狀(box-like)耦合濾波器。另外，文中也提出了一種新的參數萃取法，此法可以從濾波器的響應同時萃取出耦合矩陣與無外加負載之品質因子(unloaded quality factor)。此種參數萃取法可以實際用於有損濾波器的分析與調整。

Tuning and Diagnosis of Cross-Coupled Microstrip Filters

Student: Ching-Ku Liao   **Advisor: Dr. Chi-Yang Chang**

Department of Communication Engineering
National Chiao Tung University

Abstract

This Dissertation presents how to extract the equivalent circuit parameters of cross-coupled filters. From the extracted parameters, one can decide how to tune a filter to achieve the prescribed response systematically. In most cases, the cross-coupled filters can be described by a coupling matrix. Thus, how to extract and synthesize a coupling matrix with a given response would be discussed in detail. Besides, a systematical procedure for filter design and tuning is given. With these developed methods, one can effectively analyze the effect of cross couplings and asynchronous resonant frequencies of resonators in microstrip filters. As an example, the quadruplet filters with source-load coupling are discussed in detail. And a cascade trisection filter with high selectivity in upper stopband is proposed. In addition to the design of single-mode resonator filters, we investigate how to utilize the dual-mode resonator with single-mode resonators to realize box-like filters with generalized Chebyshev response. To extract a coupling matrix and an unloaded quality factor of a filter from a simulated/measured response simultaneously, a novel parameter extraction method is proposed. This parameter extraction method can be used to analyze and tune lossy filters.

誌　　謝

　　生命中，總有要做決定的時刻。當然，有些事情容易決定，有些則很困難。對我，選擇讀博士班並不是個容易的決定。選擇讀博士班是對研究的憧憬、對未知事物的好奇。但在現實的生活中，研究會有困難，親人也未必支持自己走研究這條路。周遭不少人對我說過：『幹嘛念博士啊?』，『你做這有啥用，還不如去賺錢。』之類的話。但對我而言，念博士班的人總有一個夢，有著對未知事務的好奇，而這樣的好奇心與想做出點新奇的東西的想法驅動著自己去做研究。拿到博士學位並不是夢想的實現，而是一個小里程的結束。

　　我要特別感謝張志揚教授的指導。張教授的開朗與耐心以及對專業知識的熟稔，對於研究工作的進展有莫大的助益。在新竹的這幾年，叔叔嬸嬸的照顧以及可愛的堂弟堂妹們的陪伴，讓我在研究之餘有精神上的調劑。在佛羅里達大學的期間，常志、政寧、明旗、天宇的友誼，讓身在美國的我能快樂度日。在美國的期間，何雲幫了我許多忙、教了我許多事情，他的幫助讓我能很快適應在美國的生活。Bruce 帶我認識了美國同時拜訪了很多地方。 Linsay 則是最樂於糾正我的破英文的一位，我英文如有進步多要歸功於他。林仁山教授夫婦熱心的幫忙與招待讓身在異鄉的我倍感溫暖。很高興有這麼多人陪我走過這個里程。

<div align="right">

廖竟谷　　於交大

民國九十六年六月

</div>

Contents

List of Table

List of Figures

Chapter 1 Introduction

Microwave filters are essential component in a microwave system. Thus, there are lots of literatures concerning with the designs and implementations of microwave filters applied in different wireless communication systems. Concerning with the development of the microwave filters, Ralph Levy et al. [1], [2] and Ian C. Hunter et al. [3] give a clear historical review of the development of microwave filters. Among these papers, different kinds of microwave filters are introduced and discussed, and important references are also given. Among different kinds of microwave filters, this dissertation would focus on the design and tuning of microwave filters which can be described by coupling matrices.

The design of microwave filters normally starts from the synthesis of a low-pass prototype network, regardless of the eventual physical realization in transmission line, waveguide, or other media. Low pass prototype networks are two-port network with an angular cutoff frequency of 1 rad/s and operating in a 1-Ω system. A typical prototype network is shown in Figure 1-1. The ladder network prototype in Figure 1-1(a) and (b) is an all-pole network with all its transmission zeros at infinity. The alternative network shown in Figure 1-1(c) and (d) are also used. The networks in Figure 1-1(c)(d) are very useful for the design of narrow band bandpass filter since it only use the series or shunt resonator. Besides, the network in Figure 1-1(c) or (d) can be described by a coupling matrix. To achieve more selective frequency response, like generalized Chebyshev response [1], finite transmission zeros in the complex plane have to be introduced, and the corresponding prototype circuit usually can be expressed by a cross-coupled network. Filters which can be modeled by a cross-coupled network are called cross-coupled filters. Cross couplings are usually generated by either putting resonant/non-resonant circuits or introducing couplings between nonadjacent resonators.

(a)

(b)

(c)

(d)
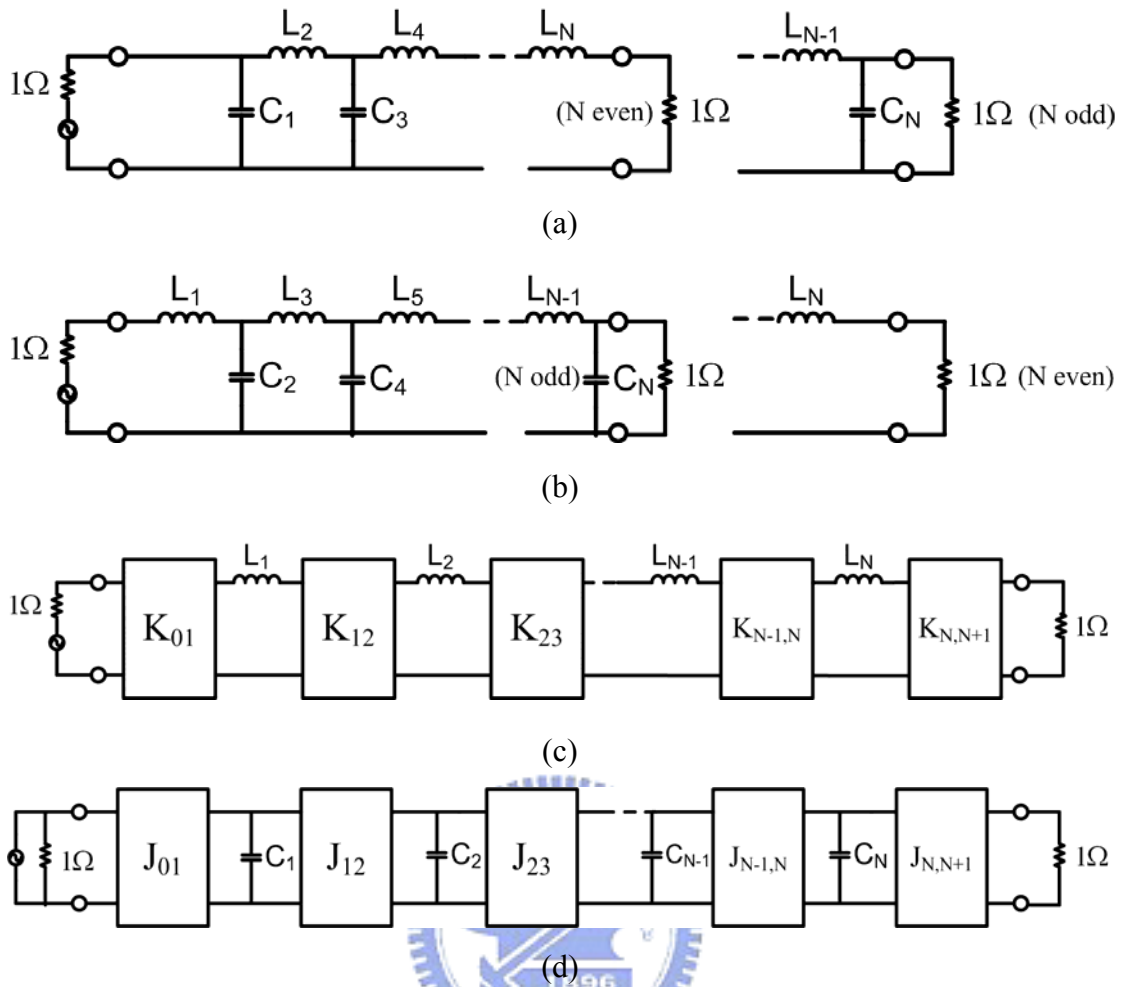
Figure 1-1. (a), (b) Lowpass prototype networks for "all-pole" filters. (c), (d) Alternative lowpass prototype networks using inverter.

1.1 Review of the Design of Cross-Coupled Resonator filters

The cross-coupled filters have been used since 1940's [1]. An example is given following to explain the basic idea behind cross-coupled filters. A filter, utilizing the cross couplings between nonadjacent resonators, is shown in Figure 1-2. These cross couplings give a number of alternative paths which a signal may take between input and output ports. The multi-path effect causes transmission zeros to appear in the transfer function, which, depending on the phasing of the signals, may cause transmission zeros at finite frequencies or group delay flattening, or both simultaneously.
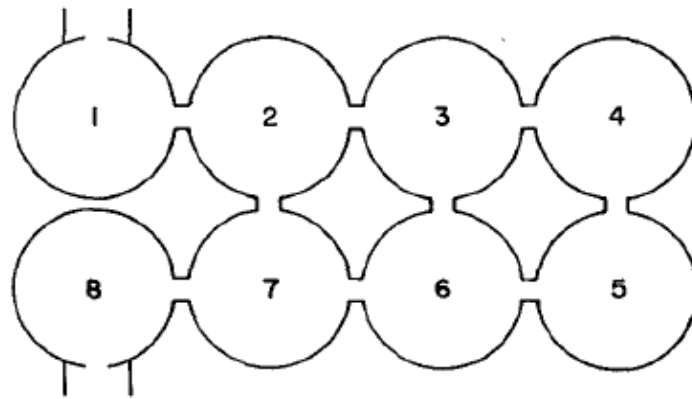
Figure 1-2. A cross-coupled resonator filter (clipped from Figure 9 in [1])

Synthesis technique and implementation methods for the cross-coupled filters have been developed for couples of decades. Among those related works, the most significant development took place in the 1970's in COMSAT by Atia and Williams [4]-[7]. The COMSAT work on elliptic function and linear-phase waveguide filters using dual-mode cavities with cross coupling was particular significant. The dual-mode cavity filters introduced by Atia and Williams have set the virtual standardization of these designs for satellite transponders. Actually, Atia and Williams have published a series of papers concerning on the synthesis, design, implementation, and tuning of the cross-coupled resonator filters. All those papers are well-written and introduce original concepts. It is highly recommended for one who is interested in the design of cross-coupled resonators filter to read the series of papers by Atia and Williams.

The most recent progress in the synthesis of cross-coupled filter is done by Richard Cameron. In 1999 and 2003, Richard Cameron published two papers focused on generalizing the synthesis technique for the cross-coupled resonator filter with the generalized Chebyshev function [8] [9]. With his work, a cross-coupled filter with N resonators can have at maximum N finite transmission zeros. Based on Cameron's

work, many researchers have developed different methods to transfer the synthesized coupling matrixes into desired forms. The details of the related synthesis techniques will be discussed in Chapter 2.

The cross-coupling concept was originally used in the waveguide filters but not applied to the microstrip filters before 1990's. But with the increasing power of computation of computers, the story was changed. Electromagnetic (EM) simulators are capable of simulating complex physical structures within a reasonable time now. Thus, it is feasible to get the S-parameters of the designed structure through the EM simulator instead of doing experiments. Hong and Lancaster took the advantage of the computer's power to calculate the external quality factor and coupling coefficients, originally experimental method, to design the microstrip cross-coupled resonator filters [10], [11]. The related works done by Hong and Lancaster are clearly described in the book [12] written by them.
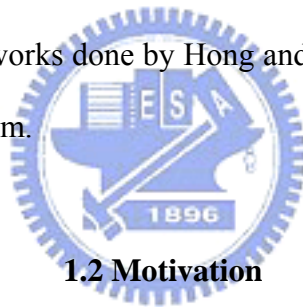
1.2 Motivation

The computer-aided diagnosis and tuning of cross-coupled resonator filters have been an active topic in the filter society for several decades. The main driving force to the art is the continuous demand on reducing the manufacturing cost and development time for various filters with different specifications. The core task in filter tuning is to diagnose the filter coupling status that corresponds to the current filter response. By comparing the desired circuit model parameters (i.e., coupling matrix) to the extracted ones, the tuning direction and magnitude can be decided.

Tuning is an essential process for optimizing filters' responses in both the simulation stage and production line. On the simulation, even though a great variety of EM simulators are commercially available, it is generally impossible to optimize microwave filters on the basis of field simulators alone because the computer

4

simulation time for it is huge, especially for higher order filter with generalized Chebyshev response. Moreover, on the production line, fabrication of high performance filters is a constant trade-off between the manufacturing cost and the accuracy required in the process. In reality, the variation in raw material and manufacturing process leads the filters' response deviate from the designed ones, which means post tuning is always required. The need of tuning on both EM simulation and fabrication urges filter designers to develop CAD tool to shorten the design period in recent decades.

In the design of cross-coupled resonator filter, especially for microstrip filter, the spurious couplings between resonators always exist. However, the method proposed by Hong and Lancaster only gives initial dimensions of microstrip cross-coupled filters [12]. The effect of spurious couplings between resonators and how to tune a filter to achieve a prescribed response were not mentioned. Thus, parameter extraction methods and tuning algorithm is needed to obtain the strength of spurious couplings and tune a filter.
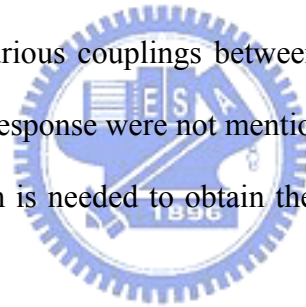
1.3 Literatures Survey

The existing computer diagnosis techniques can be basically divided into two catalogues: by optimization technique and by analytical methods. There are pros and cons for the diagnosis techniques based on optimization methods and analytic formula, respectively. In the following, we will discuss them individually.

Basically, all the diagnosis and tuning procedures involving three basic elements

1. Filter synthesis

2. Curve fitting of a simulated or measured S-parameter,

3. Update of a filter's physical dimensions.

These three basic elements in the procedure determine how good a procedure is. A simplified design flow of the filter tuning process is shown in Figure 1-3 to clarify the basic elements involved. The implementation of the flow shown in Figure 1-3 will be discussed in Chapter 2 in detail.

The methods based on nonlinear optimization are like that in [13]-[15] where different optimization strategies and schemes for parameter extraction are explored. In [13], the optimization technique is used to find a coupling matrix with the goal that the resulted response fitting well with the simulated response. However, there are many variables (coupling coefficients) involved in the optimization process, which makes the method only applicable for the cases where the order of filter is less than 6. The methods in [16], [17] are based on analytical method. Those methods extract the coupling matrix from the locations of system zeros and poles. The existing analytical models provide a recursive procedure to determine individual resonant frequencies and inter-resonator couplings. However, those analytical methods are only valid for highly restricted filter topologies. In addition, to get analytical formula for the calculation of the coupling matrix, one must derive different formula for different topologies, which is not easy even for an expert in this filed. Furthermore, the

S-parameters corresponding to an extracted coupling matrix usually can not so well fit the simulated or measured response as one can obtain by the optimization method because of the existence of dispersion effect. As we know, poles and zeros of a system determine the systems response. Moving one of the poles or zeros will change the response over all frequency. On the other hand, methods based on optimization can fit the simulated response better than the method based on analytical methods because sampling a lot of different frequency points over the interest band can average the dispersion effect.
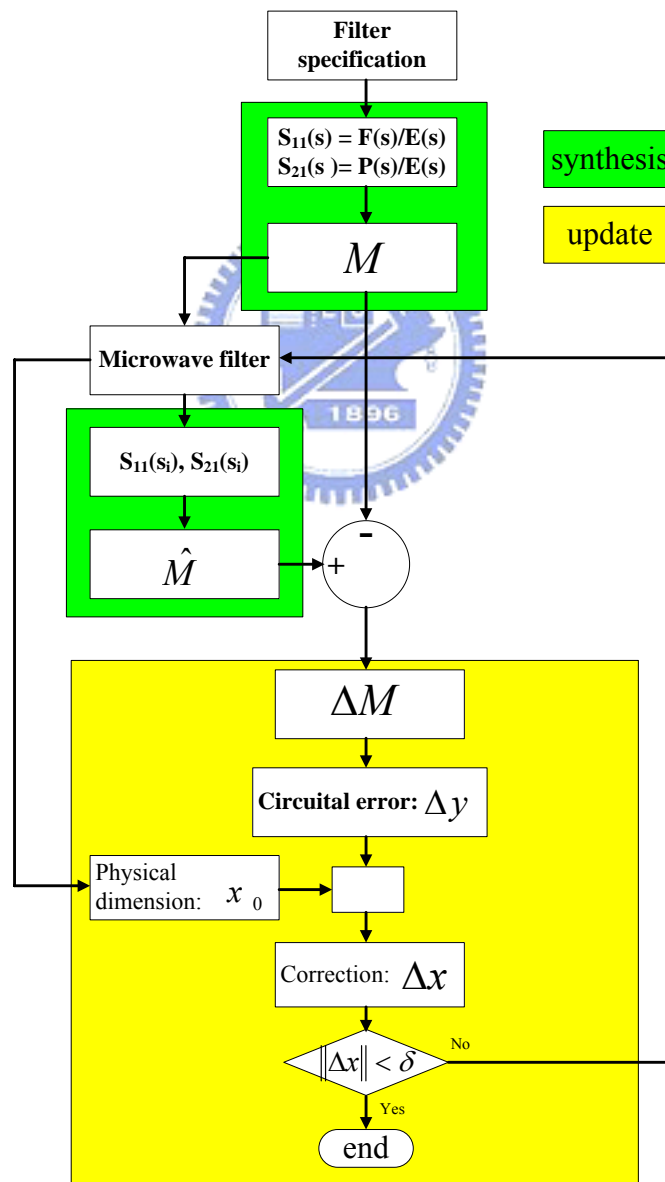
Figure 1-3. Flow diagram of the filter optimization algorithm

From the above discussion, some observations are summarized. First, optimization technique should not be directly applied to obtain the coupling matrix as that in [13] since this approach limited the method only applicable to lower order filter. Second, reconstructing the coupling network from poles and zeros of system by analytical formula may not be accurate enough and be topology-limited.

In the procedure provided in [18], the Cauchy method is applied to obtain the approximated rational polynomials of reflection and transmission function, $S_{11}(s)$ and $S_{21}(s)$, which is suitable for filter synthesis. After getting the approximated rational polynomial of $S_{11}(s)$ and $S_{21}(s)$, a variety of synthesis techniques can be applied to get the coupling matrix. The synthesis technique used in [19] is based on optimization technique and can be applied to get a coupling matrix with arbitrary topology with the order smaller than 14. In practical, most cross-coupled resonators filters have the order smaller than 14. Thus, the procedure provided in [19] is highly recommended. Besides, there is no need to calibrate the reference plane when using the Cauchy method to get the approximated $S_{11}(s)$ and $S_{21}(s)$.

The formulation based on Cauchy method in [18] is only valid for lossless case. For lossy filters, the modified Cauchy methods are proposed in [20]. However, the method in [20] is incorrect in the sense that the generated rational polynomials, $S_{11}(s)$ and $S_{21}(s)$, are not suitable for the filter synthesis. The author in [21] indicated the theoretical error in [20] and proposed a modified formulation suitable for filters with low and moderate losses. It should be noted that even the formulation in [21] can not tell how lossy a filter is. So, how to model a lossy filter and extract related parameters is still a problem under investigate.

1.4 Contribution

The main contributions of this dissertation are described in the following.

First, an optimization procedure as shown in Figure 1-3 is developed in this dissertation. The optimization procedure is used to design all the circuits presented in this dissertation. It is also applied to investigate the effect of spurious couplings in the cross-coupled microstrip filters. Coupling matrices are extracted in the course to optimize the quadruplet filter with source-load coupling. With the developed optimization methods, quadruplet filters with various responses are designed, built, and tested.

Second, a microstrip cross-coupled filter with two independently controllable transmission zeros on upper stopband is presented. The initial filter structure is a conventional Chebyshev-response parallel-coupled filter that can be easily realized by the analytical method. The newly proposed coupling/shielding lines effectively control the cross and main couplings without changing the original filter layout. With this approach, designer can eliminate tedious segmentation method for the filter design.

Third, an E-shaped dual-mode resonator is proposed to implement coupling topologies such as doublet, extended doublet, and box-section in a unified approach. The doublet and box-section filter exhibit the zero-shifting properties which can not be achieved by trisection cross-coupled filters. The extended-doublet filter can generate two finite transmission zeros to improve selectivity or flatten in-band group delay. The correspondence between the E-shaped dual-mode resonator and a coupling matrix is established, which make it possible to design those filters in a systematical way.

Finally, the formulation which is applicable to extract the loss term and a coupling matrix simultaneously from a simulated or measured response is proposed.

With this method, no matter the device under test is lossy or lossless, one can extract the coupling matrix from the simulated or measured response.

1-5 Organization

This dissertation is mainly concentrated on the design and tuning of cross-coupled resonator filters, especially for the microstrip filters.

In Chapter 2, each step taken in the flow diagram of filter optimization in Figure 1-3 is discussed in detail. The model of the cross-coupled resonator filter in low pass domain is given. From the model, the relation between a coupling matrix and S-parameters is derived. Then, how to directly relate the position of finite transmission zeros to a given coupling matrix is given. Some simple topologies such as trisection, quadruplet, doublet, extended doublet, and box-section are taken as examples, and the equations relating the position of finite transmission zeros and coupling coefficients are given. In addition, a variety of synthesis methods are discussed, and the method for updating the physical dimension is given.

In Chapter 3, the quadruplet filters with source-load coupling are presented. The effect of spurious cross couplings between resonators is discussed. The parameter extraction method is applied to extract the coupling matrix corresponding to simulated response. The examples include the quadruplet filters designed for improving skirt selectivity and in-band group delay flatness.

In Chapter 4, a cascade trisection filter with source/load to multi-resonator couplings is proposed. The initial dimension of the filter is obtained from the conventional parallel coupled line filter. The filter exhibiting two finite transmission zeros which can be independently controlled to improve the selectivity.

In Chapter 5, generalized Chebyshev microstrip filters with box-like coupling schemes are presented. The box-like portion of the coupling schemes is implemented by an E-shaped resonator. Synthesis and realization procedures are described in detail.

In Chapter 6, a parameter extraction method based on vector fitting formulation is proposed to identify the unload quality factor of resonators and coupling matrix of a filter from the simulated/measured response simultaneously.

In Chapter 7, summary and suggested future works are given.

Chapter 2 Design and Optimization of Microwave Filter

Based on Coupling Matrix

In this chapter, the design flow of cross-coupled resonator filters is given and discussed in detail. To facilitate the discussion, the cross-coupled resonators network is analyzed in the normalized frequency domain at first. The relation between the normalized network parameters and S-parameters is derived. How to obtain the position of finite transmission zeros from coupling topologies is also given. With the necessary background, each step shown in Figure 1-3 is given.

(a)

(b)
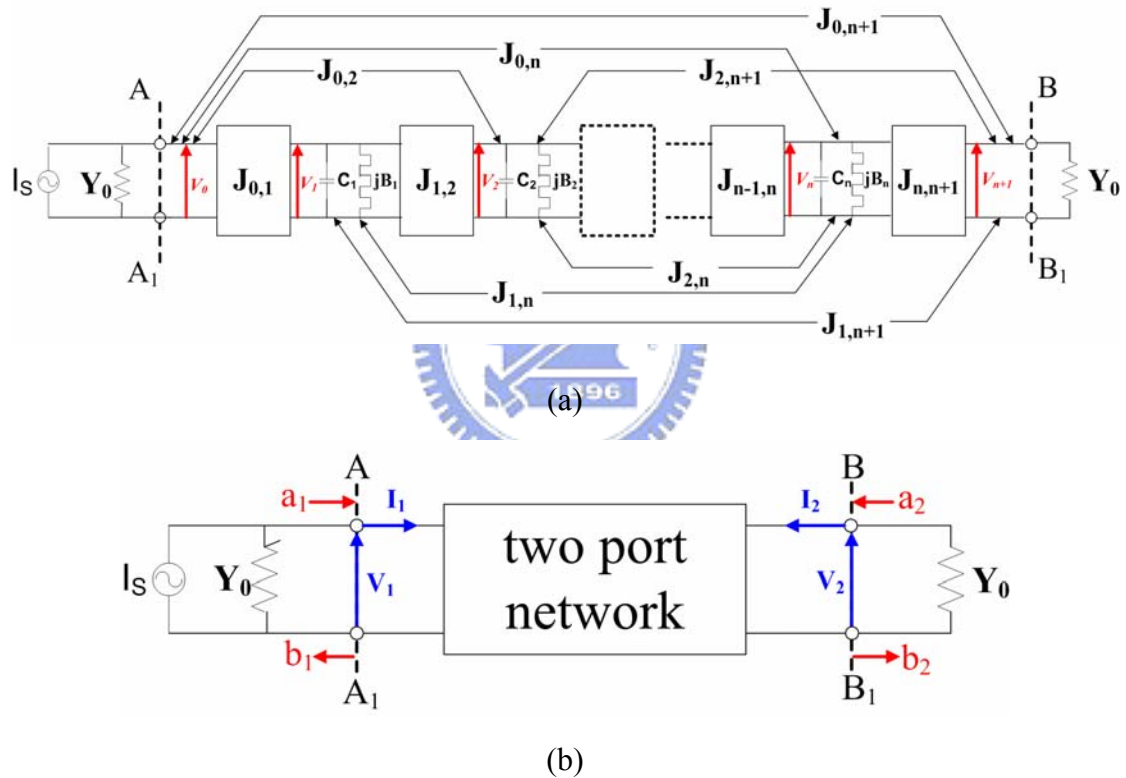
Figure 2-1 (*a*) Equivalent circuit of *n*-coupled resonators in low pass domain. (*b*) Its network representation.

2.1 Filter Model in the Normalized Domain

A prototype filter of degree n in the lowpass domain is shown in Figure 2-1 (a). The prototype filter consists of frequency independent impedance inverters $J_{ij}s$, capacitors $C_i s$ and susceptances $B_i s$. The values of all the capacitors and the

12

terminated admittances Y_0 are set equal to one. The capacitors in the low-pass domain correspond to the resonators in the bandpass domain. Thus, the frequency invariant susceptances $B_i s$ represent the frequency shift of resonators in the bandpass domain. The values of $B_i s$ are zero for the synchronously tuned filters and nonzero for the asynchronously tuned filters.

According to the current law, which is one of the Kirchhoff's two circuit laws and states the algebraic sum of the currents leaving a node in a network is zero, with a driving or external current of I_s, the node equations for the circuit of Figure 2-1(a) are

$$
\begin{bmatrix}
Y_0 & jJ_{0,1} & jJ_{0,2} & \cdots & jJ_{0,n+1} \\
jJ_{0,1} & j\Omega+jB_1 & jJ_{1,2} & \cdots & jJ_{1,n+1} \\
jJ_{0,2} & jJ_{1,2} & \ddots & & \vdots \\
\vdots & \vdots & & j\Omega+jB_n & jJ_{n,n+1} \\
jJ_{0,n+1} & jJ_{1,n+1} & \cdots & jJ_{n,n+1} & Y_0
\end{bmatrix}_{(n+2)\times(n+2)}
\begin{bmatrix}
V_0 \\
V_1 \\
\vdots \\
V_n \\
V_{n+1}
\end{bmatrix}_{(n+2)\times 1}
=
\begin{bmatrix}
I_s \\
0 \\
0 \\
\vdots \\
0
\end{bmatrix}_{(n+2)\times 1}
\quad (2\text{-}1)
$$

where Ω is the normalized frequency.

To derive the two-port S-parameters of a coupled-resonator filter, the circuit of Figure 2-1(a) is represented by a two-port network of Figure 2-1(b). Comparing Figure 2-1(a) and Figure 2-1(b), we can find that $V_1 = V_0$, $V_2 = V_{n+1}$, and $I_1 = I_s - Y_0 V_0$. And

$$
a_1 = \frac{I_s}{2}, \qquad b_1 = \frac{2V_0 - i_s}{2}
$$

$$
a_2 = 0 \quad , \qquad b_2 = V_{n+1}
$$

Thus,

$$
S_{11} = \left. \frac{b_1}{a_1} \right|_{a_2=0} = -1 + \frac{2V_0}{I_s} \qquad (2\text{-}2)
$$

$$
S_{21} = \left. \frac{b_2}{a_1} \right|_{a_2=0} = \frac{2V_{n+1}}{I_s} \qquad (2\text{-}3)
$$

From equation (2-1), we can obtain

$$\frac{V_0}{I_s} = [Y]^{-1}_{1,1} \tag{2-4}$$

$$\frac{V_{n+1}}{I_s} = [Y]^{-1}_{(n+2),1} \tag{2-5}$$

Take (2-4) into (2-2), we can obtain

$$S_{11} = -1 + 2[Y]^{-1}_{1,1} \tag{2-6}$$

Take (2-5) into (2-3), we can obtain

$$S_{21} = 2[Y]^{-1}_{n+2,1} \tag{2-7}$$

In the literatures, the matrix $\begin{bmatrix} 0 & J_{0,1} & J_{0,2} & \cdots & J_{0,n+1} \\ J_{0,1} & B_1 & J_{1,2} & \cdots & J_{1,n+1} \\ J_{0,2} & J_{1,2} & \ddots & & \vdots \\ \vdots & \vdots & & B_n & J_{n,n+1} \\ J_{0,n+1} & J_{1,n+1} & \cdots & J_{n,n+1} & 0 \end{bmatrix}$ is called the

normalized coupling matrix and denoted as matrix [M].

$$[M] = \begin{bmatrix} 0 & M_{S1} & M_{S2} & \cdots & M_{SL} \\ M_{S1} & M_{11} & M_{12} & \cdots & M_{1L} \\ M_{S2} & M_{12} & \ddots & & \vdots \\ \vdots & \vdots & & M_{nn} & M_{nL} \\ M_{SL} & M_{1L} & \cdots & M_{nL} & 0 \end{bmatrix}$$

Where $M_{ij} = J_{i,j}$, $M_{ii} = B_i$. To translate the equation (2-6) and (2-7) to the

expressions in the literatures, let

$$[Y] = s[I] + j[M] + [G] = j\left(\Omega[U]_0 + [M] - j[G]\right) = j[A],$$

where $[A] = \Omega[U]_0 + [M] - j[G]$, $[U_0] \in R^{(n+2)\times(n+2)}$ is identical to the identity

matrix, except for the element $[U_0]_{11} = [U_0]_{n+2,n+2} = 0$, and $[G] \in R^{(n+2)\times(n+2)}$ is also a

diagonal matrix, $[G] = diag\{1,0,\cdots,0,1\}$. The equations (2-6) and (2-7) can be

rewritten as

$$S_{11} = -1 - 2\,j[A]_{1,1}^{-1} \qquad\qquad (2\text{-}8)$$

$$S_{21} = -2\,j[A]_{(n+2),1}^{-1} \qquad\qquad (2\text{-}9)$$

Similarly, we can derive

$$S_{22} = -1 - 2\,j[A]_{n+2,n+2}^{-1} \qquad\qquad (2\text{-}10)$$

The equations (2-8), (2-9) and (2-10) directly related the normalized coupling matrix to the S-parameters.

2.2 The Position of Finite Transmission Zeros

From the equations (2-8) and (2-9), we can express S_{11} and S_{22} as a rational functions,

$$S_{11}(\Omega) = \frac{F(\Omega)}{E(\Omega)} \qquad\qquad (2\text{-}10)$$

$$S_{21}(\Omega) = \frac{P(\Omega)}{E(\Omega)} \qquad\qquad (2\text{-}11)$$

Obviously, the finite transmission zeros are the roots of the equation

$$P(\Omega) = 0 \qquad\qquad (2\text{-}12)$$

Solving the equation (2-12) can help us understand the dependence between the coupling coefficients and finite transmission zeros, which help us get more insight to control the finite transmission zeros. To illustrate that, let us take an example with the coupling matrix M_1

$$M_1 = \begin{bmatrix} 0 & M_{S1} & 0 & 0 & 0 & 0 \\ M_{S1} & 0 & M_{12} & 0 & M_{14} & 0 \\ 0 & M_{12} & 0 & M_{23} & 0 & 0 \\ 0 & 0 & M_{23} & 0 & M_{34} & 0 \\ 0 & M_{14} & 0 & M_{34} & 0 & M_{4L} \\ 0 & 0 & 0 & 0 & M_{4L} & 0 \end{bmatrix} \qquad (2\text{-}13)$$

The topology of M_1 is known as cross-coupled quadruplet and the graphical representation of it is drawn in Figure 2-2. This kind of graphical representation has

15

been widely used in literatures recently.
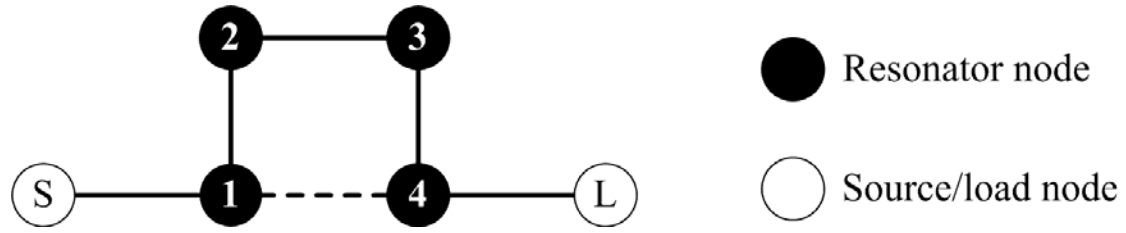
Figure 2-2 the coupling route of the example filter

By solving $P(\Omega) = 0$, we can find the roots can be expressed as

$$\Omega^2 = M_{23}^2 - \frac{M_{12}M_{23}M_{34}}{M_{14}} \qquad (2\text{-}14)$$

The cross-coupled quadruplet filter is a perturbation version of the original direct-coupled Chebyshev filter. Thus, compared to the values of M_{12}, M_{23} and M_{34}, the value of M_{14} is relatively small. That is $\left| M_{23}^2 \right| < \left| \dfrac{M_{12}M_{23}M_{34}}{M_{14}} \right|$.

For the design where the shape skirt selectivity is required on both side of the pass band, the finite transmission zeros should be put on the real frequency axis, which means $\Omega^2 > 0$. On the other hand, for the group delay flattening, the finite transmission zeros should be put on the imaginary frequency axis, which means $\Omega^2 < 0$. From the equation (2-14), we can tell that if $M_{12}M_{23}M_{34}M_{14} < 0$, then $\Omega^2 > 0$ and if $M_{12}M_{23}M_{34}M_{14} > 0$, then $\Omega^2 < 0$.

The coupling topologies: quadruplet, trisection, doublet and box-section, are given in Table 2-1. The corresponding position of finite transmission zeros of these topologies are given in Table 2-1 as well.

Coupling route	Coupling matrix	Position of finite Txz
	$$M = \begin{bmatrix} 0 & M_{S1} & 0 & 0 & 0 & 0 \\ M_{S1} & 0 & M_{12} & 0 & M_{14} & 0 \\ 0 & M_{12} & 0 & M_{23} & 0 & 0 \\ 0 & 0 & M_{23} & 0 & M_{34} & 0 \\ 0 & M_{14} & 0 & M_{34} & 0 & M_{4L} \\ 0 & 0 & 0 & 0 & M_{4L} & 0 \end{bmatrix}$$	$\Omega^2 = M_{23}^2 - \dfrac{M_{12}M_{23}M_{34}}{M_{14}}$
	$$M = \begin{bmatrix} 0 & M_{S1} & 0 & 0 & 0 \\ M_{S1} & M_{11} & M_{12} & M_{13} & 0 \\ 0 & M_{12} & M_{22} & M_{23} & 0 \\ 0 & M_{13} & M_{23} & M_{33} & M_{3L} \\ 0 & 0 & 0 & M_{3L} & 0 \end{bmatrix}$$	$\Omega = -M_{22} + \dfrac{M_{12}M_{23}}{M_{13}}$
	$$M = \begin{bmatrix} 0 & M_{S1} & M_{S2} & 0 \\ M_{S1} & M_{11} & 0 & M_{1L} \\ M_{S2} & 0 & M_{22} & M_{2L} \\ 0 & M_{1L} & M_{2L} & 0 \end{bmatrix}$$	$\Omega = -\dfrac{M_{11}M_{s2}M_{2L} + M_{22}M_{s1}M_{1L}}{M_{s1}M_{1L} + M_{s2}M_{2L}}$
	$$M = \begin{bmatrix} 0 & M_{S1} & 0 & 0 & 0 & 0 \\ M_{S1} & M_{11} & M_{12} & M_{13} & 0 & 0 \\ 0 & M_{12} & M_{22} & 0 & M_{24} & 0 \\ 0 & M_{13} & 0 & M_{33} & M_{34} & 0 \\ 0 & 0 & M_{24} & M_{34} & M_{44} & M_{4L} \\ 0 & 0 & 0 & 0 & M_{4L} & 0 \end{bmatrix}$$	**Under the condition:** **$M_{44}=M_{11}$** $\Omega = -\dfrac{M_{33}M_{12}M_{24} + M_{22}M_{13}M_{34}}{M_{12}M_{24} + M_{13}M_{34}}$

Table 2-1. Coupling topologies and the position of their corresponding finite transmission zeros

2.3 Synthesis Methods for Cross-Coupled Filters

Filters may be classified into categories in several ways, one being into different classes of response functions, defined in terms of the location of poles of the insertion-loss function and of the zeros within the passband. The zeros are usually spaced throughout the passband to give a Chebyshev response since this is far more optimum and superior to the maximally flat or Butterworth response, which is rarely used. As far as the poles are concerned, the most common type of filter response has these located all at dc and infinity and is often described as an all-pole Chebyshev

filter. When one or more poles are introduced into the stopband at finite frequencies, a filter is called a generalized Chebyshev filter or a pseudo-elliptic filter.

From the discussion in section 2.1 and 2.2, we know cross-coupled filters exhibit finite transmission zeros (attenuation poles), which means the responses of cross-coupled filters may correspond to the generalized Chebyshev response. In fact, how to generate the $S_{11}(s)$ and $S_{21}(s)$ corresponding to the generalized Chebyshev function and find the corresponding coupling matrix are well-established [4]-[9]. The method about how to generate rational functions, $S_{11}(s)$ and $S_{21}(s)$, corresponding to the generalized Chebyshev response are given in [8]. The generated $S_{11}(s)$ and $S_{21}(s)$ are in the form

$$S_{11}(s) = \frac{F(s)}{E(s)} \qquad (2\text{-}15)$$

$$S_{21}(s) = \frac{P(s)}{E(s)} \qquad (2\text{-}16)$$

Synthesis methods about how to get the coupling matrix corresponding to the specified response in (2-15) and (2-16) may be divided into three categories.

1. Direct optimization

In 1998, Atia first proposed that with suitable cost function defined with positions of poles and zeros of a transfer function, we can set coupling coefficients of a filter as variables and apply the optimization method to get a coupling matrix [22] corresponding to that transfer function. Later, Amari extended Atia's work to include the source-load coupling [23]. The drawback of this kinds of method is that they are only effective for the filter with order smaller than 6. On the other hand, this kind of method is easy to follow and implement in a circuit simulator, like ADS.

2. Analytical method

The analytical method for the synthesis of cross-coupled filters was originally presented by Atia and Williams in [5]. Recently, Cameron has extended the analytical method to generate a generic matrix corresponding to a generalized Chebyshev response [8]. The generic matrix is $n \times n$ matrix having the form

$$M = \begin{bmatrix} M_{11} & M_{12} & M_{13} & \cdots & M_{1n} \\ M_{21} & M_{22} & M_{23} & \cdots & M_{2n} \\ M_{31} & M_{32} & M_{33} & \cdots & M_{3n} \\ \vdots & \vdots & \vdots & \ddots & \vdots \\ M_{n1} & M_{n2} & M_{n3} & \cdots & M_{nn} \end{bmatrix}$$

where $M_{ij}=M_{ji}$. The external coupling between the first resonator to source or last resonator to load is not shown in the matrix but expressed by two additional parameters R_1 and R_2. Since the source-load coupling is not included in the formulation, this kind of synthesis method can only apply for nth order filter with maximum of (n-2) finite transmission zeros. Besides, the matrix in generic form has to be further reduced since the coupling route is too complicated to achieve practically.

In 2003, Cameron further generalized the synthesis technique to cover the cases where source-load and source/load to multi-resonator couplings are involved. Follow the analytical formula in [9], we can get a transversal matrix with size $(n+2) \times (n+2)$. To distinguish coupling matrix with size $(n+2) \times (n+2)$ to that with size $n \times n$, we usually call a coupling matrix with size $(n+2) \times (n+2)$ an extended coupling matrix. A transversal coupling matrix is an extended coupling matrix with the following form

$$M = \begin{bmatrix} 0 & M_{S1} & M_{S2} & \cdots & M_{SL} \\ M_{1S} & M_{11} & 0 & \cdots & M_{1L} \\ M_{2S} & 0 & \ddots & \cdots & \vdots \\ \vdots & \vdots & \vdots & M_{nn} & M_{nL} \\ M_{LS} & M_{L2} & \cdots & M_{Ln} & 0 \end{bmatrix}$$

The corresponding coupling route of the transversal topology is shown in Figure 2-3
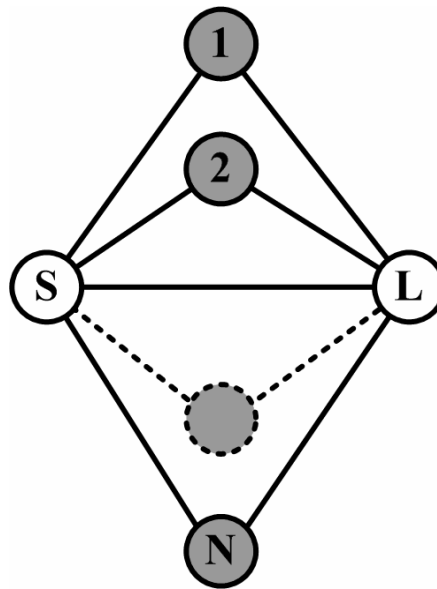
Figure 2-3. Coupling route of a transversal filter

The transversal matrix need to be further transformed into other coupling routes since the coupling route in transversal configuration is too sensitive to realize when the order of filter exceeds 2 [24]. From the above discussion, we know that both the generic and transversal coupling matrix are impractical. Thus, how to annihilate some couplings to make a coupling matrix simpler and keep the same electrical performance is important.

The technique of annihilating some specific couplings in a coupling matrix is called matrix reduction. The method for matrix reduction has been studied for several

decades. In principle, we can apply a sequence of similarity transforms to a generic or transversal matrix until more convenient form with a minimal number of couplings is obtained [5], [8], [9]. The similar transformation would not change the eigenvalues and eigenvectors of the coupling matrix, which means a transferred coupling matrix would exhibit the same response as the original coupling matrix. There are only a few patterns of coupling matrix can be achieved in a predetermined way, and most of them are proposed by Cameron [8], [9]. The analytical method is very powerful in the sense that the order of filter is not limited. However, how to transfer the generic or transversal coupling matrix into suitable topologies is not easy at all.

In view of the difficult of determine the rotation angles of the sequence of similar transformation, optimization method is introduced [25]. The method in [25] is reported to be effective for filter with order below 12. Another power optimization method based on the conservation of eigenvalues is proposed in [19], which is effective for filter with order under 14 and taken in this dissertation.

2.4 Obtaining a Initial Design for a Microwave Filter

With the information of a coupling matrix, we may obtain the initial dimension of microwave filters. A widely applied method to get the initial dimension of a filter is the segmentation method. In the segmentation method, the coupling strength between resonators is tested pair by pair to obtain the approximated coupling strength. The external coupling, the coupling between the first/last resonator to the source/load, is calculated by excluding other resonators. The detail of segmentation method formulated in low-pass domain is provided in Chapter 4 in the book [26]. In addition, formulation in the bandpass domain is given in the chapter 8 in the book [12]. In principle, it is better to do the calculation in the low-pass domain since the formulas are much simpler.

2.5 Tuning Procedures

The tuning of a microwave filter consists of two major steps. First, extract the coupling matrix from the simulated or measured response. Second, decide how to adjust the geometrical dimension of the filter under test by comparing the difference between extracted coupling matrix and the wanted coupling matrix.

A. parameter extraction

As we discussed in section 2.2 and 2.3, it is feasible to express the S-parameters of a filter as a rational polynomials in normalized frequency domain. So, if we can identify the S-parameters in rational polynomials in normalized frequency domain from the simulated or measured response, we can use the synthesis technique to obtain a coupling matrix. For S-parameter identification, an effective method, called Cauchy method, is proposed. The detail of the method is given in [18]. Here, we just give a brief review of the Cauchy method and point out some important characteristics of it.

The purpose of Cauchy method is to obtain the approximated rational polynomials of $\widetilde{S}_{11}(s)$ and $\widetilde{S}_{21}(s)$ in the following form

$$\widetilde{S}_{11}(s) = \frac{\widetilde{F}(s)}{\widetilde{E}(s)} = \frac{\sum_{k=0}^{n} a_k^{(1)} s^k}{\sum_{k=0}^{n} b_k s^k} \qquad (2\text{-}17)$$

$$\widetilde{S}_{21}(s) = \frac{\widetilde{P}(s)}{\widetilde{E}(s)} = \frac{\sum_{k=0}^{n_z} a_k^{(2)} s^k}{\sum_{k=0}^{n} b_k s^k} \qquad (2\text{-}18)$$

In the Eq. (2-17) (2-18), n is the order of filter and n_z is the number of finite transmission zeros. Note that the $\widetilde{S}_{11}(s)$ and $\widetilde{S}_{21}(s)$ have common denominator. Instead of directly fitting the simulated or measured data into the rational polynomial $\widetilde{S}_{11}(s)$ and $\widetilde{S}_{21}(s)$, the first step is to fit the characteristic function

$K(s) = \tilde{S}_{11}(s)/\tilde{S}_{21}(s)$. In this step, one can obtain the $\tilde{F}(s)$ and $\tilde{P}(s)$. The second step is to reconstruct the polynomial $\tilde{E}(s)$ by the Feldtkeller's equation:

$$\tilde{F}(s)\tilde{F}^*(-s) + \tilde{P}(s)\tilde{P}^*(-s) = \tilde{E}(s)\tilde{E}^*(-s) \qquad (2\text{-}19)$$

Note that there is no need to calibrate the reference plane before applying the Cauchy method, which makes the Cauchy method a perfect CAD tool. After obtaining the approximated rational polynomials in (2-17) and (2-18), the synthesis method given in section 2.3 can be directly applied to obtain the coupling matrix $\tilde{M}$. The $\tilde{M}$ represents the equivalent electrical parameters of the filter corresponding to the present geometrical dimensions.

B. Update the geometrical parameters

The cross-coupled network shown in Figure 2-1 can be treated as a surrogate model. The status of the surrogate model is represented by a coupling matrix. The object of filter diagnosis is to decide how to adjust the geometrical dimension of a filter by comparing the extracted coupling matrix $\tilde{M}$ to the object coupling matrix M_{obj}, where M_{obj} correspond to the desired response.

In a coupling matrix, only the nonzero elements are significant since they represent either the coupling coefficients or the shifting of resonant frequencies. To facilitate the discussion, we collect those nonzero elements to form a vector $\bar{y}$ and collect the geometrical parameters of the filter to form a vector $\bar{x}$. The relation between vector $\bar{y}$ and vector $\bar{x}$ can be denote as $\bar{y} = f(\bar{x})$. The object surrogate parameters can be denoted as $\bar{y}_{obj}$. The present geometrical parameters of the filter can be donated as $\bar{x}_0$ and its corresponding significant surrogate parameters can be donated as $\bar{y}_0$. The goal of optimization is to find an optimal geometrical parameter

$\bar{x}_{opt}$ to let the corresponding $\bar{y}_{opt}$ approach $\bar{y}_{obj}$ So, updating the vector $\bar{x}$ from

$\bar{x}_0$ to $\bar{x}_{opt}$ is the core of the optimization. The update method used in [13] is taken in

this dissertation and outlined in the following.

Before the surrogate model can be optimized, the sensitivities of the parameters

with respect to the geometrical parameters must be determined. This is done by using

finite difference approximation as described in the following four steps:

1. Calculate S-parameter of the filter structure in basis (non-ideal) position using the

   field solver and extract the characteristic parameters : $\widetilde{M}_{ij}^{\,basis}, \widetilde{M}_{ii}^{\,basis}$

2. Change first geometry parameter to $x_1 + \Delta x_1$, and repeat step 1➔ $\widetilde{M}_{ij}^{\,x_1+\Delta x}, \widetilde{M}_{ii}^{\,x_1+\Delta x}$

3. Repeat step2 for all other geometry parameters $x_2, x_3, ..., x_n$

The above information is to construct the first order Taylor expansion with respect to

the initial design (the initial design must be near the solution, otherwise the

convergence is not guaranteed).

4. The surrogate model can be approximated as

$$M_{ij}^{surrogate}(x_1 + d_1, x_2 + d_2, ..., x_n + d_n)$$

$$= \widetilde{M}_{ij}^{\,basis}(x_1, x_2, ..., x_n) + \sum_{k=1}^{n}\left(\frac{\widetilde{M}_{ij}^{\,x_k+\Delta x_k} - \widetilde{M}_{ij}^{\,basis}}{(x_k + \Delta x_k) - x_k}\right)d_k$$

$$= \widetilde{M}_{ij}^{\,basis}(x_1, x_2, ..., x_n) + \sum_{k=1}^{n}\left(\frac{\widetilde{M}_{ij}^{\,x_k+\Delta x_k} - \widetilde{M}_{ij}^{\,basis}}{\Delta x_k}\right)d_k$$

$M_{ij}^{basis}(x_1, x_2, ..., x_n)$, and $\left(\dfrac{M_{ij}^{\,x_k+\Delta x_k} - M_{ij}^{\,basis}}{(x_k + \Delta x_k) - x_k}\right)$ are determined in the first three steps.

The object of optimization is to determine the set $\{d_1, d_2, ... d_n\}$ which minimize

the difference between coupling matrix of surrogate model and object coupling matrix

get from standard filter synthesis. The cost function is defined as

$$U(d_1, d_2, ..., d_n)$$

$$= \sum_i (M_{ii}{}^{surrogate}(x_1 + d_1, x_2 + d_2, ..., x_n + d_n) - M_{ii}{}^{obj})^2$$

$$+ \sum_j \sum_i (M_{ij}{}^{surrogate}(x_1 + d_1, x_2 + d_2, ..., x_n + d_n) - M_{ij}{}^{obj})^2$$

The termination condition can be set by the value of cost function $U(d_1, d_2, ..., d_n)$ or

by the value of $\left\| \vec{d} \right\|^2$, where $\vec{d} = (d_1, d_2, \cdots, d_n)$. If the updated geometric parameters

do not exhibit the desired response, repeat the step1 to step 4 until the termination

condition is achieved. It usually takes several times for the optimization   since   in

most case the parameters of surrogate model are not a linear function of the geometry

parameters. However, this method is attractive since the step can easily be followed in

practice. Besides, testing the sensitivity is crucial since it not only give the

information of how to update the filter but also give a measure of how sensitive a

filter is.
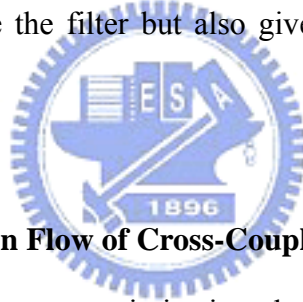
2.6 The Optimization Flow of Cross-Coupled Microwave Filters

In this section, the step by step optimization algorithm is given. The flow of the

optimization algorithm is shown in Figure 2-4. Each step is numbered.

1. Give a specification.

2. Generation of the ideal characteristic polynomials, $F(s), P(s), E(s)$ which satisfy

    specifications.

3. Synthesis of the ideal coupling matrix M which would be the object matrix we

    want to achieve in the optimization process.

The methods for the first three steps are given in section 2.3.

4. Computation of the initial dimensions of the microwave filter from the

    information of the ideal coupling matrix by segmentation method. Detail is given

in section 2.4.

5. Simulate the circuit in an EM simulator. Then, acquire N samples points of S-parameters, $S_{11}(s_i)$ $S_{21}(s_i)$ from the simulated response to reconstruct the rational model, $\widetilde{S}_{11}(s)$ and $\widetilde{S}_{21}(s)$, by Cauchy method. The detail is given in section 2.5.

6. Synthesize the coupling matrix corresponding to the rational functions $\widetilde{S}_{11}(s)$ and $\widetilde{S}_{21}(s)$. The obtained coupling matrix is $\widetilde{M}$. The synthesis technique is the same as that used in step 3.

7. Calculate the difference between the object coupling matrix M_{obj} and extracted coupling matrix $\widetilde{M}$. $\Delta M = \widetilde{M} - M_{obj}$.

8. Do the sensitivity test

9. Generate the correction vector, $\vec{d}$, for the geometric parameters of the filter. The methods for Step 7 to step 9 are given in section 2.5.

10. If the change of the geometric dimension is small enough (depending on the limitation of the fabrication), then stop the optimization procedure. Otherwise, change the geometric dimension to be $x_0 + \Delta x$ and repeat step 4 to step 10.
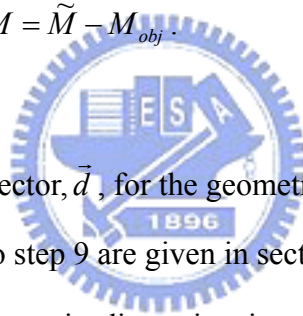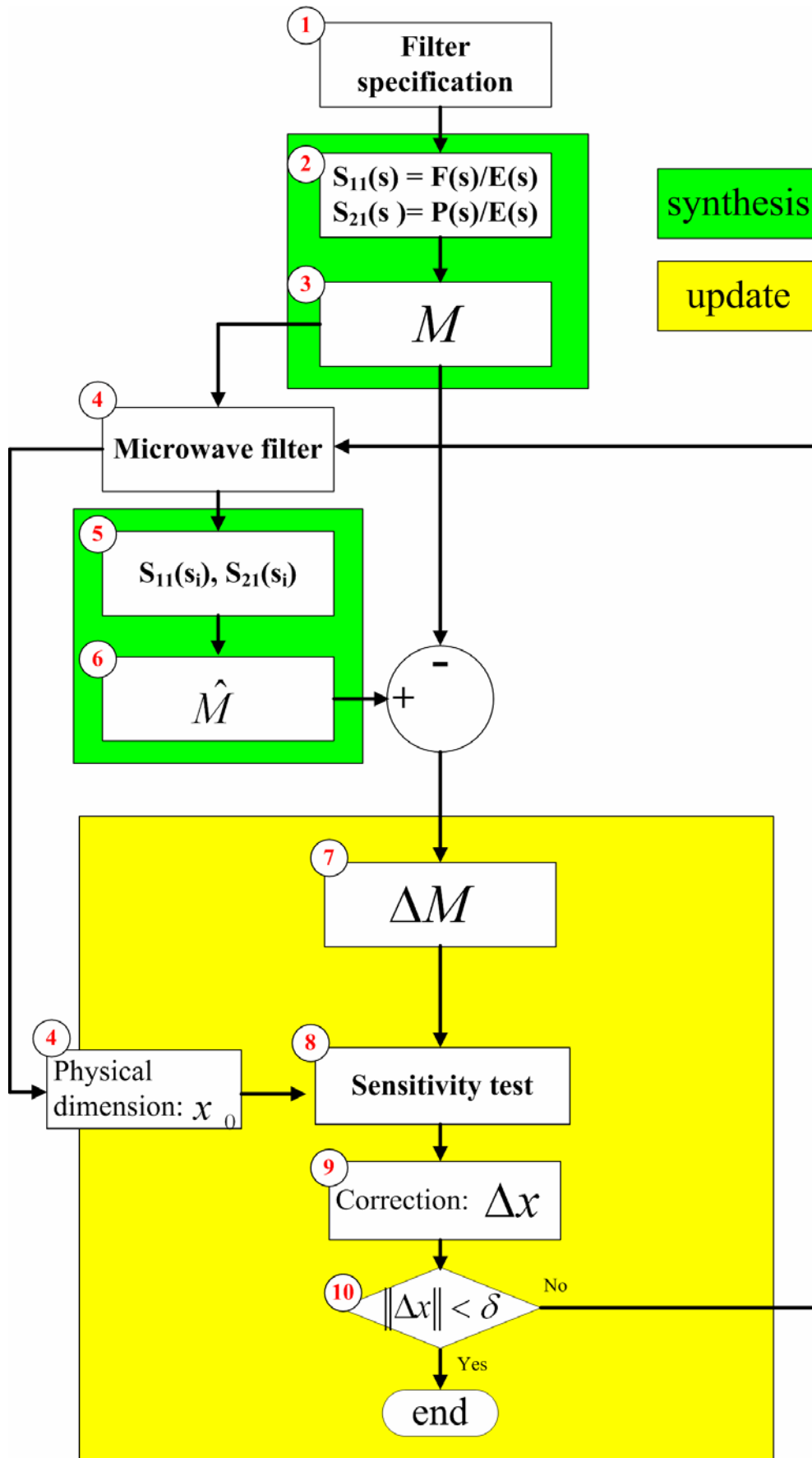
Figure 2-4 The flow of the optimization algorithm

2.7 Limitations of the Proposed Design Flow

The diagnosis and tuning process presented in this Chapter is only true for filters which can be described by the cross-coupled network shown in Figure 2-1(a). Thus, the correspondence between a physical layout and a cross-coupled prototype network, served as surrogate model, must be tested at first. This kind of test can be achieved in the process of sensitivity test. By observing the shift of the resonant frequencies or variation of coupling coefficients as the physical dimension is changed, we can tell whether the correspondence between the physical layout and surrogate model exists.

The surrogate model used in this dissertation can only apply for narrow band filters. The maximum fractional bandwidth may range from 10% to 40% depending on the type of resonators and coupling methods. The diagnosis and tuning process is not a "black box" process, which means knowing more about the design process would help do the parameter extraction and diagnosis. For example, when doing the design, the formula for lowpass to bandpass transformation may differ from design to design. When doing the diagnosis, we must map the frequency response from bandpass domain to lowpass domain by the bandpass to lowpass transformation. Definitely, the bandpass to lowpass transformation is the reverse operation of the lowpass to bandpass transformation used in the design. Thus, knowing the lowpass to bandpass transformation used in the design is important for the process of filter diagnosis.

Chapter 3 Cross-Coupled Filters with Source-Load Coupling

In this chapter, quadruplet microstrip filters with source-load coupling are proposed to achieve similar skirt selectivity and/or in-band flat group delay as that of a sixth-order canonical form or an extracted pole microstrip filter. Diagnosis method of unwanted effects such as asynchronous resonant frequencies and unwanted couplings, which often occurs in microstrip's open environment, is described in detail. A systematic design flow to implement a quadruplet microstrip source-load coupled filter with proper filter response is also provided. Two trial filters exhibited quasi-elliptical and flat group delay response are designed and fabricated. Both theoretical and experimental results are presented.

3.1 Introduction

High performance microstrip filters with high selectivity and linear in-band phase response has been studied over the last two decades [12]. Additional cross coupling between nonadjacent resonators are often used to generate finite transmission zeros for high selectivity, or linear phase. Naturally, the topology of the coupling network determines the number of finite transmission zeros, whereas the relative signs and magnitudes of the different coupling coefficients control the positions of finite transmission zeros. Some well-known topologies such as canonical form, cascade quadruplet (CQ), cascade trisection (CT) [12], and extracted-pole [27] have been successfully realized using microstrip. For instance, Jokela [28] has shown that sixth-order canonical form filter can achieve both high selectivity and linear phase, which is attractive when comparing the passband insertion loss with the CQ filter. In the CQ configuration, a minimal of eighth order is required to generate the real-frequency transmission zeros pair for selectivity, and real-axis transmission zeros

pair for linear phase. An eighth-order CQ filter introduces more insertion loss than that of a sixth-order canonical form filter, but it gains the independent control of transmission zeros where the design and tuning becomes easy. However, there are some disadvantages attached to the canonical structure as mentioned in [27]. Besides, according to Jokela's paper [28], the in-band flat group delay and skirt selectivity can be obtained simultaneously but a requirement of $M_{25}=0$ should hold for easy implementation. This requirement simplifies the coupling routine but greatly constrains the freedom of choice of filter response.

(a)

Controlling line of source-load coupling

Controlling line of source-load coupling

(b)
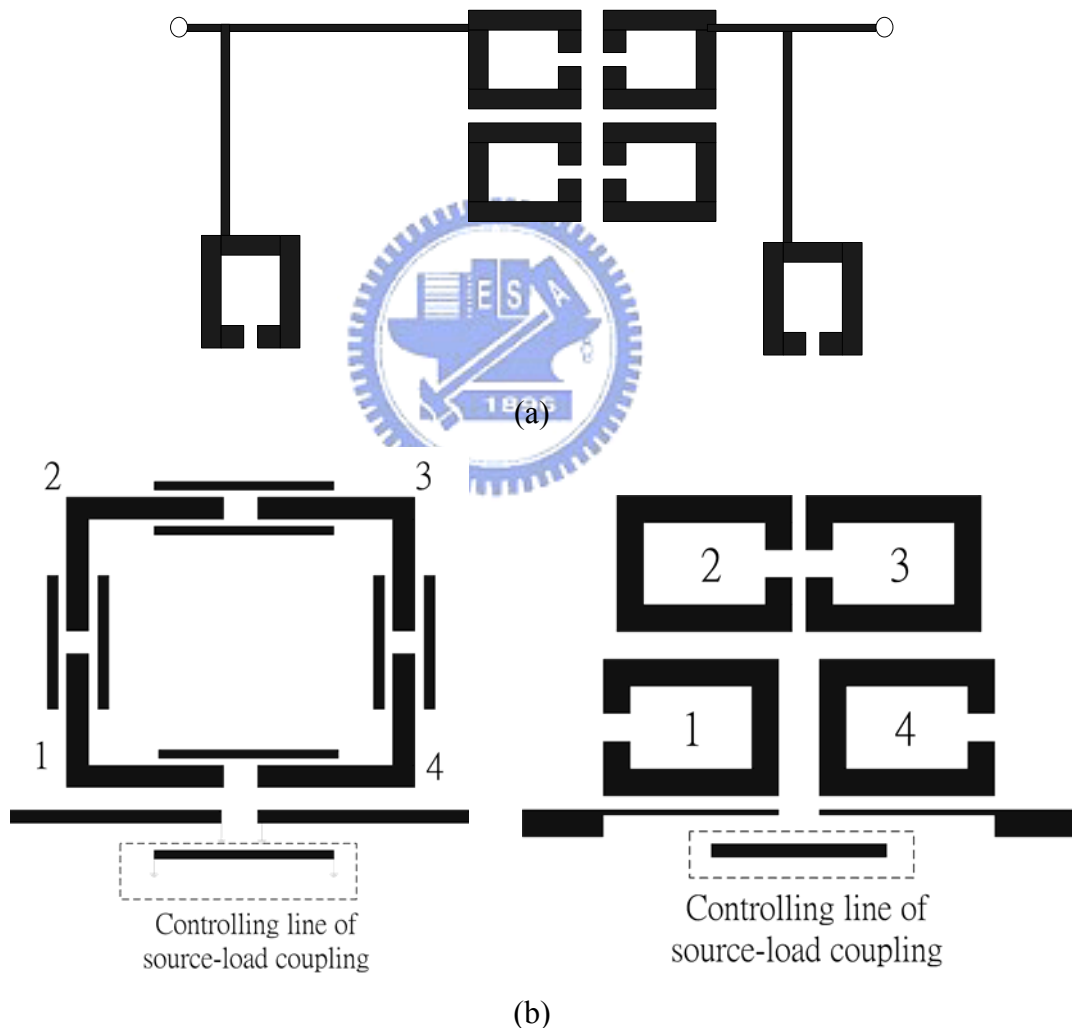
Figure 3-1 Microstrip implementation for (a) sixth-order quasi-elliptic filter with linear phase response using extracted-pole technique (b) proposed quadruplet filter with source-load coupling.

To avoid the disadvantage of the canonical form filter, Yeo et al. [27] proposed the extracted-pole microstrip filter as shown in Figure 3-1(a) where the concept is originally used in a waveguide filter. The extracted-pole filter depicts better control of finite transmission zeros than that of canonical form filter, but it is relatively large due to the need of phase shifters. Here, we propose the fourth-order filter with source-load coupling, as shown in Figure 3-1(b), to generate two pairs of transmission zeros as sixth-order canonical form or eighth-order CQ filter does. The synthesis methods of the symmetric resonator filters with source-load coupling are well documented in literatures [23, 29]. Coupling diagram of the symmetric fourth-order filter with source-load coupling is shown in Figure 3-2(a). However, in realistic implementation of microstrip filter, the unwanted cross couplings always exist and lead the coupling route becomes complicated as shown in Figure 3-2(b). To identify all parameters corresponding to unwanted cross couplings, frequency alignment, and source-load coupling, powerful CAD tools are needed. Recently, an elegant diagnosis method is proposed to help designing of symmetric coupled-resonator filters [17]. However, the method in [17] has not taken the source-load coupling into account. In this chapter, we propose a diagnosis scheme, which is applicable to arbitrary topologies with or without source-load coupling.

This chapter is organized as follows. In section 3.2, the phenomenon of asymmetric responses of quadruplet filter is discussed and design guidelines are provided. In section 3.3, the CAD method is introduced to extract the coupling matrix with prescribed topologies. In section 3.4, the diagnosis method is applied to designing the proposed filter. Both theoretical and experimental results are presented for comparison.
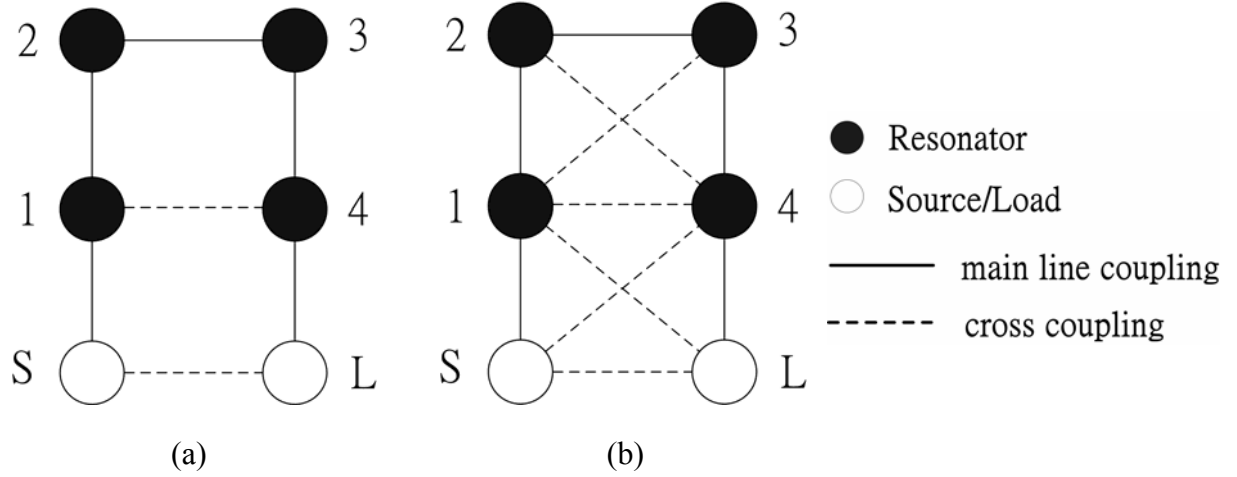
Figure 3-2 Coupling and routing scheme of symmetric cross-coupled quadruplet filter with source-load coupling (a) ideal case, (b) including the unwanted diagonal cross couplings.

3.2 Asymmetric Frequency Responses

The fourth order cross-coupled quadruplet filter is the well-known building block for generating a pair of finite transmission zeros, which can improve skirt selectivity or in-band group delay flatness. The conventional coupling diagram of quadruplet filter is similar to Figure 3-2(a) except source-load coupling is excluded. The explicit relation between the finite transmission zeros and the coupling coefficients of it can be expressed in lowpass domain as follows

$$\Omega^2 = M_{23}{}^2 - \frac{M_{12}M_{23}M_{34}}{M_{14}} \qquad (3\text{-}1)$$

In Eq. (3-1), Ω is the normalized frequency and M_{ij} are the coupling coefficients in lowpass prototype. The relation between Ω and actual frequency f is $\Omega = (f_0/\Delta f)(f/f_0 - f_0/f)$, where f_0 is the center frequency of the filter, and Δf is the bandwidth of the filter. For improving the skirt selectivity of the filter, the finite transmission zeros are put in real frequency axis and the relation $M_{12}M_{23}M_{34}M_{14} < 0$ must be satisfied. On the other hand, to generate the imaginary frequency transmission zeros for in-band group delay flatness, $M_{12}M_{23}M_{34}M_{14} > 0$ must hold.

However, the unwanted diagonal cross couplings always exist in the microstrip cross-coupled filter due to microstrip's open environment. Both unwanted diagonal cross couplings and asynchronous resonant frequencies of resonators would distort the ideal symmetric response of the reflection coefficient $|S_{11}|$ and transmission coefficient $|S_{21}|$. In [17, 30], the authors have shown how to extract the unwanted diagonal cross couplings and to adjust the resonant frequencies of resonators to compensate the distortion of return loss for a skirt selectivity filter. However, in the case of flat group delay filter we find that the unwanted cross couplings seriously degrade the flatness of in-band group delay and should be suppressed to a negligible level. Figure 3-3 shows some examples to demonstrate the phenomena. In Figure 3-3(a), an ideal response of the synchronous-tuned quadruplet filter with symmetric finite transmission zeros at $\Omega = \pm 2$ is shown. If the values of unwanted cross couplings M_{13} and M_{24} are equal to -0.06, the frequency response after adjusting the resonant frequencies is shown in Figure 3-3(b). It can be observed that the transmission zeros drift slightly and the height of $|S_{21}|$ bumps tilts. In many practical applications this change of $|S_{21}|$ is acceptable. However, in the case of flat group delay filter as shown in Figure 3-3(c), the finite transmission zeros are located at $\Omega = \pm j1.55$. Set $M_{13}=M_{24}=-0.06$, which is similar to the previous case, and adjust the resonant frequency to optimize the in-band return loss, we would get the results as shown in Figure 3-3(d). It is obvious that the response of $|S_{21}|$ has negligible change but the in-band group delay tilts seriously. In most of linear phase filter applications this tilting of group delay is not allowed.

From the above discussion, some observations are summarized as follows. First, higher order symmetric filters in folded form are hard to design since tuning of resonant frequencies is needed for compensating the in-band return loss distortion. Besides, controlling more than one pair of finite transmission zeros and keep the

return loss good is even more difficult. On the contrary, the source-load coupling has extremely small contribution to the passband response and is much easier to implement extra pair of transmission zeros. In other words, we can control the additional pair of finite transmission zeros and keep the original finite transmission zeros nearly unchanged by merely adjusting source-load coupling without fine-tuning other portion of the filter. Second, the unwanted cross coupling is surprisingly harmful to the performance of in-band flap group delay response. The only way to implement a good in-band flap group delay filter is to avoid the unwanted cross coupling.
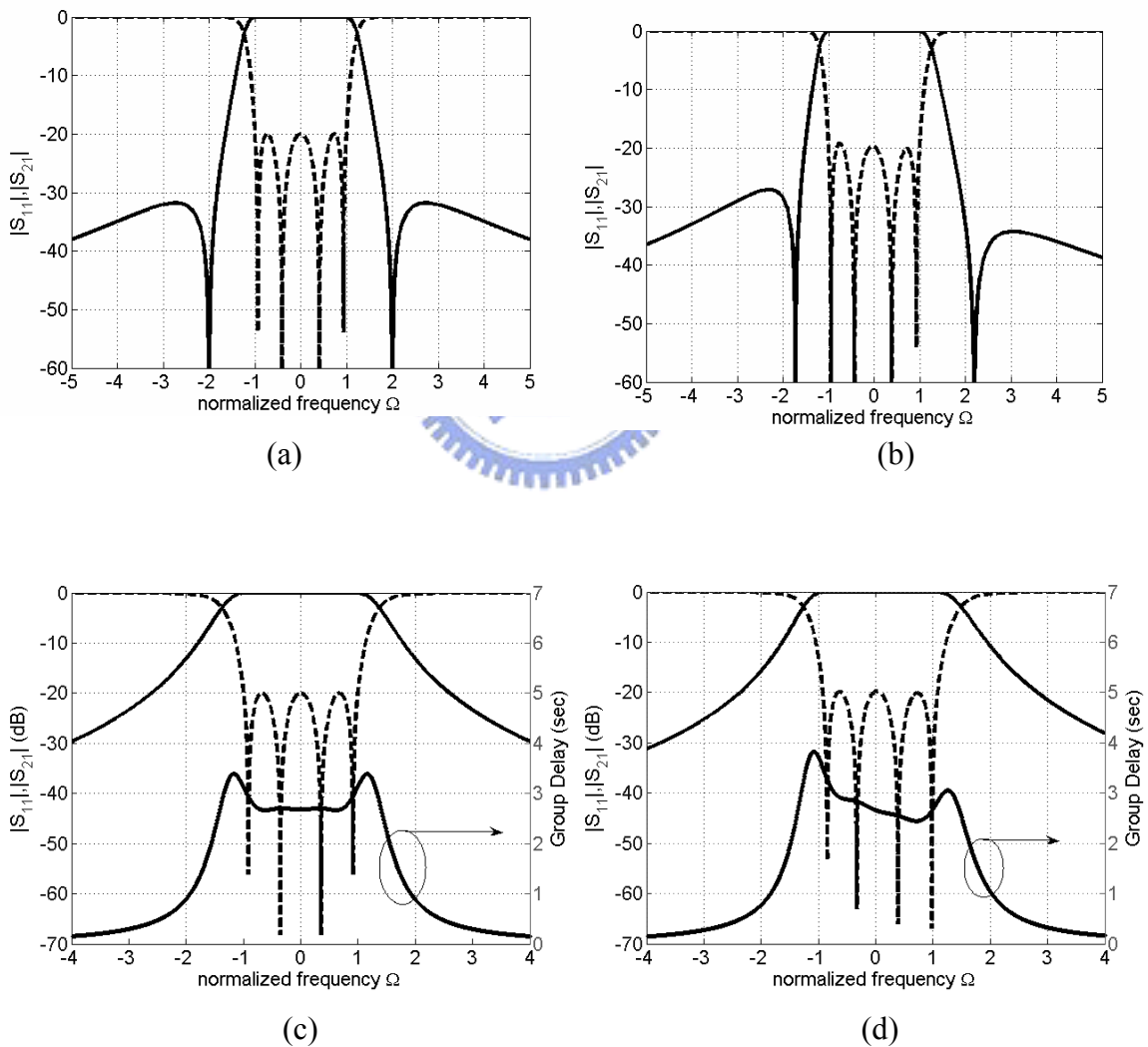
Figure 3-3. Quadruplet filters with (a) ideal quasi-elliptical response, (b) including unwanted cross coupling, (c) ideal flap group delay response, and (d) including unwanted cross coupling.

34

3.3 CAD Methods for Filter Diagnosis

In previous section, we ignore the coupling term, M_{L1}, M_{S4}, and M_{SL} to facilitate the discussion and give some design guidelines for the quadruplet filter. To get further insight about the correspondence between the proposed physical layout in Figure 3-1(b) and the coupling diagram shown in Figure 3-2(b), we introduce the CAD tool to extract the entire filter network parameters from the EM simulated results in this section.

The extraction method proposed here has two major steps. In the first step, we extract the $(N+2) \times (N+2)$ transversal coupling matrix, for the filter of order N, from the EM simulated response as Alejandro et al. have done in [18]. In [18], the authors apply the Cauchy method to get the rational polynomial approximation of $S_{11}(\Omega)$ and $S_{21}(\Omega)$ from the EM simulated results, and then generate the corresponding transversal coupling matrix by the method proposed by Cameron [9]. Extracting the coefficients of the rational function by Cauchy method is attractive since there is no need of calibrating the reference plane as that in [16, 17]. In this step, we would get the transversal coupling matrix like the follows (take the proposed quadruplet filter for instance).

$$M = \begin{bmatrix} 0 & M_{S1} & M_{S2} & M_{S3} & M_{S4} & M_{SL} \\ M_{S1} & M_{11} & 0 & 0 & 0 & M_{1L} \\ M_{S2} & 0 & M_{22} & 0 & 0 & M_{2L} \\ M_{S3} & 0 & 0 & M_{33} & 0 & M_{3L} \\ M_{S4} & 0 & 0 & 0 & M_{44} & M_{4L} \\ M_{SL} & M_{1L} & M_{2L} & M_{3L} & M_{4L} & 0 \end{bmatrix} \qquad (3\text{-}2)$$

The coupling matrix is related to the responses of $S_{11}(\Omega)$ and $S_{21}(\Omega)$ via the following equation

$$S_{11} = 1 + 2j[A^{-1}]_{11} \qquad (3\text{-}3)$$

$$S_{21} = -2j[A^{-1}]_{N+2,1} \qquad (3\text{-}4)$$

Here, $A = \Omega[U_0] + [M] - j[R]$, $\Omega = (f_0/\Delta f)(f/f_0 - f_0/f)$, $[U_0]$ is similar to the (N+2)×(N+2) identity matrix except that $[U_0]_{11} = [U_0]_{N+2,N+2} = 0$, $[M]$ is the (N+2)×(N+2) symmetric coupling matrix, f_0 is the center frequency of the filter and Δf is its bandwidth, and $[R]$ is the diagonal matrix $[R] = diag\{1, R_{loss}, ..., R_{loss}, 1\}$. R_{loss}, which value is $\dfrac{f_0}{\Delta f}\dfrac{1}{Q_u}$, accounts for the resonator loss. Q_u is the unloaded quality factor of the resonator. Note that R_{loss} is set to be zero in the filter parameter extraction process since the assumption of lossless network must be satisfied in the extraction of $S_{11}(\Omega)$ and $S_{21}(\Omega)$ [18]. After getting the coupling matrix of prescribed topology, one can put the R_{loss} back to calculate the practical filter response.

In the second step, the transversal coupling matrix is transformed into the prescribed topology. It is known that by applying the multiple similarity transformations to the coupling matrix, one can get the equivalent coupling matrix with the same electrical performance as the original coupling matrix. Some methods may be found in the literature, which describe how to find the sequence of rotations (and the corresponding angles) required for obtaining a few specific topologies [8, 9, 31]. However, to the best of authors' knowledge, how to transfer the transversal coupling matrix into the topology shown in Figure 3-2 is still not known. Fortunately, one can apply the numerical optimization technique to determine the sequence and rotation angles of the multiple similarity transformations as Macchiarella has done in [25]. The method, reported in [25], works well for the synthesis of a filter with order up to 12. The initial coupling matrix being used in [25] is the canonical folded form or

generic form, which corresponds to the filter of order N with maximum of N-2 finite transmission zeros.

We apply the optimization method as proposed by Macchiarella to transform the transversal coupling matrix to the prescribed topology as shown in Figure 3-2 (b). Note that using the transversal coupling matrix as initial coupling matrix extends the method of [25] applicable to a filter of order N with maximum of N finite transmission zeros. In the follows, we take the quadruplet filters as an example since they will be used in the next section. Applying the multiple similarity transformations to the transversal coupling matrix M in Eq. (3-2), we would get the new coupling matrix $\overline{M}$ and $\overline{M}$ can be expressed as

$$
\begin{aligned}
\overline{M} &= (R_{23} \cdot R_{24} \cdot R_{25} \cdot R_{34} \cdot R_{35} \cdot R_{45}) \\
&\quad \cdot M \cdot (R_{45}{}^t \cdot R_{35}{}^t \cdot R_{34}{}^t \cdot R_{25}{}^t \cdot R_{24}{}^t \cdot R_{23}{}^t) \\
&= S(\vartheta_{23}, \vartheta_{24}, .., \vartheta_{45}) \cdot M \cdot S^t(\vartheta_{23}, \vartheta_{24}, .., \vartheta_{45})
\end{aligned}
\tag{3-5}
$$

where $R_{ij}(\vartheta_{ij})$ is the rotation matrix of order N+2 corresponding to pivot (i, j), and angle ϑ_{ij}. $R_{ij}(\vartheta_{ij})$ is defined as follows:

$$
\begin{aligned}
R_{ij}(i,i) &= R_{ij}(j,j) = \cos(\vartheta_{ij}) \\
R_{ij}(i,j) &= -R_{ij}(j,i) = \sin(\vartheta_{ij}) \\
R_{ij}(k,k)\big|_{k \neq i,j} &= 1 \qquad , (i < j) \neq 1, N+2 \\
R_{ij}(k,i)\big|_{k \neq i,j} &= 0 \qquad , R_{ij}(j,k)\big|_{k \neq i,j} = 0
\end{aligned}
\tag{3-6}
$$

The cost function U for the topology shown is Figure 3-2(b) is defined as

$$
\begin{aligned}
&U(\vartheta_{23}, \vartheta_{24}, .., \vartheta_{45}) \\
&= |\overline{M}_{S2}|^2 + |\overline{M}_{S3}|^2 + |\overline{M}_{2L}|^2 + |\overline{M}_{3L}|^2 \\
&\quad + |\overline{M}_{11} - \overline{M}_{44}|^2 + |\overline{M}_{22} - \overline{M}_{33}|^2 + |\overline{M}_{13} - \overline{M}_{24}|^2 + |\overline{M}_{S4} - \overline{M}_{1L}|^2
\end{aligned}
\tag{3-7}
$$

The first four terms in the cost function indicate which cross coupling elements must vanish while the last four terms indicate the symmetry of the coupling route. If the

symmetric condition was not included in the cost function, we might get the non-physical solutions. In the practical implementation of the minimization procedure, the Gauss-Newton method is used to determine the rotation angles $(\vartheta_{23}, \vartheta_{24}, .., \vartheta_{45})$, which minimize the cost function U. Once the rotation angles are determined, we can get the corresponding coupling matrix $\overline{M}_{model}$.

It should be mentioned that the proposed extraction scheme could be applied to arbitrary topologies once their feasibility has been assessed. Depending on the setting of different cost functions, different topologies can be obtained after multiple similarity transformations. For the filter of order N, one can choose the $N \times N$ coupling matrix or $(N+2) \times (N+2)$ coupling matrix as the initial coupling matrix, depending on the maximum number of finite transmission zeros. If the maximum number of finite transmission zeros is less than N-2, either $N \times N$ coupling matrix or $(N+2) \times (N+2)$ extended coupling matrix can be chosen. Otherwise, the $(N+2) \times (N+2)$ transversal coupling matrix should be applied.

3.4 Filter Design Examples

In this section, we will develop two novel quadruplet filters with source-load coupling and utilize the CAD tool introduced in previous section to do diagnosis of proposed filters. The design procedures are summarized as following. Follows the synthesis method described in [9], one would get the ideal coupling matrix with the topology shown in Figure 3-2(a). The corresponding spacing between every resonator is determined through the characterization of the couplings as described in chapter 8 of [12]. After EM simulation, the values of unwanted cross couplings are extracted. Fixing the values of unwanted couplings, the optimization technique is then applied to determining the required frequency shifts of resonators and the change of other coupling elements to compensate the distortion of $|S_{11}|$[17]. Two examples are given to show the design procedures. The first filter, shown in Figure 3-4, is designed to

have two pairs of real frequency transmission zeros at normalized frequency $\Omega = \pm 2, \pm 6$ for skirt selectivity. The second filter, shown in Figure 3-7, is intended to have one pair of real frequency transmission zero at normalized frequency $\Omega = \pm 4.5$ for selectivity and another pair at $\Omega = \pm j1.55$ for in-band flap group delay. The center frequency, the fractional bandwidth, and the maximum in-band return loss of both filters are 2.4GHz, 3.75% and 20dB respectively. The filters are built on a 20-mil-thick Rogers RO4003 substrate with $\varepsilon_r = 3.38$, $\tan\delta = 0.0021$. The commercial EM simulation software Sonnet 9.0 [32] is used to perform the simulation.
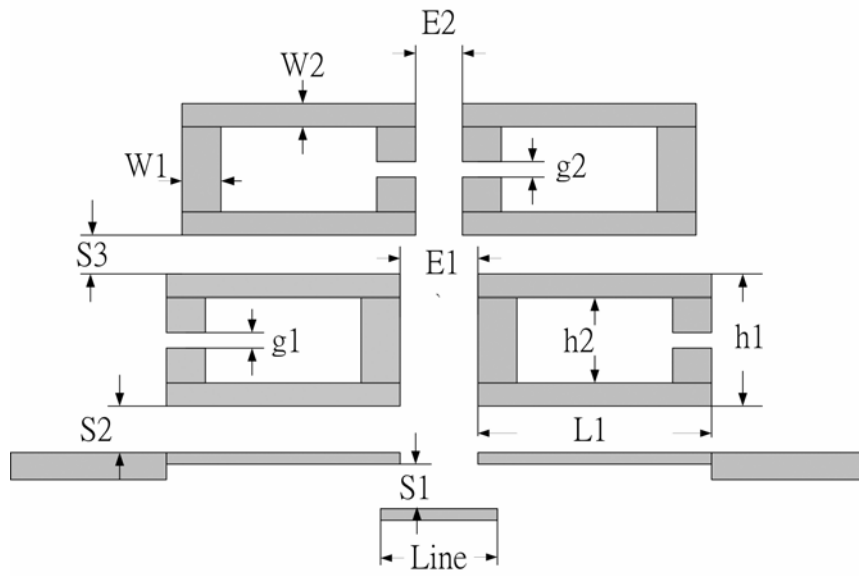
(a)
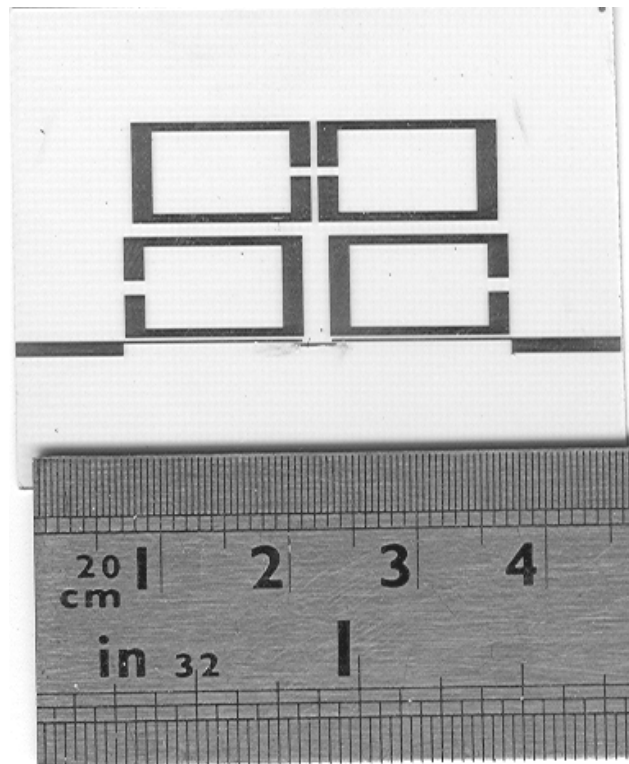
(b)

Figure 3-4. (a) quadruplet filter with the capacitive S/L coupling controlled by the controlling line (b) photograph of the fabricated filter with dimension (in mils) S1=4, S2=8, S3=41, E1=90, E2=20, W1=64, W2=30, h1=310, h2=250, g1=42, g2=26, Line=160

A. Quadruplet filter with two pair of real frequency transmission zeros

In order to see the effect of the controlling line, we exclude the controlling line at first and adjust the quadruplet filter with the previously mentioned procedures. After extracting the unwanted diagonal cross couplings of the quadruplet filter and compensate them, we would get the EM simulated response shown as circles in Figure 3-5(a). Using the CAD tool developed in section 3.3 together with the cost function defined in Eq. (3-7), the extracted coupling matrix M_1 (with the value of cost function $U = 10^{-7}$) is obtained as following.

$$
M_1 = \begin{bmatrix}
0 & 1.0089 & 0 & 0 & 0 & 0 \\
1.0089 & -0.0021 & 0.8514 & -0.0090 & -0.1436 & 0 \\
0 & 0.8514 & 0.0317 & 0.7380 & -0.0090 & 0 \\
0 & -0.0090 & 0.7380 & 0.0317 & 0.8514 & 0 \\
0 & -0.1436 & -0.0090 & 0.8514 & -0.0021 & 1.0089 \\
0 & 0 & 0 & 0 & 1.0089 & 0
\end{bmatrix}
$$

The corresponding response of M_1 is also shown in Figure 3-5(a) as solid line for comparison.

After adding the controlling line of source-load coupling, the EM simulated response is shown in Figure 3-5(b) as circles. The corresponding extracted coupling matrix M_2 (with the value of cost function $U = 10^{-7}$) is

$$
M_2 = \begin{bmatrix}
0 & 1.0189 & 0 & 0 & 0.0032 & 0.0035 \\
1.0189 & -0.0120 & 0.8572 & -0.0057 & -0.1420 & 0.0033 \\
0 & 0.8572 & 0.0204 & 0.7390 & -0.0058 & 0 \\
0 & -0.0057 & 0.7390 & 0.0204 & 0.8571 & 0 \\
0.0032 & -0.1420 & -0.0058 & 0.8571 & -0.0120 & 1.0189 \\
0.0035 & 0.0033 & 0 & 0 & 1.0189 & 0
\end{bmatrix}
$$

The corresponding response of coupling matrix M_2 is also shown in Fig. 5(b) as solid line.
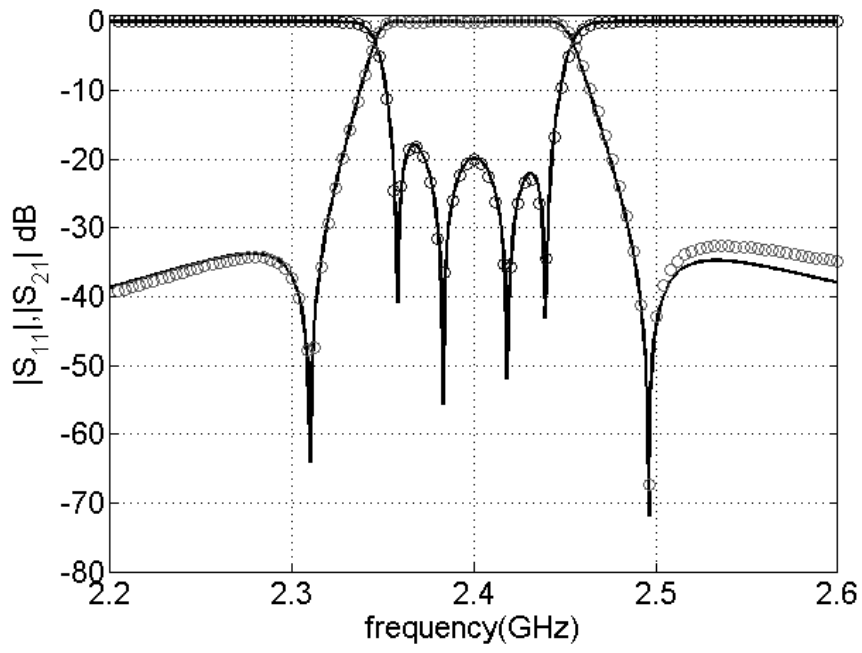
(a)
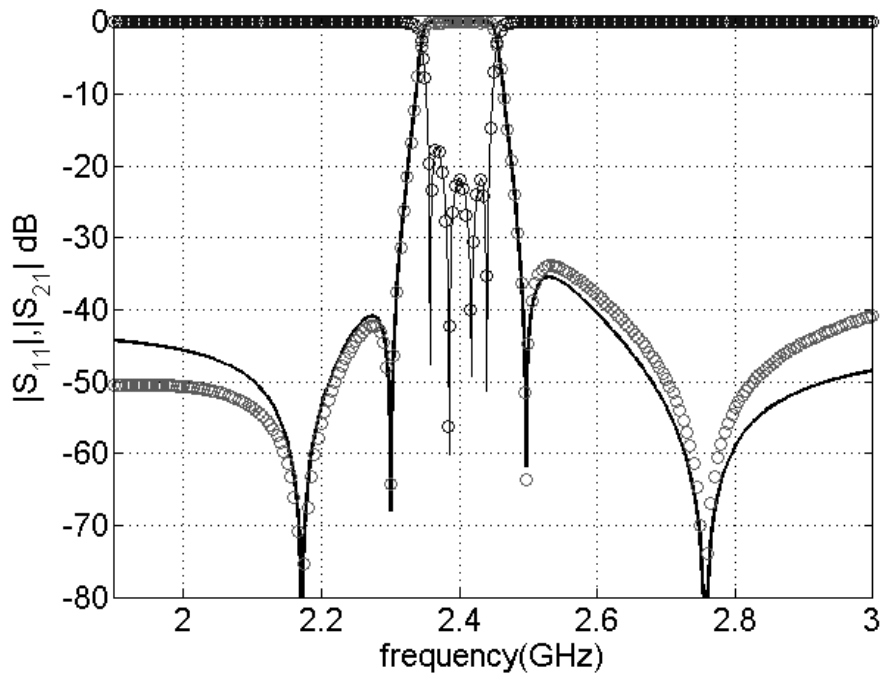
(b)

Figure 3-5. (a) response of quadruplet filter (b) response of quadruplet filter with controlling line of source-load coupling. Circle: EM simulated results; solid line: circuit model.

Comparing M_1 and M_2, it can be easily observed that the introduction of controlling line is only a small perturbation to the original quadruplet. In other words, the controlling line has negligible contribution to the passband response. Besides, the existence of the tiny unwanted diagonal cross couplings M_{S4} and M_{L1} in matrix M_2 explain why the response is asymmetric because the response becomes symmetric as the M_{S4} and M_{L1} are excluded from M_2. Taking matrix M_2 into equation (3) and (4), and setting unloaded quality factor $Q_u = 150$, the results are shown in Figure 3-6 as dashed lines. The measured responses are also shown in Figure 3-6 as solid lines. Comparing the circuit model responses with measured responses an excellent fit can be observed except some frequency drift toward lower frequency.
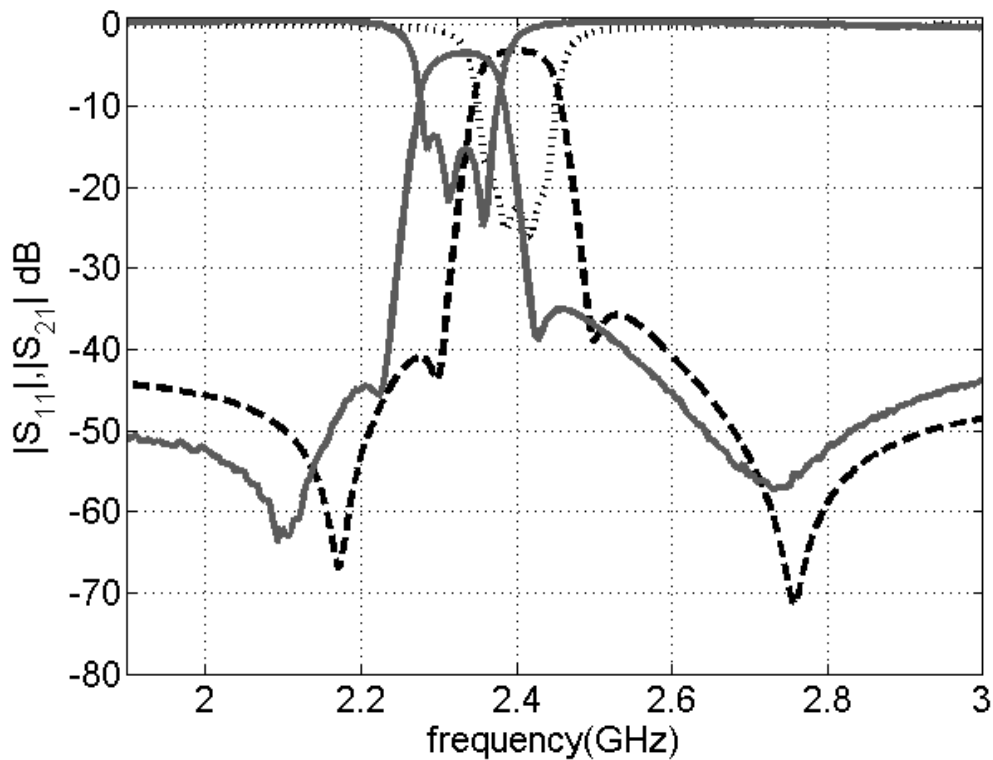
Figure 3-6. Experimental and circuit model results. Solid line: experimental results, dashed line: circuit model including loss term.
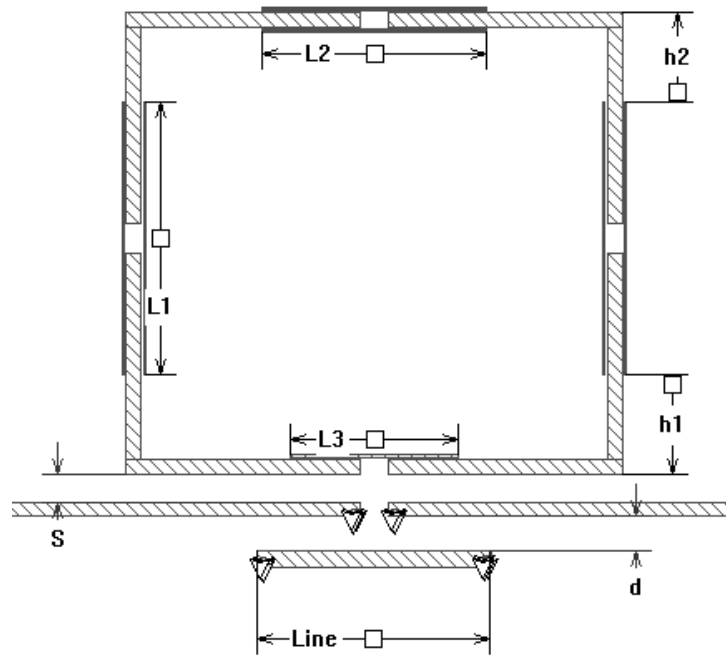
(a)
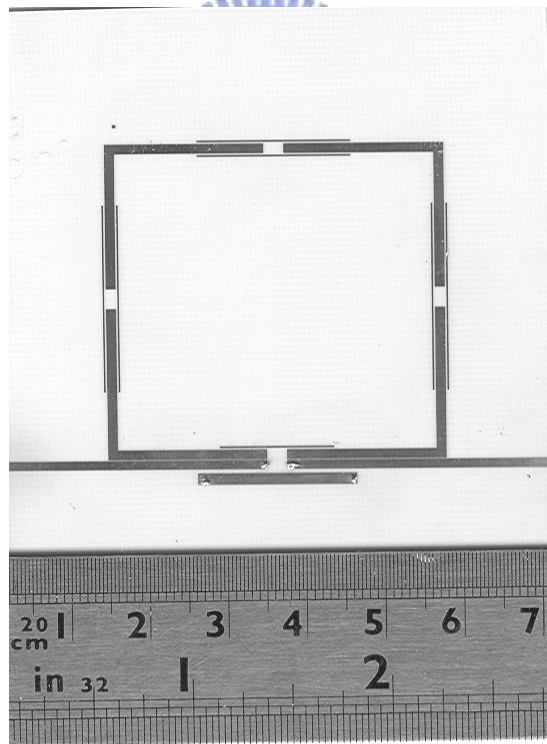
(b)

Figure 3-7. (a) quadruplet filter with the inductive S/L coupling controlled by the controlling line (b) photograph of the fabricated filter with dimension (in mils) d=20, Line=800, s=4, L3=575, L1=940, L2=770, L3=575, h1=340, h2=304.

B. Quadruplet filter for flap group delay and skirt selectivity

As mentioned in section 3.2, the unwanted cross couplings M_{13} and M_{24} would destroy the in-band group delay flatness. To reduce the strength of unwanted couplings, we use the L-shaped resonator and arrange the resonators in square to maximize the distance between diagonal resonators as shown in Figure 3-7. The coupled lines with length L_1, L_2, and L_3 control the strength of coupling between L-shape resonators respectively. The inductive source-load coupling is effectively controlled by changing the length of controlling line with both ends connected to ground. Resonant frequencies of resonators can be tuned by adjusting the length h1 and h2. Following similar procedures in the previous design, we can get the extracted coupling matrix M_3 as

$$M_3 = \begin{bmatrix} 0 & -1.0945 & 0 & 0 & 0.0052 & 0.0099 \\ -1.0945 & 0.3663 & -1.0093 & -0.0274 & -0.1681 & 0.0054 \\ 0 & -1.0093 & 0.3402 & -0.6241 & -0.0272 & 0 \\ 0 & -0.0274 & -0.6241 & 0.3404 & -1.0089 & 0 \\ 0.0052 & -0.1681 & -0.0272 & -1.0089 & 0.3664 & -1.0936 \\ 0.0099 & 0.0054 & 0 & 0 & -1.0936 & 0 \end{bmatrix}$$

The corresponding response of M_3 fit well with the EM simulated results as shown in Figure 3-8. Taking M_3 into equation (3-3) and (3-4) and setting unloaded quality factor $Q_u = 150$, we have the filter responses shown in Figure 3-9 as doted lines. The experimental results are also shown in Figure 3-9 as solid lines that they are similar to the circuit model results except similar frequency drift as the former example. The frequency drift might come from the discrepancy of the substrate dielectric const. In other words, the dielectric const ε_r might be greater than data sheets' value 3.38.

(a)

(b)
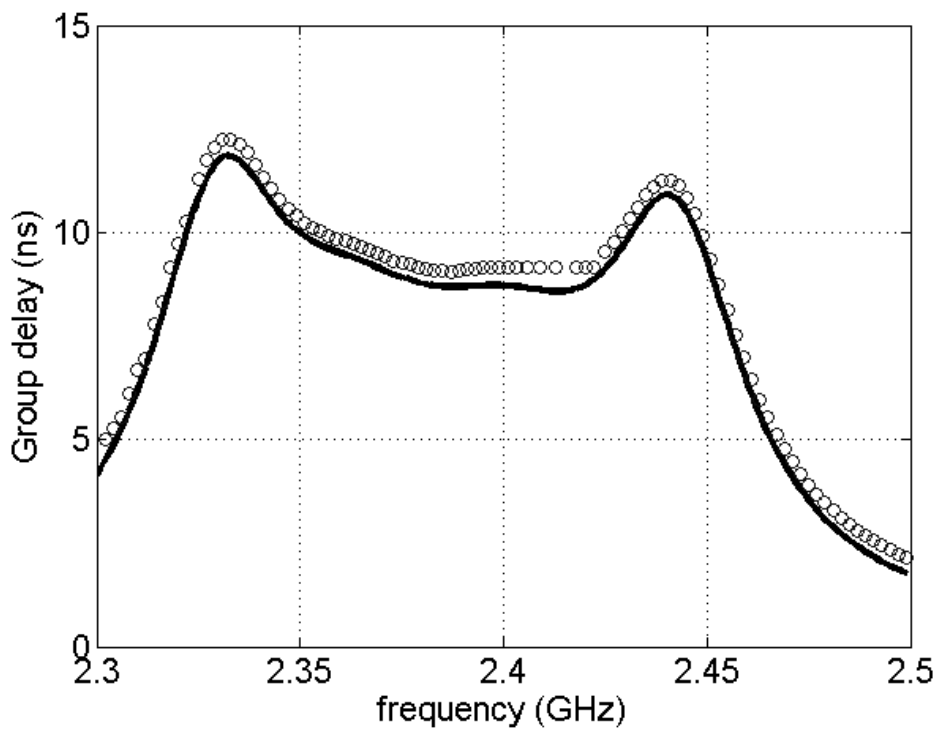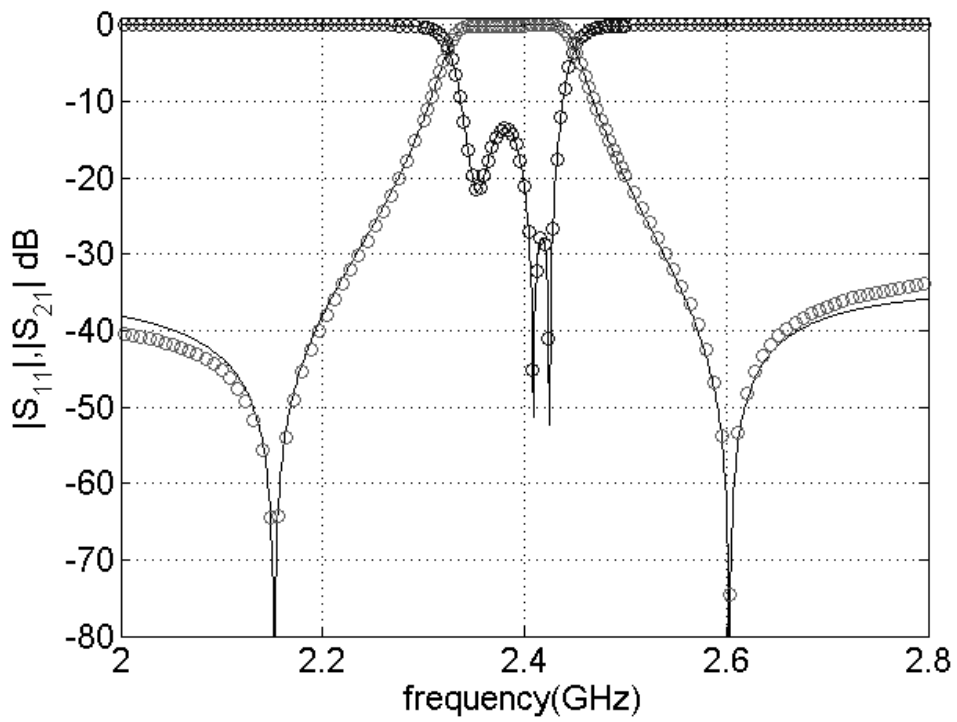
Figure 3-8. Response of quadruplet filter with controlling line of source-load coupling.

Circle: EM simulated results; solid line: circuit model.

From above two examples, we can conclude that the controlling line of source-load coupling can effectively adjusting the position of finite transmission zeros with negligible perturbation to the passband. It is suggested that one can design the symmetric folded coupled-resonator filter at first and then adds the controlling line to control the source-load coupling without fine-tuning other portion of the filter. The design method may apply to higher order symmetric folded coupled-resonator filter.
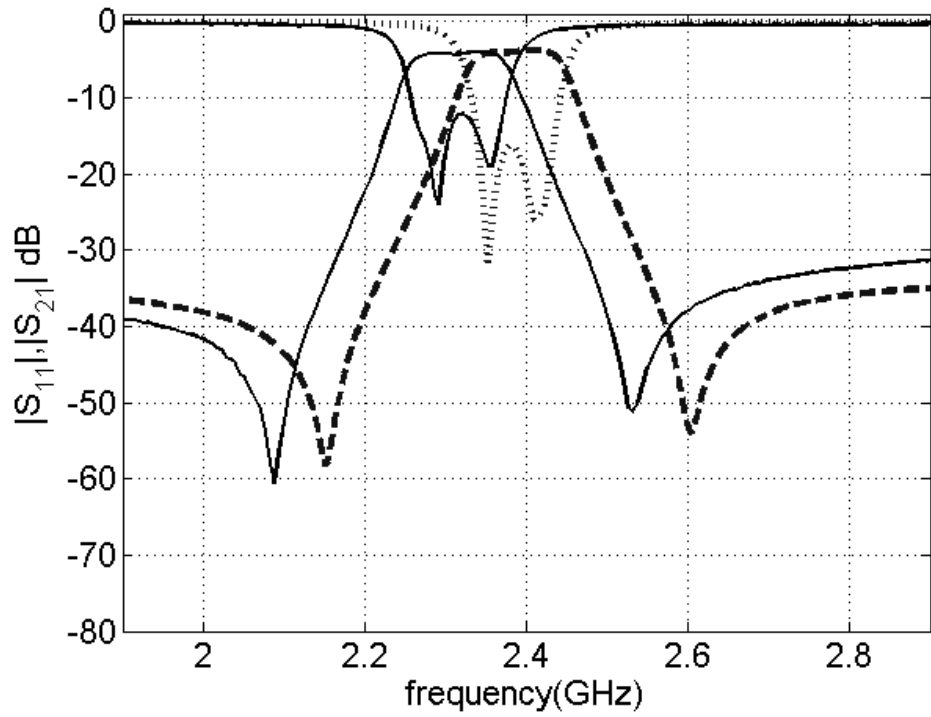
(a)
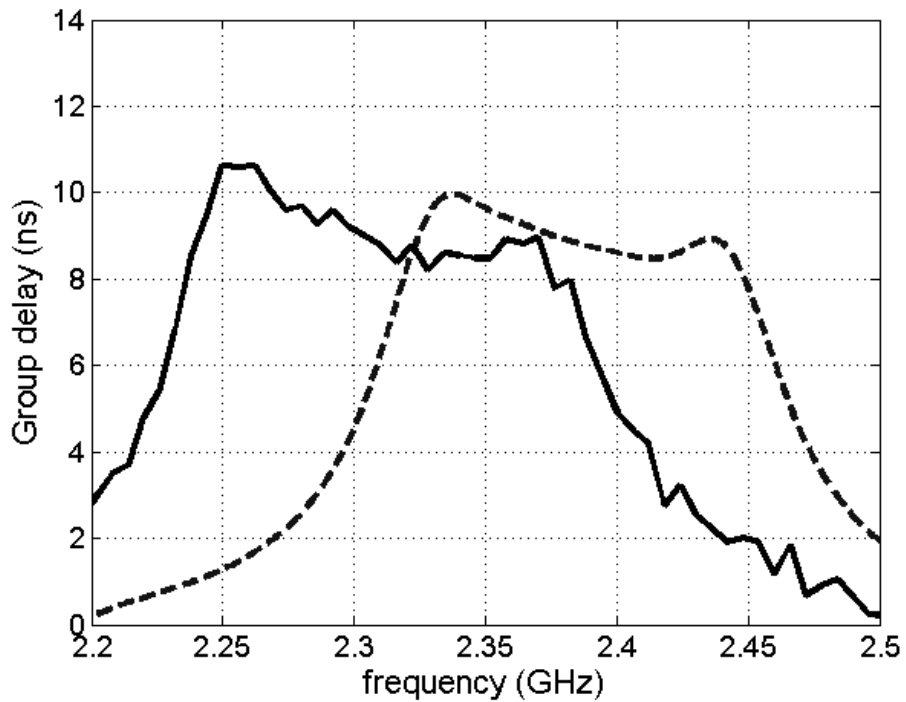
(b)

Figure 3-9. Experimental and circuit model results (a) return loss and insertion loss (b) group delay. Solid line: experimental results, dashed Line: circuit model including loss term.

Chapter 4 Modified Parallel-Coupled Filter with Two Independently Controllable Upper Stopband Transmission Zeros

In this chapter, a microstrip cross-coupled filter with two independently controllable transmission zeros on upper stopband is presented. The initial filter structure is a conventional Chebyshev-response parallel-coupled filter that can be easily realized by the analytical method. The newly proposed coupling/shielding lines can effectively control the cross and main couplings without changing the original filter layout. This approach allows designer to eliminate tedious segmentation method, which is usually used to establish the relation between coupling coefficient and physical distance between resonators. A 3-order filter is designed and fabricated for demonstration.

4.1 Motivation

The cross-coupled microstrip filters have been extensively studied in recent years. Research efforts are focused mainly on two aspects. One is finding new shape of resonator. Another is developing novel synthesis methods, which enable designer to arrange resonators in different ways to achieve advanced response such as generalized Chebyshev response. Resonators with different shape, such as loop [11], hairpin [33], and patch [34], have been arranged in specific topologies for improving the selectivity or in-band group delay of filters. Some widely applied topologies are cascade quadruplet (CQ) and cascade trisection (CT). Besides CQ and CT, novel synthesis methods have leaded to novel topologies containing couplings of source/load to multi-resonator [23, 35]. In a word, novel physical structures accompanied with advanced synthesis methods have enriched the possibilities of a microstrip filter. However, the designs of cross-coupled filters are not as straightforward as conventional ones such as parallel-coupled filter, end-coupled filter, etc. In the design

of cross-coupled filter, there are no explicit expressions to relate synthesized electrical parameters to physical dimensions of a filter. Therefore, when designing a cross-coupled filter, the first step is to synthesize a coupling matrix. Then, use segmentation method to relate coupling strength to physical distance between resonators [12]. The drawback of the design procedures is that once the size of resonator changes, designers must redo the segmentation method to find physical dimensions of filters. Moreover, since segmentation method can provide only approximated dimensions of filter, fine tunings are always needed.

To skip the tedious designing routine of segmentation method, we propose an easy designing procedure to realize a filter with two upper stopband transmission zeros. The basic structure of proposed filter utilizes the conventional microstrip parallel-coupled filter [36], as shown in Figure 4-1(a), to serve as the initial design. Then, vertically flip feeding lines of the source and the load as shown in Figure 4-1(b). As described by Chang and Itoh in [37] that the physical dimensions keep the same during flipping. Next, adding the proposed coupling/shielding lines at the ends of input and output feed lines as depicted in Figure 4-1(b). Figure 4-1(c) shows the coupling diagram of Figure 4-1(b) and the coupling elements can be optimized and fine-tuned by the method given in Chapter 2. The proposed layout of the filter is somewhat similar to those of [37]. Nevertheless, the strengths of couplings M_{S2} and $M_{L,n-1}$ in the filters described in [37] are extremely weak and not taken them into account during filter design procedures. In this paper, we introduce these coupling/shielding lines to control the strength of M_{S2} and $M_{L,n-1}$, which makes it possible to independently control two transmission zeros in upper stopband.

(a)

(b)

(c)
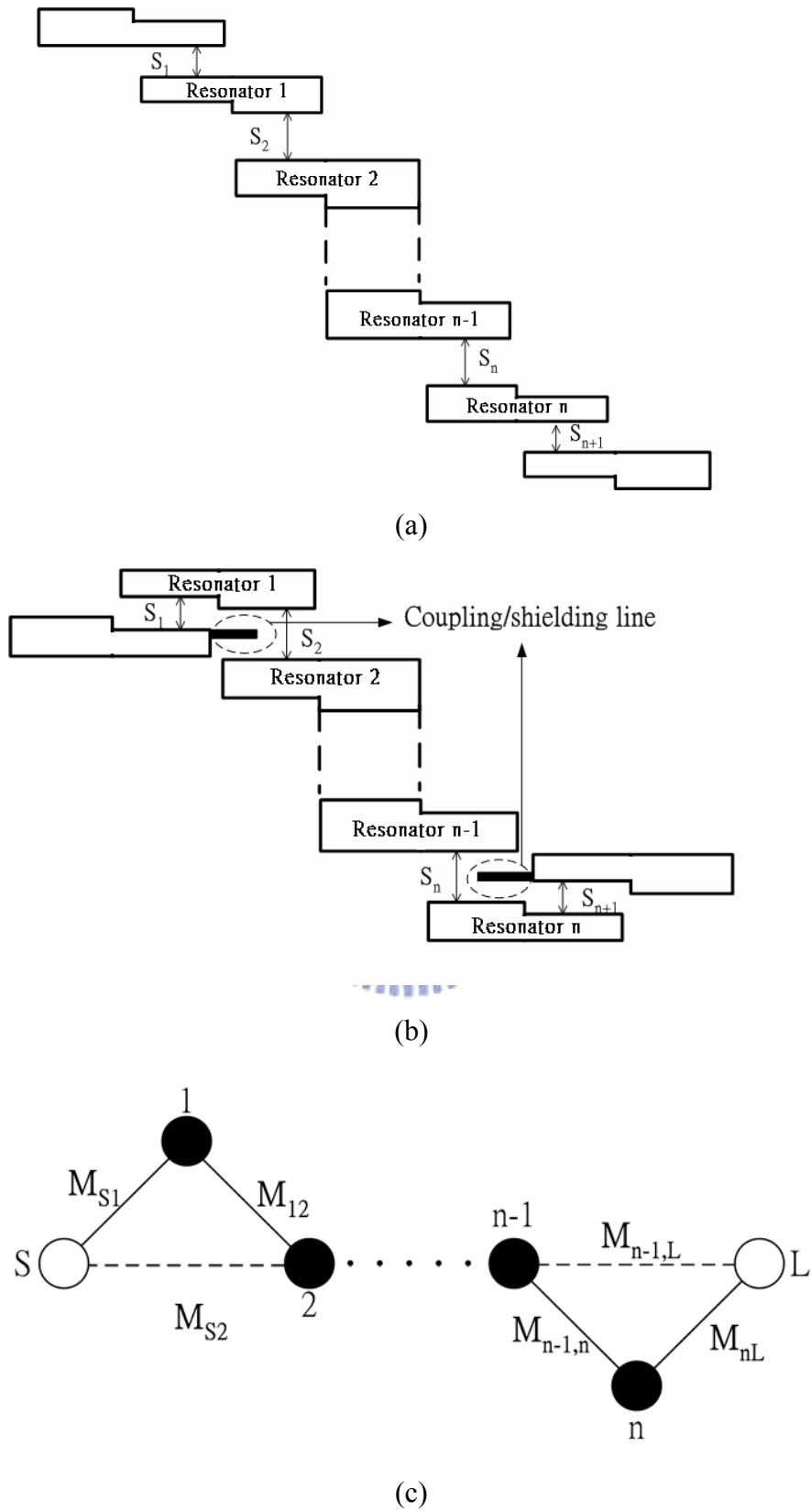
Figure 4-1. (a) The conventional parallel-coupled filter. (b) The modified filter. (c) The coupling route of the modified filter.

4.2 Circuit Description and Design Feasibility

The design procedures are started with the conventional microstrip parallel-coupled filter. Following easy design procedures, dimensions of a Chebyshev-response parallel-coupled filter as shown in Figure 4-1(a) can be obtained. Then, vertically flip feeding lines of the source and the load with respect to the resonator "1" and resonator "n" respectively, which is shown in Figure 4-1(b). Note that the gap spacing S_i in Figure 4-1(a) is identical to that in Figure 4-1(b). During practical layout, designers may shorten resonators in advance to prevent the feed lines from directly connecting to the resonator "2" or resonator "n-1" if needed.

To introduce two independently controllable transmission zeros on the upper stopband, the design procedures could be started with the Chebyshev-response coupling matrix and perturb it by introducing cross couplings $M_{S,2}$ and $M_{L,n-1}$ to form two trisection blocks as shown in Figure 4-1(c). During this procedure, it is found that in order to keep equal ripple in-band response, the strength of $M_{1,2}$ and $M_{n-1,n}$ must be decreased and the frequencies of resonators need to be adjusted. Therefore, a suitable manner to simultaneously introduce the couplings, M_{S2} and $M_{L,n-1}$, and decrease the strength of $M_{1,2}$, and $M_{n-1,n}$ is needed. The coupling/shielding lines shown in Figure 4-1(b) seem to be a perfect candidate. The coupling/shielding lines can introduce couplings, M_{S2} and $M_{L,n-1}$, and decrease the strength of M_{12} and $M_{n-1,n}$ by shielding part of the coupling gaps of them. Practically, length, width, and vertical position of the coupling/shielding line can be adjusted. Here, we fix the line width and adjust the line length and vertical position. The vertical position of the coupling/shielding line has little effect on shielding but has strong influence on cross-coupling. In Chebyshev-response parallel-coupled filters, the relations $S_1 < S_2$ and $S_{n+1} < S_n$ always hold, which makes it possible to add coupling/shielding line at the end of feed lines. Another merit of the parallel-coupled filter structure is that when adjusting the length

of resonator to align the resonant frequencies, the coupling between resonators is nearly unchanged. The feasibility of nearly independently tuning the coupling and frequencies makes it easy to implement the asynchronous tuned filter as that in Figure 4-1(c).
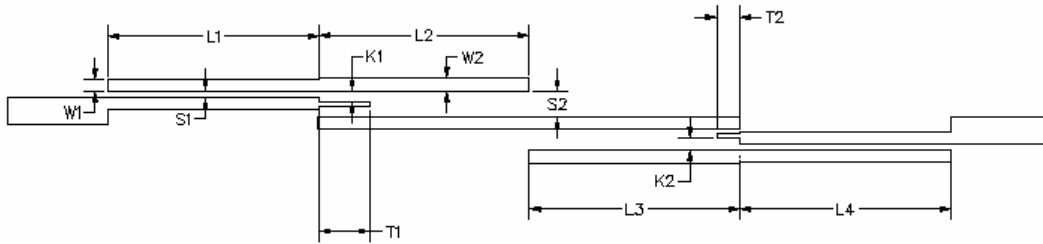
Figure 4-2. The layout of the fabricated filter (unit: mil). L1=354, L2=354, L3=354, L4=354, S1=11, S2=35, W1=19, W2=21, K1=19, K2=20, T1=87, T2=39. The line with of coupling/shielding lines is 8mil.

4.3 Design Example and Experiment

To show the feasibility of the proposed structure, an example is given below. The center frequency, in-band return loss, and fractional bandwidth of the filter are chosen to be 5GHz, 20dB, and 5% respectively. The filter is built on a Rogers RO4003 substrate with $\varepsilon_r = 3.58$, thickness=20mil, and $\tan \delta = 0.0021$. The initial dimensions of the parallel-coupled filter are obtained by analytical method described in [7]. The coupling/shielding lines with length T_1 and T_2 are added at the ends of feed lines as shown in Figure 4-2, to introduce two transmission zeros separately. Two prescribed transmission zeros are located at 5.35GHz, and 5.7GHz respectively. The initial value of T_1 and T_2 can be arbitrarily set, say, T_1=50 mil, T_2=30 mil. The S-parameters of the filter is then obtained with the help of the commercial EM simulator Sonnet [32]. Next, the method described in chapter 2 can be used to extract the coupling matrix from the simulated S-parameters. The physical dimensions of filter are then adjusted

according to the extracted coupling matrix to match the prescribed response. After totally five of EM-simulation, matrix extraction, and physical parameters adjusting loops, one can get the simulated results as shown in Figure 4-3. The measured results are also shown in Figure 4-3 for comparison. The corresponding physical sizes are shown in Figure 4-2. And the corresponding coupling matrix M is extracted as follows

$$
M = \begin{bmatrix}
0 & 1.0103 & 0.4275 & 0 & 0 \\
1.0103 & -0.7811 & 0.8549 & 0 & 0 \\
0.4275 & 0.8549 & 0.4562 & 1.0258 & 0.2334 \\
0 & 0 & 1.0258 & -0.3857 & 1.1058 \\
0 & 0 & 0.2334 & 1.1058 & 0
\end{bmatrix}
$$
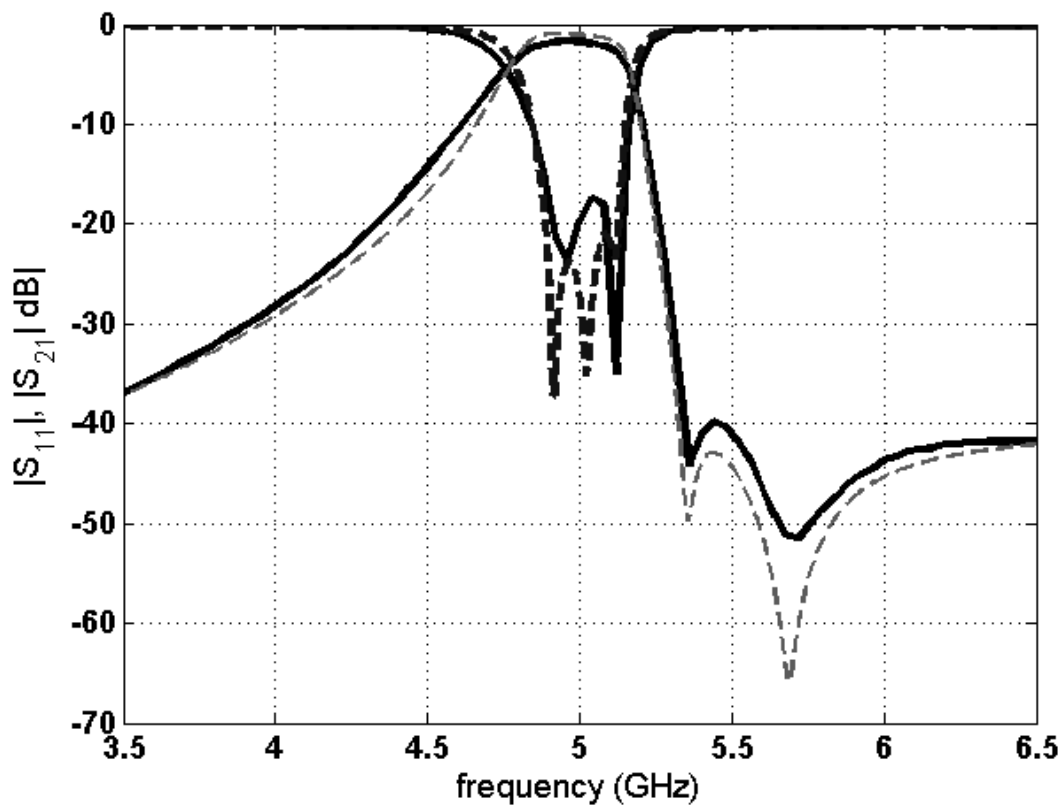
Figure 4-3. Simulated and measured responses. Solid line: measured results. Dashed lines: EM simulated results.

It should be emphasized that filter shown in Figure 4-2 has exactly the same layout as the initial design except two coupling/shielding lines. So, designers can

easily realize this filter even by trial and error method without using of matrix extracting procedure.
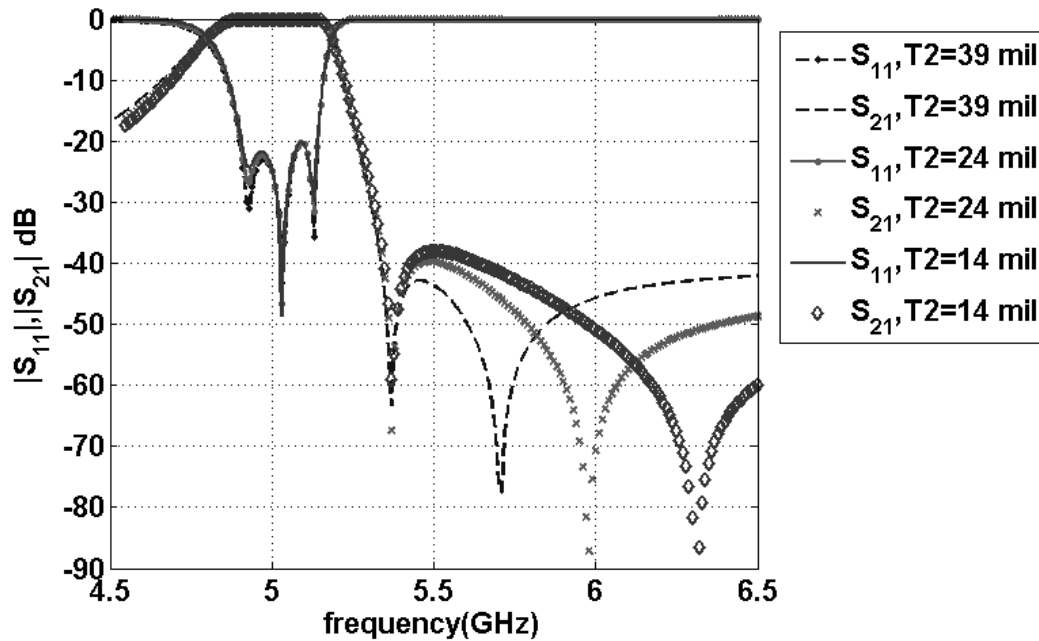
Figure 4-4. EM simulated results of three different cases. The dimensions of the simulated filter are the same as these shown in Figure 4-2 except T2 is set to different values.

It is mentioned in section 4-2 that the introduction of the coupling/shielding lines in this way can effectively adjust the transmission zeros with slight perturbation of the passband return loss. To demonstrate the merits of easy tuning of the proposed structure, three EM simulations are taken in which the length of the coupling/shielding line, T2, are set to 14mil, 24mil, and 39mil respectively while the other dimensions are the same as these given in Figure 4-2. From the EM simulated results shown in Figure 4-4, it is obvious that the transmission zero can be tuned over a wide range with negligible change in the passband return loss.

Chapter 5 Microstrip Realization of Generalized Chebyshev Filters with Box-Like Coupling Schemes

In this chapter, generalized Chebyshev microstrip filters with box-like coupling schemes are presented. The box-like coupling schemes taken in this chapter include doublet, extended doublet, and fourth-order box-section. The box-like portion of the coupling schemes is implemented by an E-shaped resonator. Synthesis and realization procedures are described in detail. The example filters show an excellent match to the theoretical responses.

5.1 Introduction

The microstrip filters with generalized Chebyshev response attract considerable attention due to its lightweight, easy fabrication and ability to generate finite transmission zeros for sharp skirts. In the literature, most of them are based on cross-coupled schemes such as cascade trisection and cascade quadruplet. Some representative examples of cross-coupled microstrip filters are available in the book [12].

Recently, with the progress of the synthesis technique, new coupling schemes such as "doublet", "extended doublet", and "box-section" are introduced [38]-[40]. As shown in Figure 5-1, these coupling schemes have a box-like center portion, so we call them box-like coupling schemes. These coupling schemes impact the filter design since they do not only provide new design possibilities but exhibit some unique and attractive properties as well. They differ from the conventional cascade trisection and cascade quadruplet mainly on two aspects. First, there are two main paths for the signal from source to load while there is only one main path in the case of cascade trisection and cascade quadruplet. Second, the configuration of doublet and box-section exhibit the zero-shifting property which make it possible to shift transmission zero from one side of the passband to the other side simply by changing

the resonant frequencies of the resonator while keeping other coupling coefficients unchanged. The zero-shifting property implies that the similar physical layout can implement a filter with transmission zero at the lower stopband or at the upper stopband, which is not feasible on the conventional trisection configuration. Besides, the third-order extended-doublet configuration, as shown in Figure 5-1(b), exhibits one pair of finite transmission zeros as that of a cross-coupled quadruplet filter. Pairs of finite transmission zeros can be used to improve the selectivity of the filter or flatten the in-band group delay. However, to the author's knowledge, only a few studies in the literature are focused on realization of the coupling schemes shown in Figure 5-1 with microstrip line [41], [42].

(a)   (b)

(c)
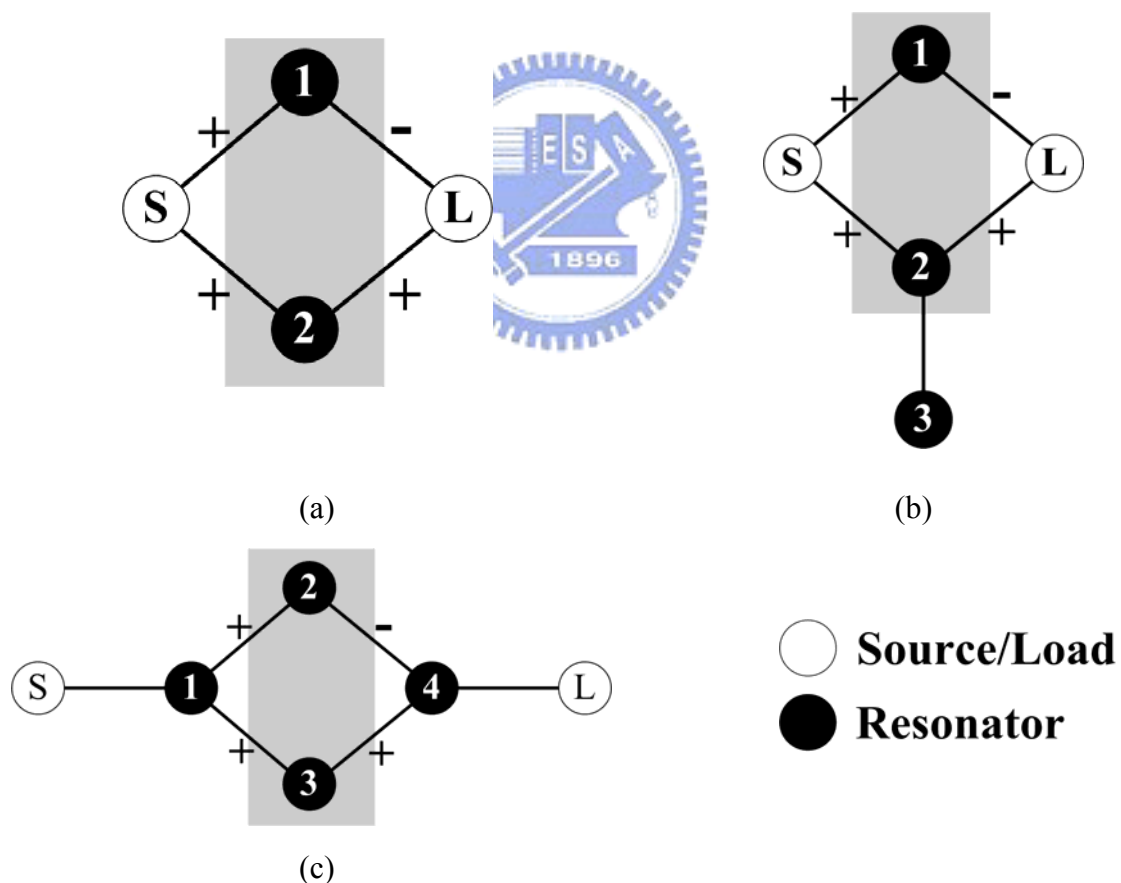
Figure 5-1. Basic box-like coupling schemes for generalized Chebyshev-response filters discussed in this paper. (a) doublet. (b) extended doublet (c) box-section. (The gray area is realized by the proposed E-shaped resonator)

An important property of the schemes in Figure 5-1 is that one of the coupling coefficients on the two main paths must be negative while others are positive. The simplest way to obtain the required negative sign is to use higher-order resonance [39], [42]. Unfortunately, higher-order resonance leads to a spurious resonance in the lower stopband. Instead of using higher-order resonance, loop resonators are arranged carefully to satisfy the required sign of coupling coefficients for the box-section configuration [41]. However, a similar method can not apply to doublet or extended-doublet. To overcome these difficulties, an E-shaped resonator as shown in Figure 5-2(a) is proposed to implement the required coupling signs.
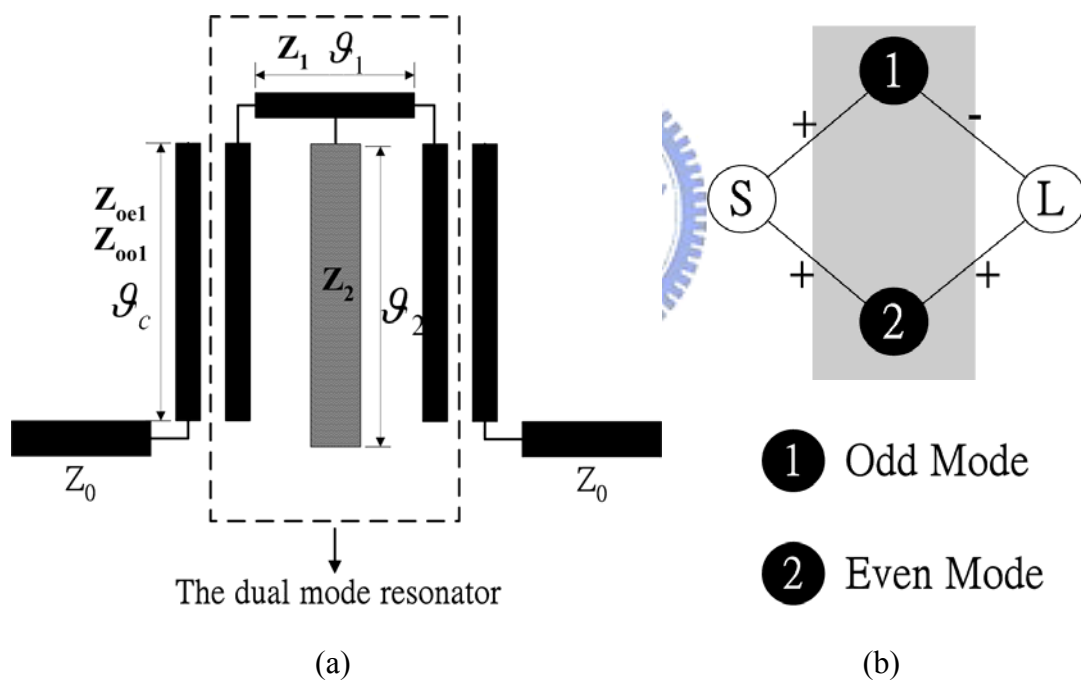
Figure 5-2. A doublet filter (a) the proposed layout (gray area indicate the E-shaped resonator) (b) the corresponding coupling scheme.

The E-shaped resonator can achieve the required magnitude and sign of the coupling schemes shown in Figure 5-1. As shown in Figure 5-2(a), the E-shaped resonator comprises a hairpin resonator and an open stub on its center plane. This symmetric

structure can support two modes: even mode and odd mode. Thus, the source and the load are coupled to both modes of the E-shaped resonator. That is even though only one physical path exists between source and load, there are two electrical paths between them. Consequently, the layout in Figure 5-2(a) can be modeled by the coupling scheme, a doublet, in Figure 5-2(b). The doublet filter illustrates how an E-shaped resonator directly couples to external feeding network.

Based on the proposed E-shaped resonator, filters with extended-doublet and box-section configuration can be realized as well. The E-shaped resonator can use either its even mode or odd mode to couple an extra resonator. Thus, the extended-doublet configuration in Figure 5-1(b) is achievable. Besides, the E-shaped resonator can couple to external resonators with two of its modes simultaneously and forms the box-section configuration in Figure 5-1(c). The feasibility of realization of the basic coupling schemes in Figure 5-1 with proposed E-shaped resonator makes it possible to realize a class of coupled microstrip filters in a unified approach.
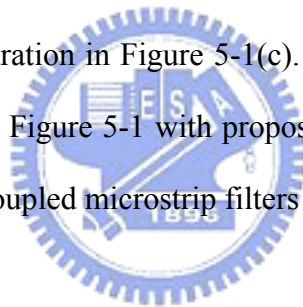
5.2 Circuit Modeling

A. Filters in the doublet configuration

The E-shaped resonator filter in Figure 5-2(a) was originally reported in [43]. In [43], the E-shaped resonator was not modeled as a two-mode resonator. Instead, the circuit was modeled as two quarter-wavelength resonators with a tapped open stub in the center plane. The open stub is considered as a K-inverter between two quarter-wavelength resonators to control the coupling strength and as a quarter-wave open stub to generate a transmission zero at the desired frequency. However, the filter cannot be designed with a prescribed quasi-elliptic response since there is no suitable prototype corresponding to the circuit model in [43].

In this dissertation, a doublet as shown in Figure 5-2 (b) is used to model the

circuit in Figure 5-2 (a). In Figure 5-2(b), the resonator 1 represents the odd-mode resonance, where the center plane of the E-shaped resonator is an electric wall (E-plane). On the other hand, the resonator 2 represents even-mode resonance, where the center plane of the E-shaped resonator is a magnetic wall (H-plane). With the notation shown in Figure 5-2(b), the corresponding coupling matrix M can be written down as

$$M = \begin{bmatrix} 0 & M_{S1} & M_{S2} & 0 \\ M_{S1} & M_{11} & 0 & M_{1L} \\ M_{S2} & 0 & M_{22} & M_{2L} \\ 0 & M_{1L} & M_{2L} & 0 \end{bmatrix} \qquad (5.1)$$

There are some interesting properties of the doublet filter in Figure 5-2(a). First, since the E-shaped resonator exhibits symmetry, the relationship $M_{S1}=-M_{1L}$ and $M_{S2}=M_{2L}$ holds. Second, $|M_{S1}|>|M_{S2}|$ is always true for this structure since the coupling strength between the odd mode and external feeding network is always larger than that of the even mode.

To get more insight of how to control a transmission zero of a doublet filter in this configuration, an explicit expression relating the coupling elements and the transmission zero Ω is provided in a low-pass domain as follows

$$\Omega = (M_{11}M_{S2}^2 - M_{22}M_{S1}^2)/(M_{S1}^2 - M_{S2}^2) \qquad (5.2)$$

Note that the mapping between normalized frequency ω' and actual frequency f is $\omega' = (f/f_0 - f_0/f)\Delta f/f_0$, where f_0 and Δf are center frequency and bandwidth of a filter, respectively.

Based on the Eq (5.2), observations are summarized in the following:

1. The transmission zero is always located at finite frequency since $M_{S1} \neq M_{S2}$. In

other words, the structure exhibits finite transmission zero inherently.

2. The transmission zero can be moved from upper stopband to the lower stopband, or vice versa, by changing the sign of M_{11} and M_{22} simultaneously. This property makes it possible to generate upper stopband or lower stopband finite transmission zero with similar structure.

3. If $M_{11} > 0$ and $M_{22} < 0$, Ω would be greater than zero. In a more explicit expression, M_{11} and M_{22} can be related to the resonant frequencies of odd mode, f_{odd}, and even mode, f_{even}, respectively by the following equations.

$$f_{odd} = f_0 (1 - \frac{M_{11} \times \Delta f}{2 f_0}) \qquad (5.3)$$

$$f_{even} = f_0 (1 - \frac{M_{22} \times \Delta f}{2 f_0}) \qquad (5.4)$$

where f_0 and Δf are center frequency and bandwidth of a filter, respectively. That is if $f_{odd} < f_0$ and $f_{even} > f_0$, the transmission zero would be on the upper stopband.

4. If $M_{11} < 0$ and $M_{22} > 0$, Ω would be smaller than zero. That is if $f_{odd} > f_0$ and $f_{even} < f_0$, the transmission zero would be on the lower stopband.

To get the related electrical parameters indicated in Figure 5-2(a), one can take the following procedures. First, synthesize a coupling matrix M corresponding to the prescribed response. Then, consider parameters concerning the odd mode only by removing the open stub on the center plane. Once the open stub is removed, the circuit becomes a first-order hairpin filter. The first-order hairpin filter can be synthesized by the conventional method [44] with the center frequency set to be the resonant frequency of odd mode, which can be expressed as $f_{odd} = f_0 (1 - M_{11} \times \Delta f / 2 f_0)$. At this step, one can specify the values of ϑ_C, Z_1 and ϑ_1 and obtain the values of Z_{oe}, Z_{oo} by analytical method [44]. Second, put the open stub back. The two parameters of the open stub, Z_2 and ϑ_2, can be adjusted to

achieve the desired resonant frequency and the needed external coupling strength of the even mode. Here, the resonant frequency of the even mode is $f_{even} = f_0 (1 - M_{22} \times \Delta f / 2 f_0)$.

To illustrate the procedure, an example is taken of a second order generalized Chebyshev filter with a passband return-loss of 20-dB and a single transmission zero at a normalized frequency $\Omega = 3$. The corresponding coupling coefficients are M_{S1}=1.1110, M_{S2}=0.6170, M_{11}=1.4545, and M_{22}=-1.6260. For filter with center frequency f_0=2.4 GHz and fractional bandwidth FBW=0.05, the ideal response is depicted in Fig. 3 as solid lines. After getting the coupling matrix, ϑ_C could first be specified. Here, we set $\vartheta_C = 60^o$, $Z_1 = 50$ ohm, and $\vartheta_1 = 60^o$ and obtain $Z_{oe} = 75.2552$ ohm, $Z_{oo} = 38.1022$ ohm for a uniform impedance resonator with characteristic impedance $Z_0 = 50$ ohm at frequency $f_{odd} = 2.3127$ GHz. Next, put the open stub back and adjust the values of Z_2 and ϑ_2 by the optimization method to let the response of the circuit match with the ideal response calculated from the M matrix. The optimized values of Z_2 and ϑ_2 are 62 ohm and 86.8^o, respectively, at frequency $f_{even} = 2.4976$ GHz. According to the obtained electrical parameters in Figure 5-2 (a), the corresponding response is shown in Figure 5-3 as circled lines. The frequency response contributed only by the odd mode is also depicted in Figure 5-3 as dashed lines to let us understand the procedures clearer.
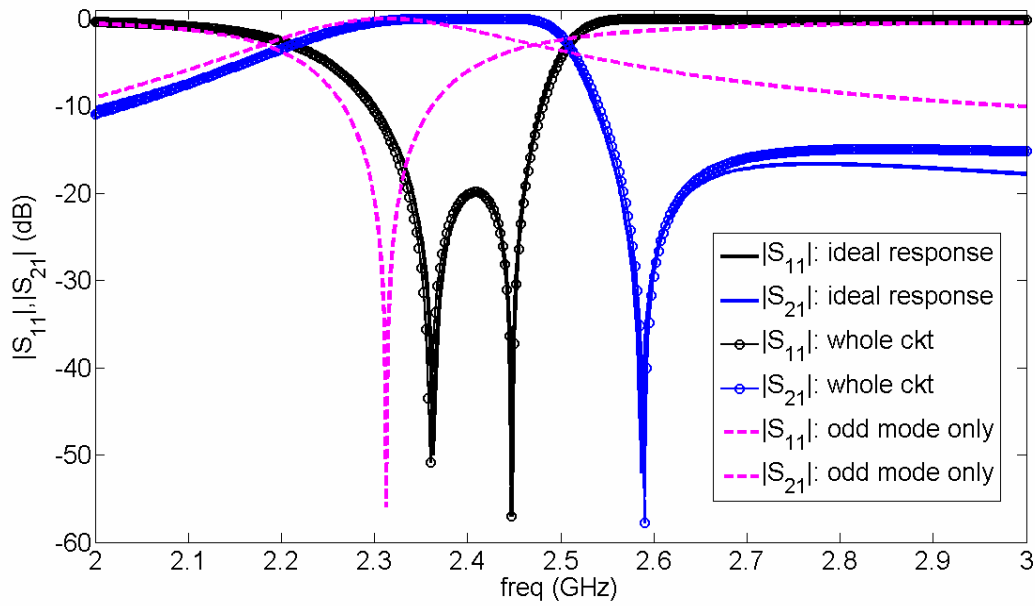
Figure 5-3. Responses generated from the coupling matrix and from electrical network shown in Fig. 2(a) with synthesis parameters.

B. Extended-Doublet Filters

Based on the doublet filters developed in previous section, the emphasis is put on how to extend the design to extended-doublet filters in this section. There are two possible arrangements suitable to form extended-doublet filters. One possible arrangement is indicated in Figure 5-4 where the extended doublet filter consists of a doublet filter plus a grown resonator. The grown resonator is a half-wavelength resonator with both ends open. In this case, the grown resonator would mainly couple to the odd mode of the E-shaped resonator. And for the even mode of the E-shaped resonator, it acts as a non-resonant element, which slightly perturbs the resonant frequency of the even mode. Another possible design is shown in Figure 5-5 where both ends of the grown resonator are shorted to ground. In this case, the grown resonator mainly couples to the even mode of the E-shaped resonator and acts as a non-resonant element to the odd mode of the E-shaped resonator. To clarify the

coupling relationship between each resonator, the coupling routes are accompanied with layouts in Figure 5-4 and Figure 5-5.
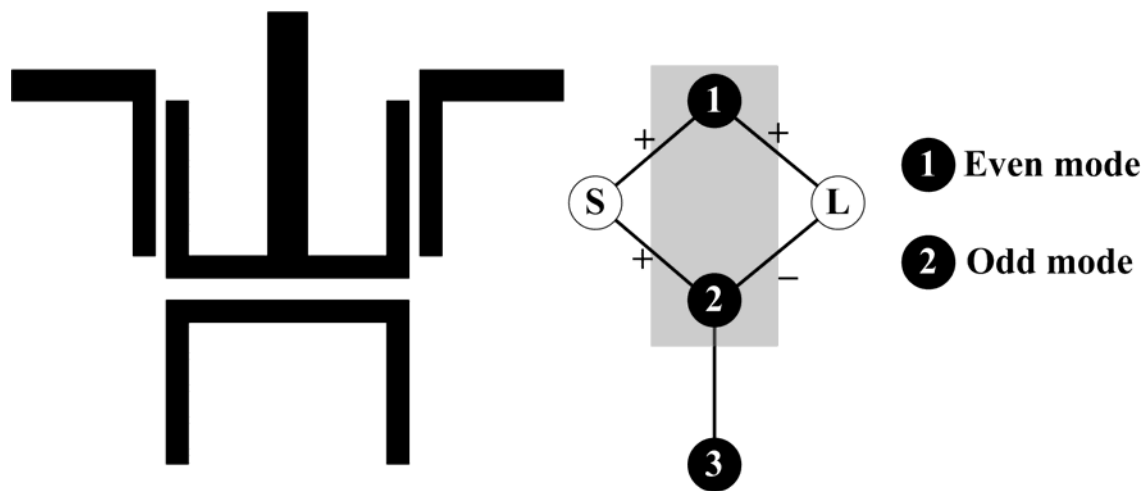
Figure 5-4. A layout of extended-doublet filter and its corresponding coupling scheme. The design is for flat group delay response
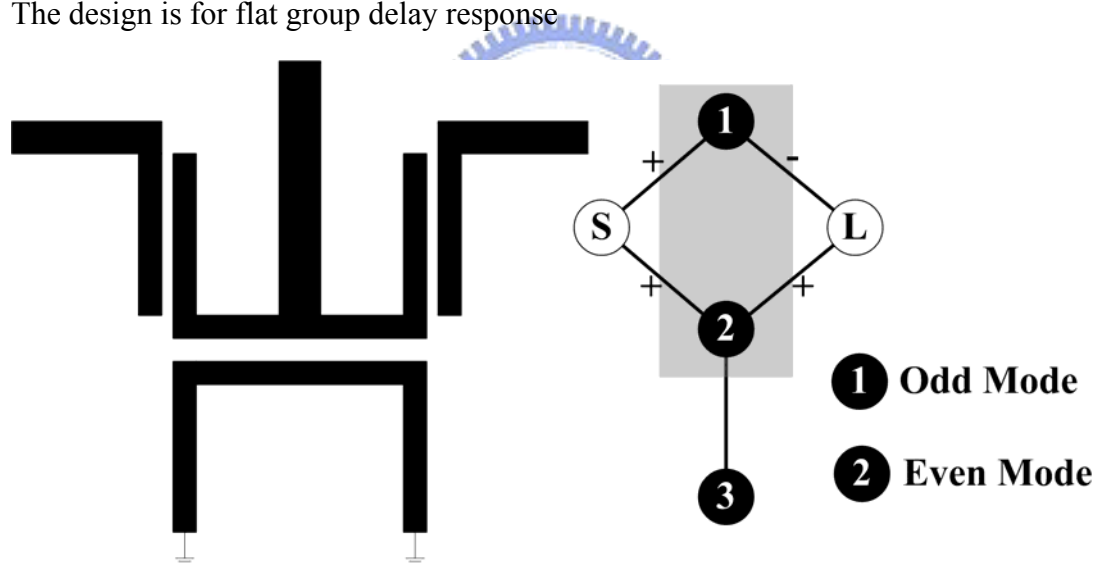
Figure 5-5. A layout of extended-doublet filter and corresponding coupling scheme. The design is for skirt selectivity response

The extended-doublet filter has a pair of finite transmission zeros. For the design in Figure 5-4, the pair of transmission zeros is on the imaginary-frequency axis. On the other hand, to generate a pair of real-frequency transmission zeros, the design in Figure 5-5 must be adopted. The difference between the two designs can be

understood from the governing equation of finite transmission zeros. Since the proposed extended doublet filters are symmetric structures, the relations $|M_{S1}|=|M_{1L}|$ and $|M_{S2}|=|M_{2L}|$ always hold. Thus, the governing equation of finite transmission zero can be expressed as

$$\Omega^2 = \frac{M_{S1}^2 M_{23}^2}{M_{S1}^2 - M_{S2}^2} \qquad (5\text{-}5)$$

As discussed in the design of doublet, the coupling coefficient of source to odd mode is stronger than that of source to even mode. Thus, for the design in Figure 5-4, $|M_{S2}|>|M_{S1}|$, which leads to $\Omega^2 < 0$. On the contrary, for the design in Figure 5-5, $|M_{S2}|<|M_{S1}|$, which results in $\Omega^2 > 0$. In conclusion, the design in Figure 5-4 can be used to generate delay-flattening transmission zeros while the design in Figure 5-5 can be used to generate a pair of attenuation poles.

To illustrate the procedure of the design, a generalized Chebyshev filter with passband return loss of 20-dB and a pair of transmission zeros at $\Omega = \pm 2$ is taken as an example. The design of an extended doublet starts from the synthesis of coupling matrix, which can be done using the technique in [9]. The synthesized coupling matrix is shown in Figure 5-6(a). Using the information of M_{S1} and M_{S2}, one can construct the doublet by the method provided in section 5-2A. Excluding the M_{23} and M_{32} in the coupling matrix, one can calculate the response contributed from the doublet only. For instance, if the center frequency and fractional bandwidth of the designed filter are 2.4GHz and 5% respectively, the responses of the doublet are shown as dotted lines in Figure 5-6(b). After getting the initial design of doublet, add the grown resonator. Since $\Omega^2 > 0$ in this case, the layout in Figure 5-5 must be adopted. Ideally, the response of the extended-doublet would be the solid lines shown in Figure 5-6. The physical implementation of this design will be presented in section 5-3 to confirm the validity.

M	S	1	2	3	L
S	0	0.8613	0.6202	0	0
1	0.8613	0	0	0	-0.8613
2	0.6202	0	0	1.3878	0.6202
3	0	0	1.3878	0	0
L	0	-0.8613	0.6202	0	0

(a)
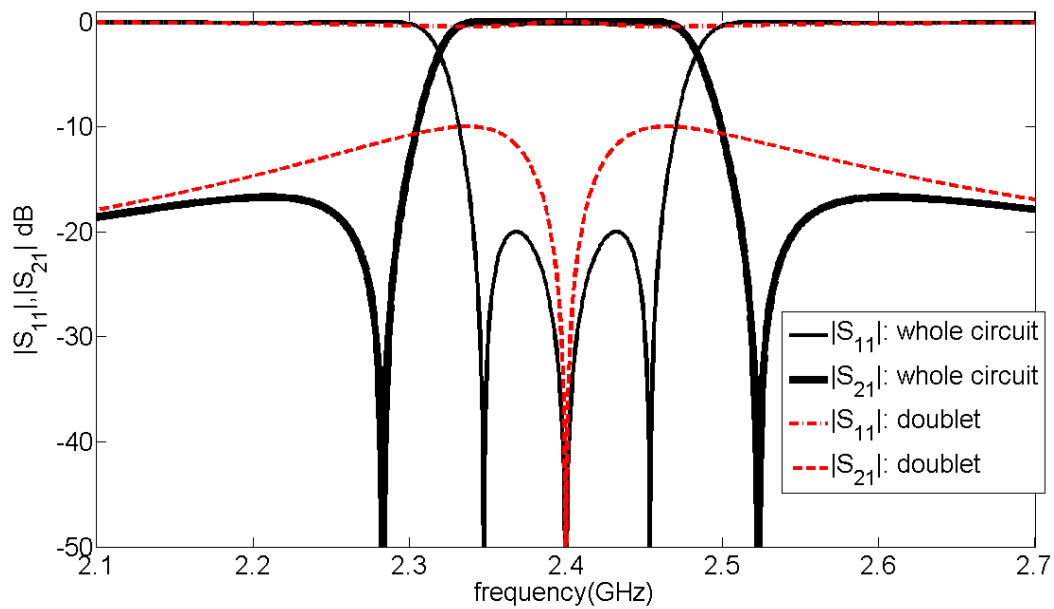
(b)

Figure 5-6. The extended-doublet filter with in-band return loss RL=20dB, normalized transmission zeros at $\Omega = \pm 2$. (a) its coupling matrix (b) Responses of extended doublet filter and responses contributed by doublet only.

C. Box-section Filters

The fourth order filter in the "box-section" configuration was first proposed in [38] and realized by coaxial resonators. With the zero-shifting property, it is possible to use the similar filter structure to realize the finite transmission zero either on the upper stopband or on the lower stopband. The box-section filter is suitable for the complementary filters of a transmit /receive duplexer [42] since it has asymmetric response with high selectivity on one side of the passband. The microstrip box-section filter was first reported in [41] with open square loop resonators. Because the box-section coupling diagram is symmetric where $M_{S1}=M_{4L}$, $M_{12}=-M_{24}$, $M_{13}=M_{34}$, and $M_{11}=M_{44}$ should be held in the coupling route shown in Fig. 5-7(a). Therefore, it is preferable to layout the filter symmetrically because a symmetrical-layout filter can inherently obtain symmetrical coupling coefficients. The asymmetrical layout causes the filters in [41] to be difficult to keep the coupling coefficients to be symmetric. Another microstrip box-section filter was proposed in [42]. Although the layout of the filters in [42] is symmetric, it suffers from spurious response in the filter's lower stopband due to one of filter's resonators to be a higher order mode resonator. In this paper, the layout depicted in Figure 5-7(b) solves the problems mentioned. The E-shaped resonator is symmetric and is free from lower stopband spurious resonances. Due to the symmetry, only half of the electrical parameters are shown in Fig. 5-7(b). As explained in doublet filter, the circuit layout in Fig. 5-7(b) satisfies the required sign of couplings.

(a)

(b)
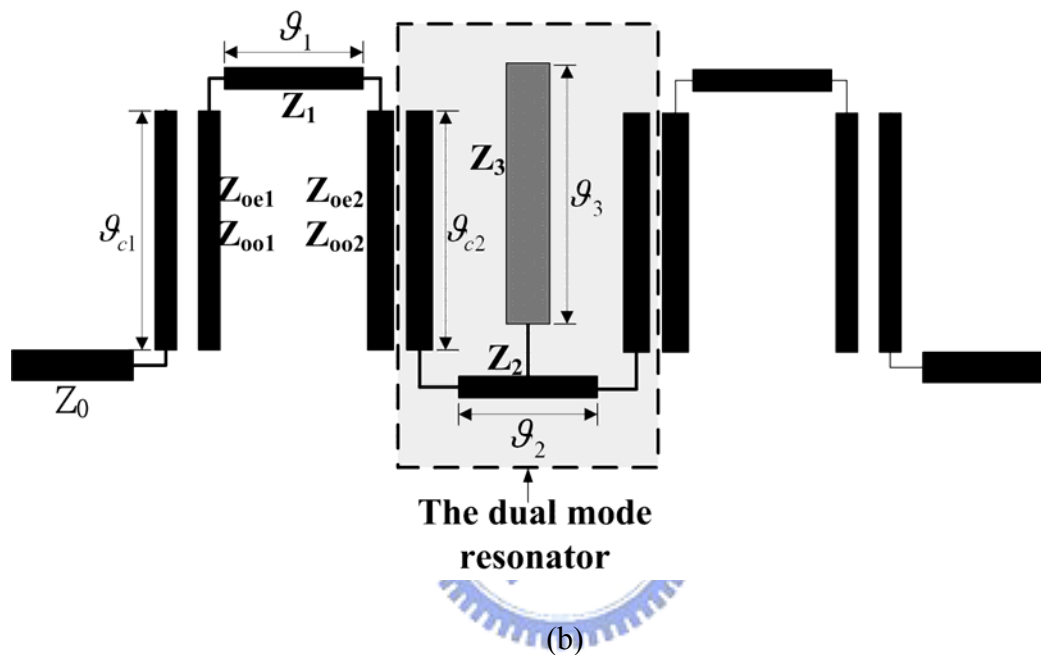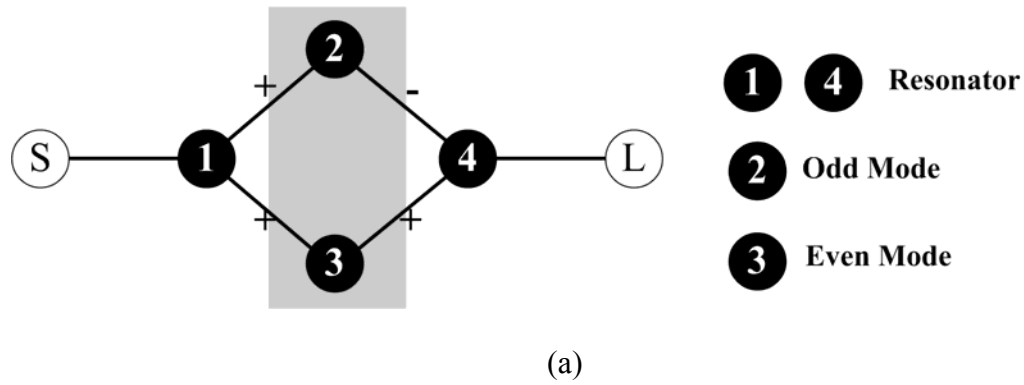
Figure 5-7. A Box-section filter. (a) filter's coupling scheme. (b) the proposed layout.

To illustrate how to obtain the corresponding electrical parameters in Figure 5-7(b) from a prescribed response, examples are taken as follows. The first example is a fourth order generalized Chebyshev filter with a passband return-loss of 20-dB, a single transmission zero at $\Omega = -2.57$ which gives a lobe level of -48 dB on the lower side of the passband. The corresponding coupling matrix M is shown in Figure 5-8(a). After the lowpass-to-bandpass transformation, the ideal bandpass response of this filter with center frequency of 2.4 GHz and fractional bandwidth of 5% is shown in Figure 5-8(b).

The design procedures are described as follows. First, remove the open stub in the E-shaped resonator in Figure 5-7(b), which is equivalent to discarding the even mode (resonator 3 in the Figure 5-7(a)) of the E-shaped resonator. After removing the open stub, the circuit becomes a third-order hairpin-like filter. The coupling matrix M_1 of this hairpin-like filter is identical to the coupling matrix M in Figure 5-8(a) except M_{3i} and M_{i3} being zero. The ideal response of this hairpin-like filter can be calculated from M_1 matrix as circled lines in Figure 5-8(b). To get the electrical parameters associated with the asynchronously tuned third-order hairpin-like filter, a synchronous tuned third-order hairpin filter provides the initial design and is synthesized at first. The synchronous tuned hairpin filter has coupling matrix M_2 which is identical to M_1 except $M_{ii}=0$. When synthesizing the synchronously tuned hairpin filter, we set $\vartheta_{C1} = 90^o$, $\vartheta_{C2} = 60^o$, $Z_1 = 50$ ohm, $Z_2 = 50$ ohm at $f = f_0$, and the characteristic impedance of each resonator to be 50 ohm. With these settings, the electrical parameters of the synchronously tuned hairpin filter are calculated and shown in Table. 5.1, which provides the initial values for the asynchronous-tuned hairpin-like filter. Then, an optimization routine is involved. The goal of optimization routine is to find a set of electrical parameters which can make the response match with the response of the ideal asynchronously-tuned hairpin-like filter calculated from M_1 matrix. The optimized parameters are shown in Table 5.1 for comparison. Note that the optimized values of associated parameters are nearly identical to the initial values; therefore, the optimization routine can converge within a few times. Finally, put the open stub back and optimize the parameters Z_3 and ϑ_3 to make the response matched with the response of the desired box-section filter's response as solid lines in Figure 8(b). The optimized values of Z_3 and ϑ_3 are given in Table 5.1 as well.

M	S	1	2	3	4	L
S	0	1.0343	0	0	0	0
1	1.0343	−0.0342	0.7291	0.5441	0	0
2	0	0.7291	−0.5572	0	−0.7291	0
3	0	0.5441	0	0.8282	0.5441	0
4	0	0	−0.7291	0.5441	−0.0342	1.0343
L	0	0	0	0	1.0343	0

(a)

(b)
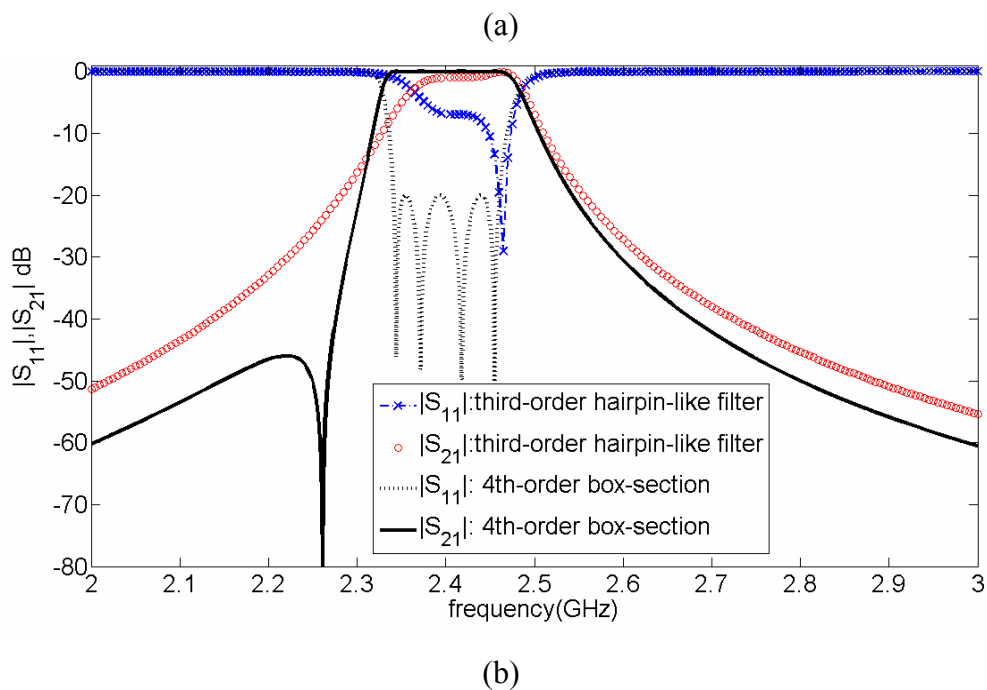
Figure 5-8. A fourth order box-section filter: (a) its coupling matrix (b) the responses of the box-section filter and ideal responses of the asynchronous tuned third-order hairpin-like filter calculated by M_1 matrix.

Instead of a lowpass prototype filter with a transmission zero at $\Omega = -2.57$ in the first example, the second example locates the transmission zero at a normalized frequency $\Omega = 2.57$ and keeps all other parameters unchanged. According to the synthesis procedures in [38], the inter-resonator couplings are unchanged but self-couplings (principal diagonal matrix elements, M_{11}, M_{22},…etc., of the coupling

matrix in Figure 5-8(a)) must change sign. Following the same procedures in the previous design, one can get the electrical parameters given in Table 5.1. In Table 5.1, the column of design #1 corresponds to lowpass prototype filter transmission zero at $\Omega = -2.57$ and the column of design #2 corresponds to a lowpass prototype filter transmission zero at $\Omega = 2.57$. The responses obtained from the electrical parameters listed in Table 5.1 and responses calculated from M matrix in Figure 5-8(a) are both plotted in Figure 5-9 for comparison.

	Initial values	Design #1	Design #2
Z_{oe1} (ohm)	68.6941	68.6967	68.6169
Z_{oo1} (ohm)	39.7079	39.7204	39.7758
Z_{oe2} (ohm)	53.5286	54.2217	52.5632
Z_{oo2} (ohm)	46.9091	47.5517	46.0413
ϑ_1 (degrees)	30	30.2141	29.7113
ϑ_2 (degrees)	60	58.1787	61.635
Z_3 (ohm)	NaN	19.1823	20.2808
ϑ_3 (degrees)	NaN	95.9949	84.3721

Table 5.1. Electrical parameters corresponding to box-section filters shown in Fig. 7(b). Here, $\vartheta_{C1} = 90^o$, $\vartheta_{C2} = 60^o$, $Z_1 = 50\,\text{ohm}$, $Z_2 = 50\,\text{ohm}$. All of the electrical lengthes are corresponding to the center frequency of the filter.

Design 1: in-band return loss RL=20dB, $\Omega = -2.57$, and FBW=5%

Design 2: in-band return loss RL=20dB, $\Omega = 2.57$, and FBW=5%

5.3 Design Examples and Experimental Results

The extended-doublet filter discussed in Section 5-2-B with its ideal response shown in Figure 5-5, and the design #1 of box-section filter discussed in Section 5-2-C with its ideal response shown in Figure 5-9(a) are fabricated to verify the designs. Although all of the electrical parameters obtained in Section 5-2 can be transformed to physical parameters, it does not include the junction effect. Therefore, a commercial EM simulator Sonnet [32] is adopted to take all the electromagnetic effects into consideration. To efficiently tune the physical dimensions of the filter to achieve the prescribed response, the diagnosis and tuning methods given in Chapter2 are taken. Figure 5-10 shows the physical dimensions and the corresponding responses for the extended-doublet filter where a RO6010 substrate with dielectric constant of 10.8 and thickness of 50mil is used. Figure 5-11 depicts the physical dimensions and corresponding responses for the box-section filter where an RO4003 substrate with dielectric constant of 3.63 and a thickness of 20mil is used. The measured in-band insertion loss of the filters in Figure 5-10 and Figure 5-11 are 1.4dB and 2.7dB, respectively. In Figure 5-10 (b), the experimental results show a larger passband than the simulated ones. The deviation mainly results from the fabrication error. In Figure 5-11 (b), the measured response is shifted about 30MHz. Further investigation showed that the dielectric constant of the substrate is closer to 3.4 rather than 3.63. The wideband measurement results of the fabricated box-section filter are shown in Figure 5-11 (c).
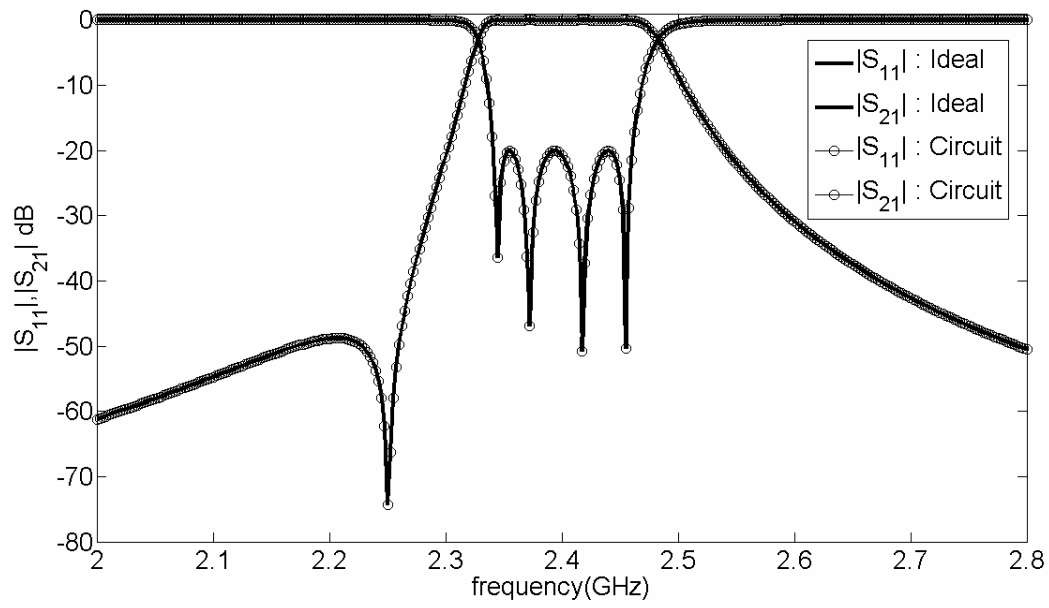
(a)
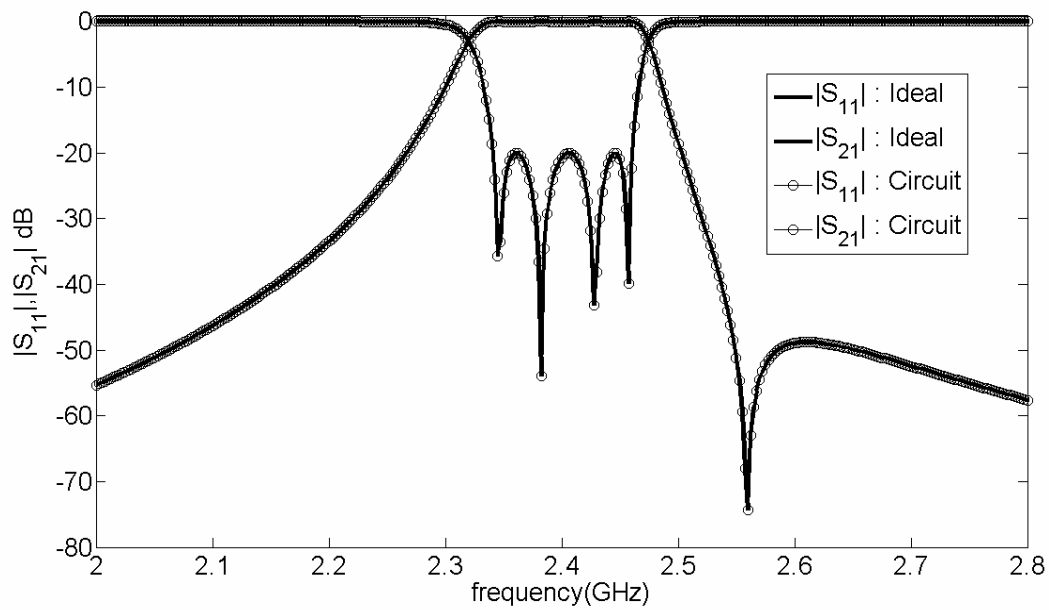
(b)

Figure 5-9 Responsess of the box-section filters. (a) Responses obtained by electrical parameters of design #1 in Table 5.1 and its coupling matrix respectively. (b) Responses obtained by electrical parameters of design #2 in Table 5.1 and its coupling matrix respectively.

(a)
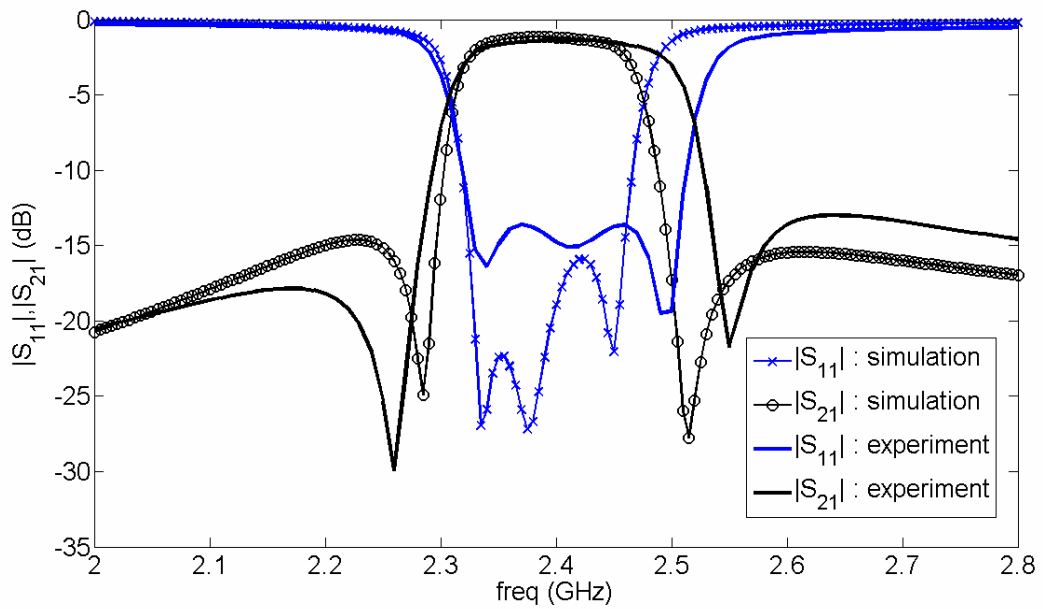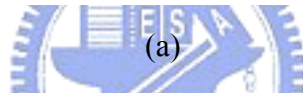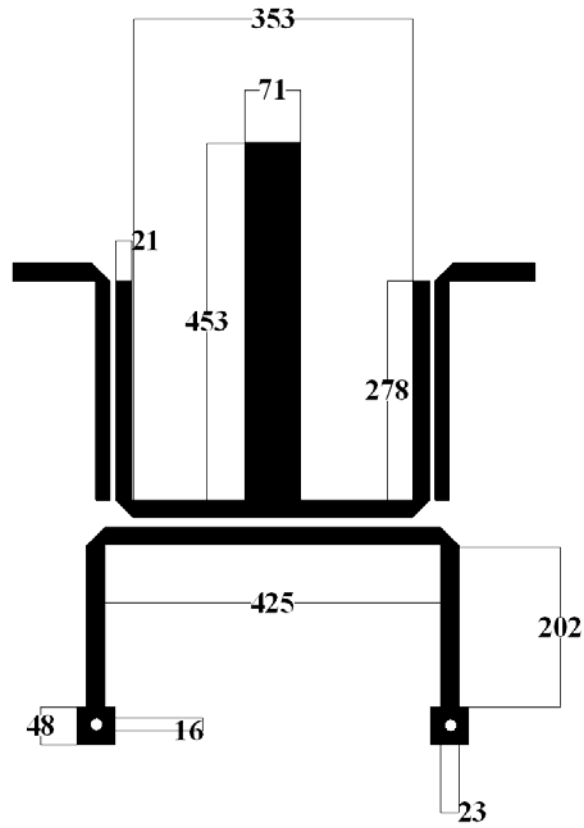
(b)

Figure 5-10. Fabricated extended-doublet filter (a) layout(unit:mil) (b) simulated and measured response.
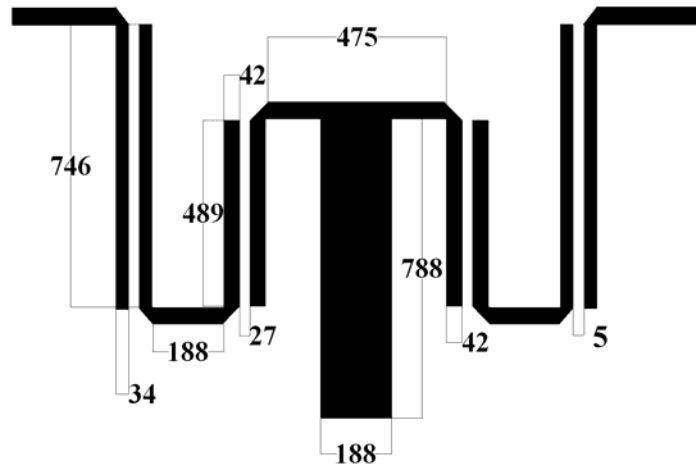
(a)
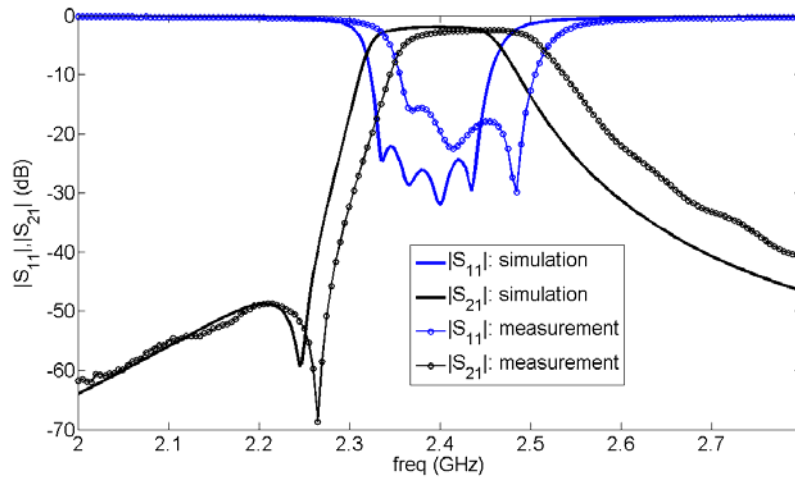
(b)
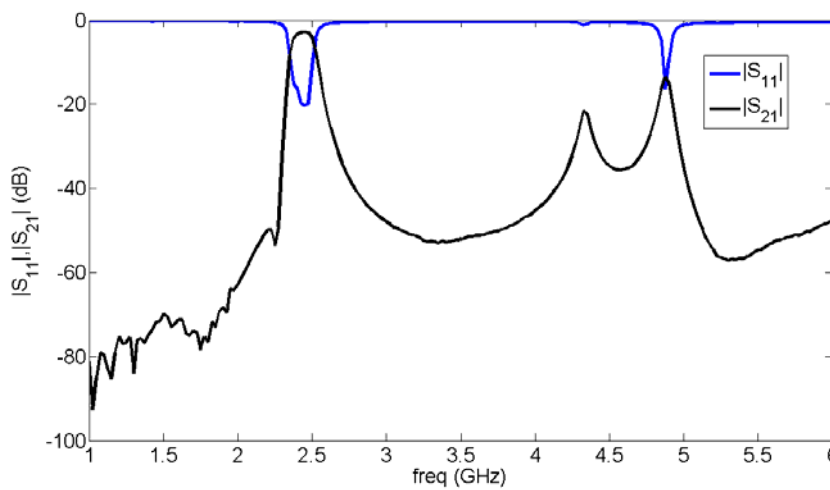
Figure 5-11. fabricated box-section filter (a) layout (unit:mil) (b) simulated and measured response. (c) the measured wideband response

5.4 Discussion

In Section 5-2, we have discussed how to get the electrical parameters of a filter network in doublet, extended-doublet, and box-section configuration from the corresponding coupling matrices. With the understanding of the correspondence between the coupling matrix and physical structure, the layout is not limited to those provided in this paper. A filter can be modeled by the box-like coupling scheme as long as it contains a two-mode resonator that is physically symmetric and supports two resonant modes. For instance, the filters in Figure 5-12 can also be modeled as a doublet filter since it is symmetric and has two resonant modes. However, for the filter in Figure 5-12, it is not easy to get the initial physical dimensions. On the contrary, the initial dimensions of the layouts proposed in this paper can easily be obtained. Besides, using the E-shaped resonator and the design procedures provided in this paper, all electrical parameters of a filter with box-like coupling schemes can be easily obtained. These parameters can be applied to filters with the same low-pass prototype and fractional bandwidth but a different center frequency and a different substrate. Having clear initial dimensions of a filter can save quite a lot of time in the design when comparing to the conventional design procedures of cross-coupled filters, e.g. the filters in [11]. In the design of a conventional cross-coupled filter, once the substrate, shape of resonator, or center frequency of a filter is changed, one must redo the design from the very beginning of the procedures.
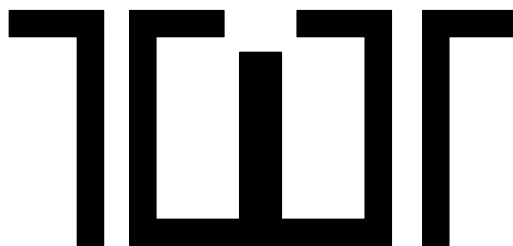
Figure 5-12. A possible filter layout that can be modeled as a doublet configuration.

The sensitivity analysis of the box-like coupling routes can be performed by the method proposed in [45]. The most sensitive part of the proposed structures is the coupling section between the E-shaped resonator and the source/load or other resonators because the coupling section controls the coupling strengths of two modes of E-shaped resonator to external circuit simultaneously.

Chapter 6 Parameter Extraction Method Based on

Vector Fitting Formulation

In previous chapters, the parameter extraction method applied to all of the mentioned filters is based on a lossless condition. In this Chapter, a formulation based on the vector fitting is applied to extract the equivalent circuit model from the frequency response of lossy cross-coupled microwave filters. By approximating the lossy response with short-circuit admittance parameters in partial fractional expansion form, the proposed method can evaluate the unloaded quality factor of resonators and extract the transversal coupling matrix simultaneously. The methodology of the vector fitting can identify the poles and residues of the short-circuit admittance parameters even when the poles are on the complex plane. And the extracted transversal coupling matrix can further transform into the prescribed form corresponding to the physical layout. The proposed method can be used in the tuning process of filter designs where the extraction of a coupling matrix is essential. To verify the method, a cross-coupled quadruplet filter is used as an example.

6.1 Introduction

The cross-coupled filters based on the model proposed in [5], [23] have found wide applications in wireless communication systems since they can provide the generalized Chebyshev response which exhibits the optimal in-band response and selectivity. However, the tuning of the filters based on cross-coupled topologies is time-consuming. In order to tune the cross-coupled filters more efficiently, therefore, diagnosis methods are needed to guide the process of the filter tuning [13]-[18]. Since the model proposed in [5], [23] can be expressed by a coupling matrix, most diagnosis methods in literatures are focused on extracting a coupling matrix from the simulated or measured response. By comparing the extracted coupling matrix to the desired coupling matrix, one can determine how to adjust the filter [13], [18].

Most parameter extraction methods are only valid for lossless filters since this is the assumption in their formulations. Thus, getting a coupling matrix from a lossy filter response is still an important research topic. Recently, a modified formulation of the Cauchy method which can extract the parameters of a lossless model from the response of a lossy bandpass filter is proposed [21]. The formulation in [21] can generate characteristic polynomials suitable for the synthesis of a low pass prototype associated with the lossless model of the filter, which is not feasible in the formulation proposed in [18], [20]. Strictly speaking, the methods in [21] would require lossless measured data and can not give a measure of how lossy a filter is.

To take the loss of a filter into consideration, we propose to use the model in Figure 6-1. The model in Figure 6-1 was modified from the model first proposed in [9] for filter synthesis and known as transversal network. The only difference between the model used in [9] and here is that we added the conductance, G_k, in each branch of the transversal network to model the loss, as shown in Figure 6-1(b). As the formulation in [9], the short-circuit admittance parameters, also known as Y-parameters, of the model in Figure 6-1, can be expressed by a polynomial in partial fractional expansion form. Here, the introduction of the loss positions the poles of the Y-parameters on the complex plane instead of on the imaginary axis as in the lossless case. To effectively get the short-circuit admittance parameters in the form of partial fraction expansion, the technique of vector fitting [46] is applied. The formulation based on the vector fitting can identify the positions of poles and calculate the residue of the Y-parameters. The poles of the Y-parameters contain the information of how lossy a filter is. Thus, the proposed method allows:

1. the evaluation of how lossy a filter is from the simulated or measured data;

2. the generation of the Y-parameters in the partial fraction expansion form, which is suitable for the synthesis of a low-pass prototype by the method in [9].
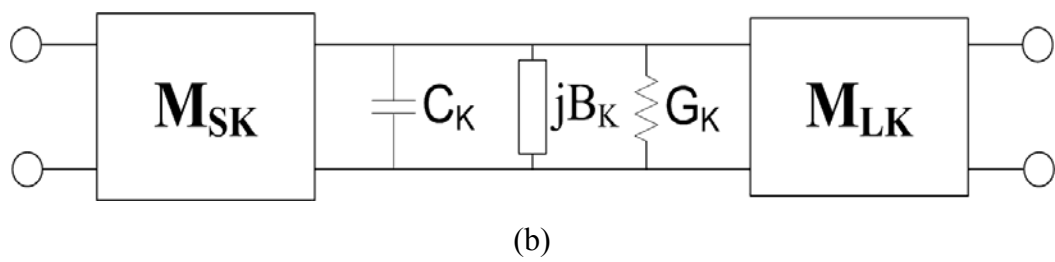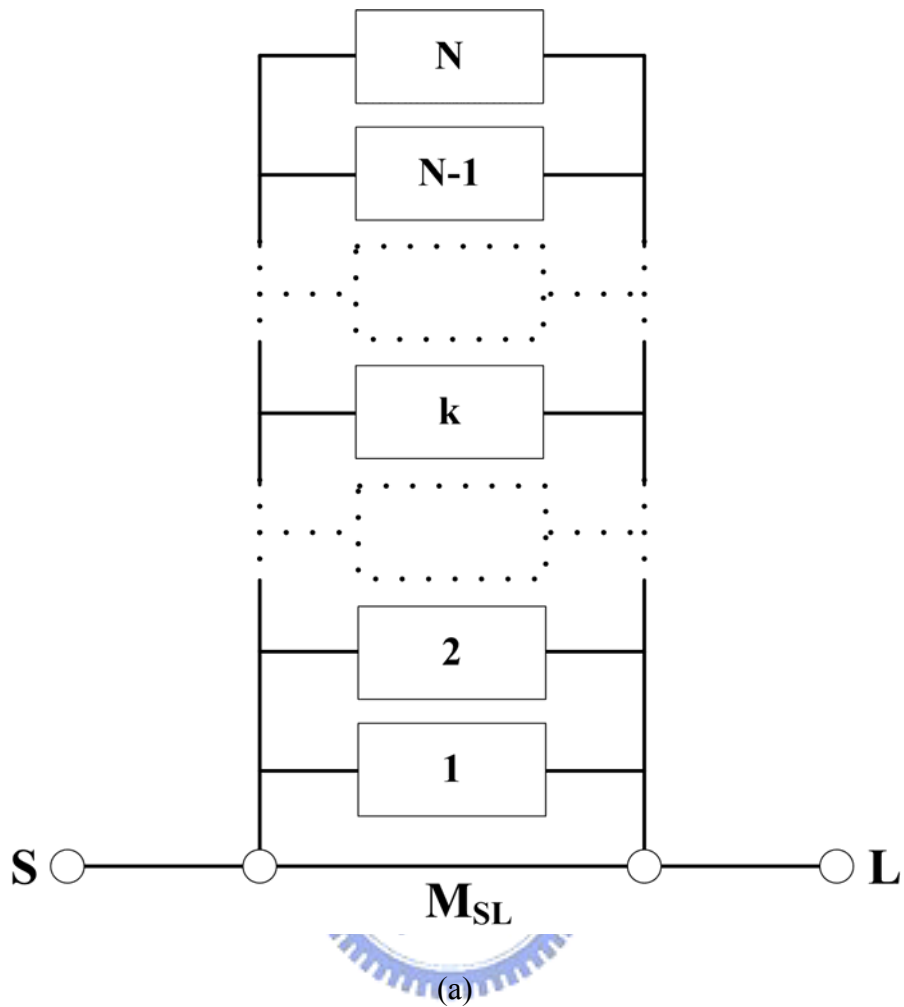
Figure 6-1. Canonical transversal array. (a) N—resonator transversal array including direct source–load coupling M_{SL}. (b) Equivalent circuit of the kth "low-pass resonator" in the transversal array.

6.2 Review of the Vector Fitting Technique

To facilitate the discussion in the next section, we briefly review the technique of vector fitting in this section. The technique of vector fitting was first proposed in 1997 by Bjorn Gustavsen and Adam Semlyen, and the authors further improved the technique in 1999 [46]. To one who is interested in the vector fitting technique, the paper published by the author in 1999 is highly suggested. The review below is based on the material in [46].

Consider the rational approximation

$$f(s) = \sum_{n=1}^{N} \frac{c_n}{s - a_n} + d + sh \tag{6-1}$$

where the c_n, a_n, d and h are unknowns. Vector fitting solves the problem (6-1) sequentially as a linear problem in two stages: pole identification and residue identification. In the stage of pole identification, specify a set of starting poles $\overline{a_n}$ in (6-1) and multiply $f(s)$ with an unknown function $\sigma(s)$. The $\sigma(s)$ is expressed by rational approximation. This gives the augmented problem:

$$\begin{bmatrix} \sigma(s)f(s) \\ \sigma(s) \end{bmatrix} = \begin{bmatrix} \sum_{n=1}^{N} \dfrac{c_n}{s - \overline{a_n}} + d + sh \\ \sum_{n=1}^{N} \dfrac{\widetilde{c}_n}{s - \overline{a_n}} + 1 \end{bmatrix} \tag{6-2}$$

Multiplying the second row in (6-2) with $f(s)$ yields the following equation:

$$\sum_{n=1}^{N} \frac{c_n}{s - \overline{a_n}} + d + sh = \left(\sum_{n=1}^{N} \frac{\widetilde{c}_n}{s - \overline{a_n}} + 1 \right) f(s) \tag{6-3}$$

or

$$(\sigma f)_{fit}(s) = \sigma_{fit}(s)f(s) \tag{6-4}$$

Equation (6-3) is linear in its unknowns c_n, d, h and $\widetilde{c}_n$. Writing (6-3) for several frequency points gives the overdetermined linear problem

$$Ax = b \qquad\qquad (6\text{-}5)$$

where unknowns are in solution vector x. Equation (6-5) is solved as a least squares problem. An important fact is that the zeros of $\sigma(s)$ are the poles of $f(s)$, so we can calculate the zeros of $\sigma(s)$ from the solution vector x to be the new poles of $f(s)$. Note that the numerator and denominator of $\sigma_{fit}(s)$ have been specified in (6-2) to be of the same order. This imply that if the starting poles are correct, then the new poles (zeros of $\sigma_{fit}(s)$) become equal to the starting poles ($\sigma_{fit}(s) = 1$). In practical application, this has the consequence that the rational function will converge if the new poles are used as starting poles in an iteration procedure.

After identifying the poles of $f(s)$, we can take the poles a_n to the original problem (6-2) and solve the equation like that in (6-5) to find the unknowns c_n, d, h, which is called residue identification in the vector fitting.

6.3 Applying Vector Fitting to Parameters Extraction

Following the formulation in [9], one can determine the two-port short-circuit admittance matrix $[Y_N]$ for the parallel-connected transverse array in Figure 6-1 as

$$
\begin{aligned}
[Y_N] &= \begin{bmatrix} y_{11}(s) & y_{12}(s) \\ y_{21}(s) & y_{22}(s) \end{bmatrix} \\
&= j \begin{bmatrix} 0 & M_{SL} \\ M_{SL} & 0 \end{bmatrix} \\
&+ \sum_{k=1}^{N} \frac{1}{(sC_k + jB_k + G_k)} \begin{bmatrix} M_{Sk}^2 & M_{SK}M_{LK} \\ M_{SK}M_{LK} & M_{Lk}^2 \end{bmatrix}
\end{aligned}
\qquad (6\text{-}6)
$$

Thus, if we can approximate the measured or simulated Y-parameters by polynomials, $y_{ij,appx}(s)$, in the following form

$$\left[Y_{appx}\right] = \begin{bmatrix} y_{11,appx}(s) & y_{12,appx}(s) \\ y_{21,appx}(s) & y_{22,appx}(s) \end{bmatrix}$$

$$= j\begin{bmatrix} 0 & K_0 \\ K_0 & 0 \end{bmatrix} + \sum_{k=1}^{N} \frac{1}{(s-j\lambda_k)}\begin{bmatrix} r_{11k} & r_{12k} \\ r_{21k} & r_{22k} \end{bmatrix} \tag{6-7}$$

Note that the residues $r_{11k}, r_{12k}, r_{21k}$ and r_{22k} are real numbers while the λ_k is a complex number in general in Equation (6-7). By comparing the first column of the Equation (6-6) and Equation (6-7), we can obtain $M_{SL} = K_0$, $C_k = 1$, $M_{kk} = B_k = -\mathrm{Re}[\lambda_k]$, $G_k = \mathrm{Im}[\lambda_k]$, $M_{Sk} = \sqrt{r_{11k}}$, $M_{Lk} = r_{21k}/\sqrt{r_{11k}}$. Once the M_{kk}, M_{SK}, M_{LK}, M_{SL} are determined, the transversal matrix is formed [9]. To transform the transversal coupling matrix into another coupling matrix with the prescribed coupling route corresponding to the physical structure, the methodology in [46] is used in this paper.

To obtain approximated Y-parameters of simulated or measured data in the form of Equation (6-7), the technique of vector fitting is applied. The vector fitting technique is a general methodology for the fitting of measured or calculated frequency domain response with rational function approximation [9]. Instead of directly fitting the data into a ratio of two polynomials, the methodology generates a polynomial in partial fractional expansion form. The source code can be obtained from the authors of the paper [46], but it can not be directly used to determine the polynomials that fit the model in Figure 6-1. The reason is that the formulation in [46] is in the bandpass frequency domain s, $s = j2\pi f$, and the generated polynomials can not fit into the model in Figure 6-1 even after bandpass-to-lowpass frequency transformation. To apply the formulation of vector fitting to fit the model in Figure 6-1, the formulation in [46] is followed except that the symbol s stands for normalized frequency $s = j\Omega$. For the need of parameter extraction, one must calibrate the position of reference planes of the input and output ports [17], and then fit the $y_{11,appx}(s)$ and

$y_{21,appx}(s)$ simultaneously. Thus, stack the $y_{11,appx}(s)$ and $y_{21,appx}(s)$ to form a vector $\bar{y}(s)$, as shown in following equation:

$$\bar{y}(s) = \begin{bmatrix} y_{11,appx}(s) \\ y_{21,appx}(s) \end{bmatrix} = \begin{bmatrix} \sum_{k=1}^{N} \dfrac{r_{11k}}{(s - j\lambda_k)} \\ jK_0 + \sum_{k=1}^{N} \dfrac{r_{21k}}{(s - j\lambda_k)} \end{bmatrix} \qquad (6\text{-}8)$$

The procedure in [46] is followed to identify the poles. As mentioned in [46], final positions of poles are determined through iterative calculations and not sensitive to the starting positions of poles. It is worth noting that the complex poles come in pairs in [46]; however, for the case here, it is not necessary for the poles to be in complex pairs since they are in the normalized frequency domain. After identifying the poles, one can identify the corresponding residues and obtain the polynomials in Equation (6-8).
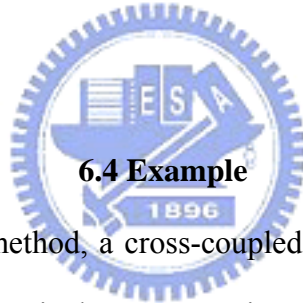
6.4 Example

To illustrate the proposed method, a cross-coupled quadruplet filter is given as an example. The layout of the filter is the same as Figure 3-4 in Chapter 3 excluding the S/L coupling controlling line. The center frequency and fractional bandwidth of the filter are 2.4 GHz and 3.75%, respectively. To demonstrate the ability of extracting the coupling matrix from a lossy filter response, the conductor loss is included. The simulation was performed using Sonnet [32] and the result is shown in Figure 6-2. The method in [17] is used to calibrate the position of the reference plane. The following bandpass-to–lowpass frequency transformation is adopted:

$$s = j\Omega = j(f_0 / \Delta f)(f / f_0 - f_0 / f) \qquad (6\text{-}9)$$

where Δf and f_0 are bandwidth and center frequency of the filter, respectively. By using the proposed method, the extracted normalized transversal coupling matrix M_1 is calculated to be

$$M_1 = \begin{bmatrix} 0 & 0.3409 & 0.5920 & 0.3704 & 0.6124 & 0 \\ 0.3409 & 1.3887 & 0 & 0 & 0 & -0.3629 \\ 0.5920 & 0 & 0.8265 & 0 & 0 & 0.5941 \\ 0.3704 & 0 & 0 & -1.0926 & 0 & 0.3886 \\ 0.6124 & 0 & 0 & 0 & -0.4793 & -0.6192 \\ 0 & -0.3629 & 0.5941 & 0.3886 & -0.6192 & 0 \end{bmatrix} \quad \text{(6-10)}$$

, along with other parameters $G_1 = 0.1472$, $G_2 = 0.1427$, $G_3 = 0.1539$, and $G_4 = 0.1501$. Then, transform the coupling matrix M_1 into the coupling matrix M_2 which corresponds to the coupling route of the cross-coupled quadruplet. The matrix M_2 is

$$M_2 = \begin{bmatrix} 0 & 1.0016 & 0 & 0 & 0 & 0 \\ 1.0016 & 0.1178 & 0.8401 & -0.0016 & -0.1496 & 0 \\ 0 & 0.8401 & 0.1592 & 0.7409 & -0.0016 & 0 \\ 0 & -0.0016 & 0.7409 & 0.1592 & 0.8401 & 0 \\ 0 & -0.1496 & -0.0016 & 0.8401 & 0.1178 & 1.0016 \\ 0 & 0 & 0 & 0 & 1.0016 & 0 \end{bmatrix} \quad \text{(6-11)}$$

With the approximation that the unloaded quality factor of each resonator is the same, we can get a measure of how lossy the filter is by calculating the average value of G_ks. In this case, the average value of G_ks is $G_{loss} = (G_1 + G_2 + G_3 + G_4)/4 = 0.1476$. From the quantity G_{loss}, we can evaluate the unloaded quality factor, Q_u, by $Q_u = \Delta f /(G_{loss} f_0)$. In this case, Q_u is equal to 180.67. A normalized coupling matrix [M] is related to the responses of $S_{11}(\Omega)$ and $S_{21}(\Omega)$ via the following equations:

$$S_{11} = -1 - 2j[A^{-1}]_{1,1} \quad \text{(6-12)}$$

$$S_{21} = -2j[A^{-1}]_{N+2,1} \quad \text{(6-13)}$$

Here, $A = \Omega[U_0] + [M] - j[G]$, $\Omega = (f_0/\Delta f)(f/f_0 - f_0/f)$, $[U_0]$ is similar to the $(N+2) \times (N+2)$ identity matrix except that $[U_0]_{1,1} = [U_0]_{N+2,N+2} = 0$, and $[G]$ is the

diagonal matrix $[G] = diag\{1, G_{loss}, ..., G_{loss}, 1\}$. Substituting the extracted coupling matrix M_2 with $G_{loss} = 0.1476$ into the Eq.(6-12) and Eq. (6-13), one can obtain the response shown in Figure 6-2.
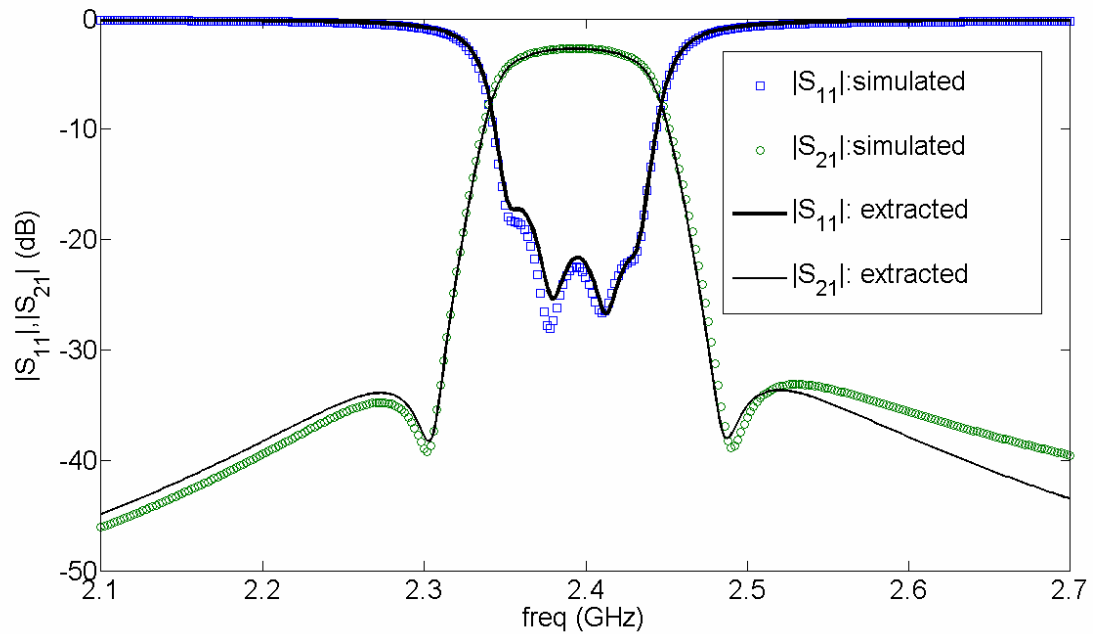

Figure 6-2. The simulated and extracted results of the cross-coupled quadruplet filter under consideration.

Chapter7 Summary and Future Work

7.1 Summary

The design of microwave filter is not a new filed, but there are always new things in this area. In recent years, a big advance is in filter design is the development of computer aided design (CAD) tools for filter diagnosis and tuning. In this dissertation, we try to keep the state of art to make filter design more systematical and faster.

A review of related algorithms and methods for the filter diagnosis and tuning are given in Chapter 2. The Pros and Cons of each method are discussed. An optimization design flow is given in Figure 2-6. Actually, each step of the flow is implemented in MATLAB except the EM simulation part which is done by commercial EM simulator. We have applied the extraction method and tuning process to design the microstrip filters in Chapter 3, Chapter 4, and Chapter 5. Although only microstrip filter are given in this dissertation, the design flow in Figure 1-3 is not limited to the microstrip filters. That is the design procedure can apply to design microwave filters with different material and guiding structure with the condition that the filter under consideration can be described by a coupling matrix with a proper topology.

A Parameter extraction method is given in Chapter 6. The proposed parameter extraction method can reconstruct the model of a lossy filter, which makes the proposed method different from other methods that are only effective for lossless filters. The ability of modeling a lossy filter makes the proposed parameter extraction method can not only be used in EM-simulation stage but also in production line.

7.2 Future work

The application interface between the commercial EM-simulator and MATLAB is needed. In the optimization procedure presented in Chapter 2, the EM-simulator is used to calculate the response of filters and export the simulated files to MATLAB. From the simulated response, programs written in MATLAB are applied to extract a coupling matrix and decide how to adjust the filter to achieve a prescribed response. The EM solver used in this dissertation is a commercial EM simulator. Thus, the application interface (API) between the EM-simulator and MATLAB is needed for the fully automatic tuning. That is to make the MATLAB able to co-simulate with a commercial EM-simulator, an interface is needed.

Although the API is not done yet, the ability of co-simulation is a trend. MATLAB is very powerful since it includes a lot of functions that can handle numerical operations and draw wonderful graphics. It is easy to develop an algorithm and verify it with MATLAB. On the other hand, it is hard for an individual to develop an EM solver to compete with the commercial EM simulators such as HFSS, IE3D, and Sonnet. Thus, if we can combine MATLAB with a commercial EM simulator, like HFSS, to solve a complicated EM problem, the design procedure would be more systematic and fast.

Reference

[1] R. Levy and S. B. Cohn, " A history of microwave filter research, design, and development", *IEEE Trans. Microwave Theory Tech.*, vol. MTT-32, pp. 1055-1067, Sep. 1984.

[2] R. Levy, R. V. Snyder, and G. Matthaei, " Design of microwave filters", *IEEE Trans. Microwave Theory Tech.*, vol. 50, pp. 783-793, March 2002.

[3] Ian C. Hunter, Laurent Billonet, Bernard Jarry, and Pierre Guillon, "Microwave filters--- applications and technology" , *IEEE Trans. Microwave Theory Tech.*, vol. 50, pp. 794-805, March 2002.

[4] A. E. Williams, " A four-cavity elliptic waveguide filter ", *IEEE Trans. Microwave Theory Tech.*, vol. MTT-18, pp. 1109–1114, Dec. 1970.

[5]A. E. Atia and A. E. Williams, "Newtypes of bandpass filters for satellite transponders," *COMSAT Tech. Rev.*, vol. 1, pp. 21–43, Fall 1971.

[6] A. E. Atia and A. E. Williams, "Narrow-bandpass waveguide filters," *IEEE Trans. Microwave Theory Tech.*, vol. MTT-20, pp. 258–265, Apr. 1972.

[7] A. E. Atia, A. E. Williams, and R. W. Newcomb, "Narrow-band multiple-coupled cavity synthesis," *IEEE Trans. Circuits Syst.*, vol. CAS-21, pp. 649–655, Sept. 1974.

[8] R. J. Cameron, "General coupling matrix synthesis methods for Chebyshev filtering functions," *IEEE Trans. Microwave Theory Tech.*, vol. 47, pp. 433–442, Apr. 1999.

[9] R. J. Cameron, "Advanced coupling matrix synthesis techniques for microwave filters," *IEEE Trans. Microwave Theory Tech.*, vol. 51, pp. 1–10, Jan. 2003.

[10] J. S. Hong and M. J. Lancaster, "Canonical microstrip filter using square open-loop resonators," *Elec. Lett.,* vol. 31, pp. 2020-2022, 1995.

[11] J. S. Hong and M. J. Lancaster, "Couplings of microstrip square open loop resonators for cross-coupled planar microwave filters," *IEEE Trans. Microwave Theory Tech.*, vol. 44, pp. 2099–2109, Nov. 1996.

[12] J. S. Hong and M. J. Lancaster, *Microstrip Filters for RF/Microwave Applications*. New York: Wiley, 2001.

[13] P. Harscher, R.Vahldieck, and S. Amari, "Automated filter tuning using generalized low-pass prototype networks and gradient-based parameter extraction," *IEEE Trans. Microw. Theory Tech.*, vol. 49, no. 12, pp. 2532–2538, Dec. 2001.

[14] G. Pepe, F.-J. Gortz, and H. Chaloupka, "Computer-aided tuning and diagnosis of microwave filters using sequential parameter extraction," in *IEEE MTT-S Int. Microw. Symp. Dig.*, 2004, pp. 1373–1376.

[15] M. Yu and W.-C. Tang, "A fully automated filter tuning robots for wireless basestation diplexers," presented at the IEEE MTT-S Int. Microwave Symp. Workshop, 2003, presentation.

[16] H.-T. Hsu, H.-W. Yao, K. A. Zaki, and A. E. Atia, "Computer-aided diagnosis and tuning of cascaded coupled resonators filters," *IEEE Trans. Microw. Theory Tech.*, vol. 50, no. 4, pp. 1137–1145, Apr. 2002.

[17] H.-T. Hsu, Z. Zhang, K. A. Zaki, and A. E. Atia, "Parameter extraction for symmetric coupled-resonator filters," *IEEE Trans. Microw. Theory Tech.*, vol. 50, no. 12, pp. 2971–2978, Dec. 2002.

[18] A. García-Lampérez, S. Llorente-Romano, M. Salazar-Palma, and T. K. Sarkar, "Efficient electromagnetic optimization of microwave filters and multiplexers using rational models," *IEEE Trans. Microw. Theory Tech.*, vol. 52, pp. 508–521, Feb. 2004.

[19] Piotr Kozakowski , Adam Lamecki, Piotr Sypek, and Michal Mrozowski, "Eigenvalue approach to synthesis of prototype filters with source/load coupling", *IEEE Microwave and Wireless Component Lett.*, vol. 15, pp.98–100,Feb. 2005.

[20] A. García-Lampérez, T. K. Sarkar, and M. Salazar-Palma, "Generation of accurate rational models of lossy systems using the cauchy method," *IEEE Microw. Wireless Compon. Lett.*, vol. 14, no. 10, pp. 490–492, Oct. 2004.

[21] Giuseppe Macchiarella, and Daniele Trina, "A formulation of the Cauchy method suitable for the synthesis of lossless circuit models of microwave filters from lossy measurements", *IEEE Microw. Wireless Compon. Lett.*, vol. 16, no. 5, pp. 243–245,

May 2006.

[22] W. A. Atia, K. A. Zaki, and A. E. Atia, "Synthesis of general topology multiple coupled resonator filters by optimization," *IEEE Microwave Theory Tech. Dig.*, pp. 821–824, 1998.

[23] S. Amari, U. Rosenberg, and J. Bornemann, "Adpative synthesis and design of resonator filters with source/load-multi-resonator coupling," *IEEE Trans. Microwave Theory Tech.*, vol. 50, pp. 1969–1978, Aug. 2002.

[24] S. Amari, and U. Rosenberg, "On the sensitivity of coupled resonator Filters without some direct couplings," *IEEE Trans. Microwave Theory Tech.*, vol. 51, pp. 1767–1773, June 2003.

[25] Giuseppe Macchiarella, "A powerful tool for the synthesis of prototype filter with arbitrary topology" in *Proc. IEEE MTT-S Int. Microwave Symp.* , June 2003, pp. 1467-1470

[26] I. Hunter, *Theory and Design of Microwave Filters*. London, U.K.: IEE Press, 2001.

[27] K. S. K. Yeo and M. J. Lancaster "The design of microstrip six-pole quasi-elliptic filter with linear phase response using extracted-pole technique," *IEEE Trans. Microwave Theory Tech.* , vol. 49, pp. 321–327, Fub. 2001

[28] K. T. Jokela, "Narrow-band stripline or microstrip filters with transmission zeros at real and imaginary frequencies," *IEEE Trans. Microwave Theory Tech.*, vol. MTT-28, pp. 542–547, 1980.

[29] J. R. Montejo-Garai, "Synthesis of N-even order symmetric filters with N transmission zeros by means of source-load cross coupling," *Electron. Lett* , vol. 36, no. 3, pp. 232–233, Feb. 2000.

[30] S. Bila, D. Baillargeat, M. Aubourg, S. Verdeyme, P. Guillon, F. Seyfert, J. Grimm, L. Baratchart, C. Zanchi, and J. Sombrin, "Direct electromagnetic optimization of microwave filters," *IEEE Microwave Mag.*, vol. 2,   pp. 46–51, Mar. 2001.

[31] H. C. Bell, Jr., "Canonical asymmetric coupled-resonator filters," *IEEE Trans. Microwave Theory Tech.*, vol. MTT-30, pp. 1333–1340, Sept.1982.

[32] *Em User's Manual*, Sonnet Software Inc., Liverpool, NY, 2004.

[33] J. S. Hong and M. J. Lancaster, "Cross-coupled microstrip hairpin-resonator filters", *IEEE Trans. Microwave Theory Tech.*, vol. 46, pp. 118–122, Jan. 1998

[34] J. S. Hong and Shuzhou Li, "Dual-model microstrip Triangular patch resonators and filters" in *Proc. IEEE MTT-S Int. Microwave Symp.*, June 2003, pp. 1901-1904

[35] J. R. Montejo-Garai, "synthesis of filters with transmission zeros at real frequencies by means of trisections including source/load to resonator coupling", Electronics Letters, Vol. 36, No. 12, September 2000, pp. 1629-1630

[36] S. B Cohn.,"Parallel-coupled transmission-line-resonator filters", IRE Trans., MTT-6, pp.223-231

[37] C.-Y. Chang and T. Itoh," A modified parallel-coupled filter structure that improves the upper stopband rejection and responsed symmetry", IEEE Trans., MTT-39, pp 310-313, 1991

[38] R. J. Cameron, A. R. Harish, and C. J. Radcliffe, "Synthesis of advanced microwave filters without diagonal cross-couplings," *IEEE Trans. Microwave Theory Tech.*, vol. 50, pp. 2862–2872, Dec. 2002

[39] Uwe Rosenberg, Smain Amari, *"Novel Coupling Schemes for Microwave Resonator Filters," IEEE Trans. MicrowaveTheory Tech.*, vol. 50, pp. 2896–2902, Dec. 2002.

[40] S. Amari and U. Rosenberg, "New building blocks for modular design of elliptic and self-equalized filters," *IEEE Trans. Microwave Theory Tech.*, vol. 52, pp. 721–736, Feb. 2004

[41] S. Amari, G. Tadeson, J. Cihlar, R. Wu, and U. Rosenberg, "Pseudo-elliptic microstrip line filters with zero-shifting properties," *IEEE Microwave Wireless Comp. Lett.*, vol. 14,pp. 346–348, July 2004

[42] A. G. Lamperez, and M. S. Palma, **"**High Selectivity X-Band Planar Diplexer with Symmetrical Box-Section Filters," in *2005 Eur. Microwave Conf.*, Vol. 1, pp.105 − 108, France, Oct., 2005

[43] J. R. Lee, J. Hoon. Cho, and S. W. Yun, "New Compact Bandpass Filter Using Microstrip λ/4 Resonator with Open Stub Inverter." *IEEE Microw. Guided wave Lett.*, vol. No. 12, pp.526-527, Dec. 2000

[44] M. Makimoto and S. Yamashita, Microwave Resonators and Filters for Wireless Communication, New York: Springer, 2001

[45] Smain Amari, and Uwe Rosenberg, "On the sensitivity of coupled resonator filters without some direct couplings," *IEEE Trans. Microwave Theory Tech.*, vol. 51, pp.1767−1773, June. 2003

[46] B. Gustavsen and A. Semlyen, "Rational approximation of frequency domain responses by Vector Fitting", *IEEE Trans. Power Delivery*, vol. 14, no. 3, pp. 1052-1061, July 1999.

簡歷

姓　名 ：廖竟谷

性　別 ： 男

出生年月日 ： 民國　67 年 10 月 16 日

籍　貫 ： 台灣省台中縣

學　歷 ：交通大學電信所碩士班畢業

經　歷 ：高中畢業於台中一中，大學畢業於交通大學電子物理學系。申請進入交通大學電信研究所電波組研讀，個人在碩博班期間之研究主題為微波被動元件之設計與製作。為斐陶斐榮譽學會(PHI TAU PHI)會員。

論文題目 ：

Tuning and Diagnosis of Cross-Coupled Microstrip Filters

Publication List

A. Journal:

[1] **Ching-Ku Liao** and Chi-Yang Chang, "Design of micorstrip quadruplet filters with source-load coupling", *IEEE Trans. Microwave Theory Tech* Vol. 53,   pp. 2302-2308, July 2005.

[2] **Ching-Ku Liao** and Chi-Yang Chang, "Modified parallel-coupled filter with two independently controllable upper stopband transmission zeros", *IEEE Microwave and Wireless Components Letters*, . pp. 841-843, Dec. 2005.

[3] **Ching-Ku Liao**, Pei-Ling Chi, and Chi-Yang Chang ,"Microstrip Realization of Generalized Chebyshev Filters with Box-Like Coupling Schemes", *IEEE Trans. Microwave Theory Tech* Vol. 53, pp. 147-153 , January 2007.

[4] Chin-Hsuing Chen, **Ching-Ku Liao**, and Chi-Yang Chang, "Novel Multifold Finite-Ground-Width CPW Quarter-Wavelength Filters With Attenuation Poles", *IEEE Trans. Microwave Theory Tech* Vol. 53, pp. 128-136 , January 2007.

[5] **Ching-Ku Liao,** Chi-Yang Chang, Jenshan Lin, "A Vector-Fitting Formulation for Parameter Extraction of Lossy Microwave Filters", *IEEE Microwave and Wireless Components Letters,* pp. 277-279, April 2007

B: Conference:

[1] Chi-Yang Chang, **Ching-Ku Liao**, and Dow-Chih Niu, "A 1.5 to 37 GHz ultra-broadband MMIC Mouw's star mixer", in 2005 EuMC Digest, pp 987-990, France, Oct. 2005

[2] Ming-Yu Hsieh, Shih-Ming Wang, **Ching-Ku Liao**, Chin-Hsien Chiang and Chi-Yang Chang, "Microstrip band-pass filters with wide stopband and sharper cutoff response", *in 2005 EuMC Digest,* pp 1247-1250, France, Oct. 2005.

[3] **Ching-Ku Liao** and Chi-Yang Chang, "A Novel Five-Pole Microstrip Cascade Quadruplet Filter", In 2005 APMC Digest, pp 433-436, SuZhou, Dec. 2005

[4] **Ching-Ku Liao**, Chi-Yang Chang, Jenshan Lin, "A Reconfigurable Filter Based on Doublet Configuration", *IEEE MTT-S International Microwave Symposium Digest* pp. 1607-1610, 2007